Model-Based Control of Soft Robots

A Survey of the State of the Art and Open Challenges

Della Santina, Cosimo; Duriez, Christian; Rus, Daniela

DOI
10.1109/MCS.2023.3253419

Publication date
2023

Document Version
Final published version

Published in
IEEE Control Systems

Citation (APA)
Della Santina, C., Duriez, C., & Rus, D. (2023). Model-Based Control of Soft Robots: A Survey of the State of the Art and Open Challenges. *IEEE Control Systems*, *43*(3), 30-65. https://doi.org/10.1109/MCS.2023.3253419

Model-Based Control of Soft Robots

A SURVEY OF THE STATE OF THE ART AND OPEN CHALLENGES

COSIMO DELLA SANTINA, CHRISTIAN DURIEZ, and DANIELA RUS

FARIMAH KHAVARINEZHAD

From a functional standpoint, classic robots are not at all similar to biological systems. If compared with rigid robots, animals' bodies look overly redundant, imprecise, and weak. Nevertheless, animals can still perform a vast range of activities with unmatched effectiveness. Many studies in biomechanics have pointed to the elastic and compliant nature of the musculoskeletal system as a fundamental ingredient explaining this gap. Thus, to reach performance comparable to nature, elastic elements have been introduced in rigid-bodied robots, leading to articulated soft robotics [1] (see "Summary"). In continuum soft robotics, this concept is brought to an extreme. Here, softness is not concentrated at the joint level but instead distributed across the whole structure. As a result, soft robots (henceforth, omitting the adjective *continuum*) are entirely made of continuously deformable elements. This design solution aims to bring robots closer to invertebrate animals and the soft appendices of vertebrate animals (for example, an elephant's trunk and the tail of a monkey). Several soft robotic hardware platforms have been proposed with increasingly higher reliability and functionalities. In this process, considerable attention has been devoted to the technological side of the problem, leading to a large assortment of hardware solutions. In turn, this abundance opened up the challenge of developing effective control strategies that can manage the soft body and exploit its embodied intelligence.

Historically and across many application domains, model-based techniques are the first advanced control algorithms to appear and substitute heuristic rules. Data-driven and machine learning approaches usually come later when moving to more extreme control scenarios. This has also been the case for standard robotics, whose history proceeded parallel to the development of control theory: from the frequency domain to linear state-space control, to the fully nonlinear domain, and, only recently, to machine learning. Vice versa, the development of control algorithms in soft robotics has followed a reversed path. In the early days, machine learning strategies were the way to control soft robots except for the quasi-static and purely kinematic scenarios. Indeed, it has long been believed that model-based strategies were unfeasible for the soft robotic application, due to the large variability of technological solutions and the overwhelming complexity of the modeling task.

Over the past few years, two main factors have been challenging this view. First, theoretical and experimental investigations have shown that feedback schemes are robust to rough approximations of the soft robot dynamics. Interestingly, even vastly simplified descriptions already provide enough information to improve the performance significantly compared to the model-free baseline. Second, a new wave of finite-dimensional modeling techniques tailored to soft robots has appeared in the literature, methods that are simultaneously accurate, manageable, and interpretable. Even if a complete application to closed-loop control has yet to come for some of these models, these theoretical works identify an underlying

Digital Object Identifier 10.1109/MCS.2023.3253419
Date of current version: 19 May 2023

1066-033X/23©2023IEEE

mathematical structure in soft robotics. Therefore, they lay a solid ground on which to study the control problem.

This article aims to introduce the control theorist perspective to this novel development in robotics (see "Summary). We aim to remove the barriers to entry into this field by presenting existing results and future challenges, using a unified language and within a coherent framework. Indeed, the main difficulty in entering this field is the wide variability of terminology and scientific backgrounds, making it quite hard to acquire a comprehensive view on the topic. Another limiting factor is that it is not obvious where to draw a clear line between the limitations imposed by the technology not being mature yet and the challenges intrinsic to this class of robots. In this work, we consider intrinsic the continuum, or multibody, dynamics; the presence of a nonnegligible elastic potential field; and the variability in sensing and actuation strategies. The hysteresis and nonideal behaviors affecting sensors, actuators, and the main body are considered relevant but not intrinsic since we believe that with the advance of the technology, these aspects should be overcome. Of the many review articles about soft robotics [1], [2], [3], [4], [5], [6], [7], [8], [9], [10], only [11] is focused on the control challenge, which does not follow a model-based approach.

FINITE-DIMENSIONAL MODELS FOR CONTROL PURPOSES

In their exact formulation, continuum soft robots belong to the domain of continuum mechanics. Thus, their dynamics are formulated as an infinite-dimensional system, that is, via partial differential equations (PDEs). Yet, recent work has clearly shown that finite-dimensional approximations of the robot's dynamics can be formulated that assume the form of standard ordinary differential equations (ODEs). These formulations are tractable and precise enough to describe the soft robot behavior with the necessary precision. Contrary to the rigid case, developing models is an integral part of the control design process in soft robotics. Commonly used models of rigid robots can be used for simulating and controlling these systems. Instead, with soft robots, models used for simulation and control design come from different assumptions and approximations. The former must be accurate, possibly at the cost of computational efficiency and simplicity of interpretation. In contrast, the latter must be low dimensional and capture only the essential features of the dynamic behavior, possibly neglecting the finer details. Moreover, control-oriented models must lend themselves to formally assess the robot's structural properties and the closed-loop behavior.

We review the main modeling strategies in the following, focusing primarily on aspects relevant to model-based control. Thus, some approximations will be made and details omitted when possible. The reader interested in knowing more about the modeling of soft robots can refer to the recent survey article by Armanini et al. [12]. Conversely, the reader interested in jumping directly to the control part is advised to first read the sections "Finite-Dimensional Approximations" and "Existence of Equilibria."

Summary

The field of soft robotics control is fascinating and full of potential, but it can be daunting to navigate. Soft robotics sits at the intersection of various disciplines, including material science, biology, continuum mechanics, and robotics, as well as distinct sub-fields within each of these areas. Each of these fields comes with its unique literature, unwritten hypotheses, notations, and terminology. On top of that, talking about control requires first agreeing on the dynamic equations that model soft robots, which is itself an open research topic currently being investigated by different communities.

Nonetheless, the challenge of controlling soft robots is particularly interesting because it combines fundamental questions with practical applications. Soft robots are inherently underactuated, highly nonlinear mechanical systems that are always immersed in an elastic potential field and subject to dissipation forces that serve as stabilizing actions. It is the task of the control engineer to harness these effects to generate precise motions with the few actuation sources available and execute controlled interactions with an external environment or store energy during dynamic movements.

This article aims to make the field of soft robotics more accessible to control theory researchers by providing a comprehensive introduction to the soft robotics control challenge through model-based control lenses. We start by presenting a unified formulation for the dynamics of a soft robot that is modeling technique independent. From there, we introduce shape control and tracking problems before exploring open challenges in the field, such as underactuation, environmental interactions, actuator dynamics, task space control, and using data in a model-based framework. Along the way, we survey the literature on soft robotics and propose several new results that leverage established techniques for controlling rigid robots.

When the Rigid Part Is Dominant

It is not uncommon to find full-fledged soft robotic technologies integrated into essentially rigid structures. This is the case for the soft neck of a rigid humanoid robot discussed in [13] and [14] and the soft muscles actuating rigid links [15], [16], [17]. In all these cases, the dynamics of the rigid part are essentially dominant with respect to the soft continuum part. Thus, the system model can be obtained with a good level of approximation by applying standard multibody dynamics machinery to the rigid portion and accounting for the soft part through a nonlinear lumped impedance.

Rod Models

Many soft robots have one physical dimension that is longer than the other two, such as the tentacle-like system shown by Figure 1(a). Their whole configuration can be effectively approximated by neglecting volumetric deformations and focusing on the behavior of their central axis. This assumption works well in practice and allows for relying on well-established theories in continuum mechanics of rods.

Consider a continuum and infinitely thin element (called a rod, from now on) of length L, as in the one in Figure 1. Its posture in space can be completely described by the spatial

Better Than Rigid Robots: Exploiting Softness in Model-Based Control

A natural way of understanding physical intelligence generated by a soft body within a model-based setting is to look at the impedance $K(q) + D(q)\dot{q}$ in (2) as a low-level feedback action. One obvious advantage of implementing such an action physically rather than digitally is that it does not require any additional sensors and actuators. Another important feature is that it acts simultaneously and in a decentralized manner along the whole infinite-dimensional structure. In other words, $\partial K/\partial q$ and D are always full rank almost everywhere, no matter the level of discretization. The number of independent directions in which standard control can be produced is limited, as concisely represented by the fact that the number of columns m of the matrix $A(q)$ in (2) is independent from the size n of the configuration space q. The consequence in terms of self-stabilization of the robot and control simplification are extensively discussed in the main body of the article.

Physical elasticity can also be used to better the execution of dynamic tasks. For example, [S1] and [S2] prove that lumped join-spring-link systems admit optimal control actions that maximize velocity and forces beyond what can be achieved by a rigid robot of equivalent inertia. During these tasks, the potential $U_K(q)$ serves as a tank in which energy can be stored and released when necessary. Thanks to multistabilities and bucklings, continuum structures can lead to even more extreme behaviors concerning pick performances, which have been thoroughly investigated in a model-based fashion [S3], [S4], [S5]. However, the proposed descriptions are generally not in the language of dynamical systems, and thus, using them for control purposes is still an open challenge. Another benefit of physical elasticity is to endow the robot with the capability of performing regular oscillations [S6], which can be excited by means of model-based control [S7], [S8], [S9]. This is especially useful in efficient and robust locomotion [7], [S10], [S11]. It is worth noting that all these capabilities are implicitly exploited by the vast range of approaches using numerical optimization for controlling soft robots [S12], [S13], [118], [162], [163], [164].

For an in-depth analysis on how the body of a soft robot can generate intelligent behaviors, refer to another article within the same special issue discussing embodied intelligence [S14].

REFERENCES

[S1] M. Garabini, A. Passaglia, F. Belo, P. Salaris, and A. Bicchi, "Optimality principles in variable stiffness control: The VSA hammer," in *Proc. IEEE/RSJ Int. Conf. Intell. Robots Syst.*, 2011, pp. 3770–3775, doi: 10.1109/IROS.2011.6048555.

[S2] S. Haddadin, M. Weis, S. Wolf, and A. Albu-Schäffer, "Optimal control for maximizing link velocity of robotic variable stiffness joints," *IFAC Proc.* vol. 44, no. 1, pp. 6863–6871, Aug. 2011, doi: 10.3182/20110828-6-IT-1002.01686.

[S3] C. Armanini, F. Dal Corso, D. Misseroni, and D. Bigoni, "From the elastica compass to the elastica catapult: An essay on the mechanics of soft robot arm," *Proc. Roy. Soc. A, Math., Phys. Eng. Sci.*, vol. 473, no. 2198, Feb. 2017, Art. no. 20160870, doi: 10.1098/rspa.2016.0870.

[S4] K. Arakawa, F. Giorgio-Serchi, and H. Mochiyama, "Snap pump: A snap-through mechanism for a pulsatile pump," *IEEE Robot. Autom. Lett.*, vol. 6, no. 2, pp. 803–810, Jan. 2021, doi: 10.1109/LRA.2021.3052416.

[S5] N. Vasios, B. Deng, B. Gorissen, and K. Bertoldi, "Universally bistable shells with nonzero gaussian curvature for two-way transition waves," *Nature Commun.*, vol. 12, no. 1, pp. 1–9, Jan. 2021, doi: 10.1038/s41467-020-20698-9.

[S6] A. Albu-Schaeffer and C. Della Santina, "A review on nonlinear modes in conservative mechanical systems," *Annu. Rev. Contr.*, vol. 50, pp. 49–71, Dec. 2020, doi: 10.1016/j.arcontrol.2020.10.002.

[S7] G. Garofalo and C. Ott, "Passive energy-based control via energy tanks and release valve for limit cycle and compliance control," *IFAC-PapersOnLine*, vol. 51, no. 22, pp. 73–78, Dec. 2018, doi: 10.1016/j.ifacol.2018.11.520.

[S8] T. Marcucci, M. Garabini, G. M. Gasparri, A. Artoni, M. Gabiccini, and A. Bicchi, "Parametric trajectory libraries for online motion planning with application to soft robots," in *Robotics Research*, N. Amato, G. Hager, S. Thomas, and M. Torres-Torriti, Eds. Cham, Switzerland: Springer, 2020, pp. 1001–1017.

[S9] C. Della Santina and A. Albu-Schaeffer, "Exciting efficient oscillations in nonlinear mechanical systems through eigenmanifold stabilization," *IEEE Contr. Syst. Lett.*, vol. 5, no. 6, pp. 1916–1921, Dec. 2021, doi: 10.1109/LCSYS.2020.3048228.

[S10] N. Kashiri et al., "An overview on principles for energy efficient robot locomotion," *Frontiers Robot. AI*, vol. 5, Dec. 2018, Art. no. 129, doi: 10.3389/frobt.2018.00129.

[S11] T. Bujard, F. Giorgio-Serchi, and G. Weymouth, "A resonant squid-inspired robot unlocks biological propulsive efficiency," *Sci. Robot.*, vol. 6, no. 50, Jan. 2021, Art. no. eabd2971, doi: 10.1126/scirobotics.abd2971.

[S12] C. Duriez and T. Bieze, "Soft robot modeling, simulation and control in real-time," in *Soft Robotics: Trends, Applications and Challenges*, C. Laschi, J. Rossiter, F. Iida, M. Cianchetti, and L. Margheri, Eds. Cham, Switzerland: Springer, 2017, pp. 103–109.

[S13] J. M. Bern, P. Banzet, R. Poranne, and S. Coros, "Trajectory optimization for cable-driven soft robot locomotion," in *Proc. Robot., Sci. Syst.*, 2019, pp. 1–8.

[S14] H. Hauser et al., "A survey on embodied intelligence in soft robots (Provisional Title)," *IEEE Control Mag.*, to be published.

curve $x:[0,1]\times\mathbb{R}\to SE(3)$. The domain $[0,1]$ is the normalized arc length of the rod, and $SE(3)$ is the special Euclidean group of dimension three. The element $x(s,t)$ is the full posture at time t of the infinitesimal element of the rod that is at a distance sL from the robot's base. So, $x(0,t)$ is the configuration of the base, $x(1,t)$ of the tip, $x(1/2,t)$ of the middle point, and so on. To each point s along the rod associate a mass density $m(s)\in\mathbb{R}^+$, an external load in the form of a generic wrench $f(s,t)\in\mathbb{R}^6$, and a velocity $\dot{x}(s,t)\in\mathbb{R}^6$. The total mass of the segment is $\int_0^1 m(s)\,\mathrm{d}s$.

It is worth stressing that despite the formulation referring to an infinitely thin structure (the rod), these models can be and commonly are applied every time a central axis can be identified. In this case, the curve x is referred to as the backbone of the soft robot. The use of framed curves as backbones for robots originated in the field of hyperredundant robots [18], [19]. Here, the rod serves as a continuum approximation of the discrete system [20]. The method was later adopted by continuum (stiff and soft) robots. Under the assumption that the cross sections of the soft robot change negligibly during deformations, the contribution of their area can be included by associating an infinitesimal rotational inertia $\mathcal{J}(s)\in\mathbb{R}^{3\times3}$ to each point along the rod.

The rod shape $x(\cdot,t)$ can, in principle, serve as the configuration of the robot at time t. An alternative that is gaining increasing popularity in soft robotics is to use the local strains to represent the robot's configuration: curvature, twist, elongation, and shear. These are the variations of x for infinitesimal variations of s. Hence, they are a function $\xi:[0,1]\to\mathbb{R}^6$ or to a smaller space in case some of the deformations are not considered. Visualizations of pure strains are provided in Figure 2. Note that, contrary to x, the codomain of ξ is the Euclidean space $\mathbb{R}^6$. This avoids the need for introducing parameterizations of $SE(3)$. Furthermore, strains are a more direct extension of the joint variables commonly used as the configuration of classic articulated robots. For these reasons, we mainly focus on strain representations in this short review of modeling techniques despite shape-based ones being wildly popular in the literature. The rod posture x can always be recovered from the strains ξ by integration. The result is a continuous version of what in classic robotics would be regarded as the forward kinematics of the robot.

At this point, the main ingredients necessary to describe a soft robot within the rod modeling framework have been laid down. The following sections focus on reviewing solutions for formulating the dynamics of these systems. We start from exact infinite-dimensional formulations, then quickly move to survey the various existing alternatives to introducing expert intuitions into the problem and getting to a finite-dimensional model of the robot that can be used for control purposes. We often refer to piecewise constant curvature (PCC) models when providing examples. This is done for simplicity and because most of the properties of more complex models are already present in this more straightforward and widespread solution.

Infinite-Dimensional Models

The Kirchhoff-Clebsch-Love and Cosserat rod theories lead to exact descriptions of the dynamics of rod-like structures [21], [22], [23], [24]. Leveraging these frameworks, the statics and dynamics of tendon-actuated continuum and soft robots are derived and experimentally validated in [25], [26], and [27], respectively. Multiple Cosserat rod models can be combined together through coupled boundary conditions to describe the kinematics of parallel soft robots [28], [29]. A tutorial on the dynamic Cosserat model for tendon-driven continuum robots is provided in [30]. These models have infinite-dimensional states, and thus, they are formulated as PDEs. This makes it hard to use them directly for control (see "Infinite-Dimensional Control" for more details). Nonetheless, they can be profitably used to extract steady-state solutions. The use of the Magnus expansion to solve the kinematics of Cosserat rods is discussed in [31] and [32]. Also, the direct application to simulation is arduous but not impossible. For example, [33] performs a time discretization that

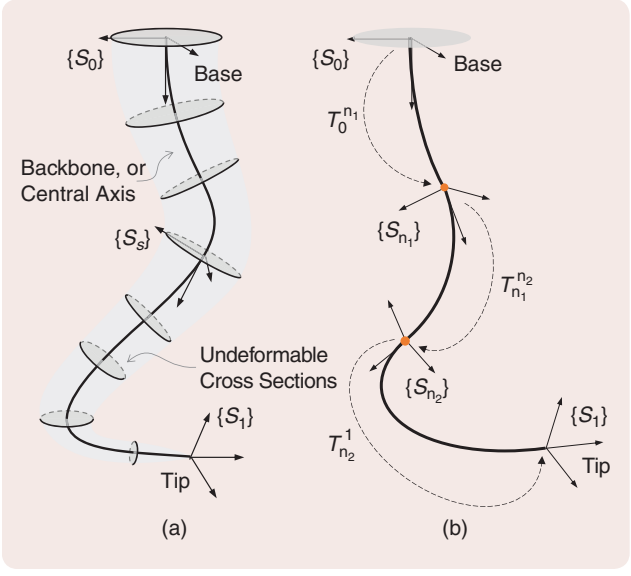

FIGURE 1 (a) A soft robot as described within rod theories. The central axis, or backbone, is a spatial curve that can deform. Cross sections are assumed to be undeformable, and they are rigidly connected to the curve. Some examples of disk-like cross sections are highlighted in the figure. To each point is also attached a reference frame $\{S_s\}$, where s is the normalized arc length. (b) Piecewise constant strain models with three segments. First, four nodes along the backbone are identified $(0, n_1, n_2, 1)$. Then, the associated transformation matrices $(T_0^{n_1}, T_{n_1}^{n_2}, T_{n_2}^{1})$ are parameterized by a finite set of variables. The robot configuration q is defined as the collection of these variables. In piecewise constant curvature models, two subsequent nodes are always connected by an arc of a circle.

transforms the PDE into an ODE in the s variable only. The latter is then solved at every time step to find the robot's shape. Nonlinear observers can be used to speed up the convergence [34].

Finite-Dimensional Approximations

The alternative to PDE formulations is to restrict the range of possible shapes x or strains ξ to a finite-dimensional functional space. For the sake of simplicity, from now on, we consider strain-based parameterizations when not differently specified.

Two classes of strategies exist to achieve this goal: piecewise constant strain models and functional parameterizations. Both of them are discussed in detail in the following. At the current stage, what is essential to keep in mind is that using these techniques, the strain ξ can be approximated as a function of the vector $q \in \mathbb{R}^n$ that serves as the configuration of the soft robot. This critical step enables the recasting of concepts from classic discrete robotics to the new continuum context. To start, the kinematics of a soft robot can now be defined as

$$\dot{x}(s, q(t)) = J(s, q(t))\dot{q}(t), \quad J(s, q) = \frac{\partial h(s, q)}{\partial q} \tag{1}$$

Infinite-Dimensional Control

The question of whether infinite-dimensional models should be directly used in the design of feedback controllers is a long-lasting one, which extends far beyond the soft robotics field [S15], [S16]. Indeed, working with a finite-dimensional approximation of the dynamics substantially simplifies the control design and already takes into account some important features of the robot's dynamics to any desired level of precision. From a practical standpoint, having results that can be proved for any level of discretization ($1 << n_S < \infty$) is de facto equivalent to dealing with the continuum case ($n_S \to \infty$). Even if appealing, it must be stressed that this approach is not mathematically accurate since it disregards important issues connected to convergence and well definiteness. Also, for this line of reasoning to hold, the level of discretization of the controller must be kept constant while increasing the discretization of the model. As a simple example, consider the feedforward controller (15). Different levels of discretization, in general, imply that the feedforward action does not perfectly match the exact one; that is, $\tau = \hat{G}(\bar{q}) + \hat{K}(\bar{q})$, with $\|\hat{G} - G\| + \|\hat{K} - K\| < \delta$ for some $0 < \delta < \infty$. As a result, a different equilibrium $\hat{\bar{q}}$ is attained, which is close to $\bar{q}$ if δ is small enough compared to the Lipschitz constants of A, K, and G. The robot's configuration converges locally to $\hat{\bar{q}}$ if a version of (22) centered around the new equilibrium is verified. This analysis becomes more and more complex as soon as nontrivial feedback actions are involved [72], [135].

On the other hand, even if it requires an arguably substantially more complex formalism, altogether avoiding state-space discretizations can have two major benefits. First, it is the only way to exclude that the controller will generate control spillover [S17], [S18]. This is a degradation of performance that can eventually bring instability due to the excitation of high-order and otherwise stable dynamics operated by controllers designed using finite-dimensional approximations. Second, infinite-dimensional analysis can result in more compact and interpretable solutions compared to the ones based on high-dimensional ordinary differential equations. However, the classic theory of partial differential equation (PDE) control has been mostly focused on linear systems [S19], [S20], [S21], with extensions to the fully nonlinear case being a topic that is currently actively researched [S22], [S23]. Consequently, the large majority of applications of PDE control to continuum mechanics [S24, Secs. 4 and 5] deal with systems that, for our goals, could be considered a small displacement approximation of the nonlinear rod dynamics [S25]: Euler-Bernoulli and Timoshenko-Ehrenfest beams. These theories study continuum elements undergoing small planar deformations as a result of an external load. Under these assumptions, their configuration is described as displacement from a neutral configuration, and their dynamics are described by linear PDEs. The suppression of vibrations in a Euler-Bernoulli beam subject to boundary actuation can be achieved using local linear feedback [S26], [S27]. This strategy can be extended to simultaneously verifying constraints in the output by means of barrier Lyapunov function theory [S28] and to deal with disturbances and input constraints using adaptive iterative learning control [S29]. Similarly, linear damping injection can be used to absorb vibrations in a Timoshenko beam subject to boundary [S30] and point-wise [S31] actuation. Damping injection can be combined with energy shaping for configuration control [S32]. The contact force regulation of a Timoshenko actuated at the base is discussed in [S33], under the hypothesis that the environment provides dissipative damping forces.

Even if the vast majority of works deal with linear beam models, attention has also been devoted to nonlinear cases. In [S34], a numerical approximation of an optimal passivity-based control is used to stabilize a Euler-Bernoulli beam undergoing deformations comparable to the ones of a soft robot. A practically stable boundary regulator for a nonlinear Timoshenko beam with large deformations is proposed in [S35]. A boundary feedback control was proposed in [S36] for a beam undergoing large deflections and rotations as well as small strains, relying on the fact that this system can be mapped to a 1D first-order semilinear hyperbolic system. Moving a further step toward the soft robot case are works dealing with Kirchhoff rods: [S37] discusses the open-loop stability

where $h(s, q) \in \mathbb{R}^6$ is the map, called forward kinematics, connecting the configuration $q(t)$ to the posture $x(s, t)$ for each point s along the backbone. The matrix-valued function J is the Jacobian of h. The following set of ODEs can be directly derived from (1) via standard Lagrangian mechanics machinery:

$$\underbrace{M(q)\ddot{q} + C(q, \dot{q})\dot{q} + G(q)}_{\text{Multibody dynamics}} + \underbrace{D(q)\dot{q} + K(q)}_{\text{Elastic and dissipative forces}} = \underbrace{A(q)\tau}_{\text{Model of underactuation}} \tag{2}$$

where $(q, \dot{q})$ forms the robot state.

The inertia matrix $M(q) \in \mathbb{R}^{n\times n}$ is evaluated as

$$M(q) = \int_0^1 J^\top(q, s)\begin{bmatrix} m(s)I & 0 \\ 0 & \mathcal{J}(s) \end{bmatrix} J(q, s)\, \mathrm{d}s \succ 0 \tag{3}$$

where $m(s)$ and $\mathcal{J}(s)$ are the mass and inertia distributions, respectively. Note that $M(q)$ may become singular in some configurations. However, this can always be avoided by properly parameterizing the configurations space. As for a rigid robot, the inertia matrix verifies

$$\| M(q) \| \leq c_{\mathrm{m}} + c'_{\mathrm{m}} \| q \|^2 \tag{4}$$

of some configurations, [S38] proposes a purely experimental validation of a kinematic controller, and [S39] proposes a quasi-static manipulation strategy for soft objects by proving that the set of equilibria corresponding to changes in boundary position and orientation constraints is a smooth manifold parameterizable with a single chart. Finally, [S40] and [S41] use energy shaping and damping injection for posture regulation of soft robots modeled through Cosserat theory and with infinite-dimensional input space. Convergence is discussed under finite-element approximation.

REFERENCES

[S15] J. Baker and P. D. Christofides, "Finite-dimensional approximation and control of non-linear parabolic PDe systems," *Int. J. Contr.*, vol. 73, no. 5, pp. 439–456, Nov. 2010, doi: 10.1080/002071700219614.

[S16] B. L. Jones and E. C. Kerrigan, "When is the discretization of a spatially distributed system good enough for control?" *Automatica*, vol. 46, no. 9, pp. 1462–1468, Sep. 2010, doi: 10.1016/j.automatica.2010.06.001.

[S17] M. J. Balas, "Modal control of certain flexible dynamic systems," *SIAM J. Contr. Optim.*, vol. 16, no. 3, pp. 450–462, 1978, doi: 10.1137/0316030.

[S18] M. Balas, "Feedback control of flexible systems," *IEEE Trans. Autom. Control*, vol. 23, no. 4, pp. 673–679, Aug. 1978, doi: 10.1109/TAC.1978.1101798.

[S19] R. Datko, "Extending a theorem of A. M. Liapunov to Hilbert space," *J. Math. Anal. Appl.*, vol. 32, no. 3, pp. 610–616, Dec. 1970, doi: 10.1016/0022-247X(70)90283-0.

[S20] A. Pazy, *Semigroups of Linear Operators and Applications to Partial Differential Equations*, vol. 44. New York, NY, USA: Springer Science & Business Media, 2012.

[S21] P. Apkarian and D. Noll, "Structured H^∞-control of infinite-dimensional systems," *Int. J. Robust Nonlinear Contr.*, vol. 28, no. 9, pp. 3212–3238, Mar. 2018, doi: 10.1002/rnc.4073.

[S22] A. Mironchenko and C. Prieur, "Input-to-state stability of infinite-dimensional systems: Recent results and open questions," *SIAM Rev.*, vol. 62, no. 3, pp. 529–614, Aug. 2020, doi: 10.1137/19M1291248.

[S23] R. Rashad, F. Califano, A. J. van der Schaft, and S. Stramigioli, "Twenty years of distributed port-Hamiltonian systems: A literature review," *IMA J. Math. Contr. Inf.*, vol. 37, no. 4, pp. 1400–1422, Mar. 2020, doi: 10.1093/imamci/dnaa018.

[S24] Z.-H. Luo, B.-Z. Guo, and Ö. Morgül, *Stability and Stabilization of Infinite Dimensional Systems With Applications*. London, U.K.: Springer Science & Business Media, 2012.

[S25] S. Timoshenko, *History of Strength of Materials: With a Brief account of the History of Theory of Elasticity and Theory of Structures*. North Chelmsford, MA, USA: Courier Corporation, 1983.

[S26] G. Chen, S. G. Krantz, D. W. Ma, C. E. Wayne, and H. H. West, "The Euler-Bernoulli beam equation with boundary energy dissipation," in *Operator Methods for Optimal Control Problems*. New York, NY, USA: Marcel-Dekker, 1987, pp. 67–96.

[S27] O. Morgul, "Dynamic boundary control of a Euler-Bernoulli beam," *IEEE Trans. Autom. Control*, vol. 37, no. 5, pp. 639–642, May 1992, doi: 10.1109/9.135504.

[S28] W. He and S. S. Ge, "Vibration control of a flexible beam with output constraint," *IEEE Trans. Ind. Electron.*, vol. 62, no. 8, pp. 5023–5030, Aug. 2015, doi: 10.1109/TIE.2015.2400427.

[S29] W. He, T. Meng, D. Huang, and X. Li, "Adaptive boundary iterative learning control for an Euler–Bernoulli beam system with input constraint," *IEEE Trans. Neural Netw. Learn. Syst.*, vol. 29, no. 5, pp. 1539–1549, May 2018, doi: 10.1109/TNNLS.2017.2673865.

[S30] J. U. Kim and Y. Renardy, "Boundary control of the Timoshenko beam," *SIAM J. Contr. Optim.*, vol. 25, no. 6, pp. 1417–1429, 1987, doi: 10.1137/0325078.

[S31] G.-Q. Xu and S. P. Yung, "Stabilization of Timoshenko beam by means of pointwise controls," *ESAIM, Contr., Optim. Calculus Variations*, vol. 9, pp. 579–600, Aug. 2003, doi: 10.1051/cocv:2003028.

[S32] A. Macchelli and C. Melchiorri, "Modeling and control of the Timoshenko beam. The distributed port Hamiltonian approach," *SIAM J. Contr. Optim.*, vol. 43, no. 2, pp. 743–767, 2004, doi: 10.1137/S0363012903429530.

[S33] T. Endo, M. Sasaki, F. Matsuno, and Y. Jia, "Contact-force control of a flexible Timoshenko arm in rigid/soft environment," *IEEE Trans. Autom. Control*, vol. 62, no. 5, pp. 2546–2553, Jan. 2016, doi: 10.1109/TAC.2016.2599434.

[S34] G. Nishida, K. Yamaguchi, and N. Sakamoto, "Optimality of passivity-based controls for distributed port-Hamiltonian systems," *IFAC Proc. Vol.*, vol. 46, no. 23, pp. 146–151, 2013, doi: 10.3182/20130904-3-FR-2041.00193.

[S35] K. D. Do, "Stabilization of exact nonlinear Timoshenko beams in space by boundary feedback," *J. Sound Vib.*, vol. 422, pp. 278–299, Mar. 2018, doi: 10.1016/j.jsv.2018.02.005.

[S36] C. Rodriguez and G. Leugering, "Boundary feedback stabilization for the intrinsic geometrically exact beam model," *SIAM J. Contr. Optim.*, vol. 58, no. 6, pp. 3533–3558, 2020, doi: 10.1137/20M1340010.

[S37] A. Majumdar and A. Goriely, "Static and dynamic stability results for a class of three-dimensional configurations of Kirchhoff elastic rods," *Phys. D, Nonlinear Phenomena*, vol. 253, pp. 91–101, Jun. 2013, doi: 10.1016/j.physd.2013.03.003.

[S38] L. B. Kratchman, T. L. Bruns, J. J. Abbott, and R. J. Webster, "Guiding elastic rods with a robot-manipulated magnet for medical applications," *IEEE Trans. Robot.*, vol. 33, no. 1, pp. 227–233, Feb. 2017, doi: 10.1109/TRO.2016.2623339.

[S39] T. Bretl and Z. McCarthy, "Quasi-static manipulation of a Kirchhoff elastic rod based on a geometric analysis of equilibrium configurations," *Int. J. Robot. Res.*, vol. 33, no. 1, pp. 48–68, 2014, doi: 10.1177/0278364912473169.

[S40] H.-S. Chang et al., "Controlling a cyberoctopus soft arm with muscle-like actuation," 2020, *arXiv:2010.03368*.

[S41] H.-S. Chang et al., "Energy shaping control of a cyberoctopus soft arm," in *Proc. 59th IEEE Conf. Decis. Contr. (CDC)*, 2020, pp. 3913–3920, doi: 10.1109/CDC42340.2020.9304408.

where c_m, c'_m are two positive scalars. If the elongation is considered negligible, then $c'_m = 0$. Coriolis and centrifugal forces $C(q, \dot{q})\dot{q} \in \mathbb{R}^n$ can be evaluated using the standard mathematical machinery (for example, Christoffel symbols). Elastic $K(q) \in \mathbb{R}^n$ and gravitational $G(q) \in \mathbb{R}^n$ actions are defined as

$$K(q) = \frac{\partial U_K}{\partial q}, \quad G(q) = \frac{\partial U_G}{\partial q} \tag{5}$$

where the scalar-valued functions U_K and U_G are the associated potential energies. They are obtained as integration along the spatial coordinate of the energetic contributions of each infinitesimal elements. The elastic force field is usually positive definite, and thus the stiffness matrix

$$\frac{\partial K(q)}{\partial q} \succ 0. \tag{6}$$

In some cases (for example, floating base and hybrid rigid-soft), this matrix may be positive semidefinite instead. Gravitational forces are bounded as

$$\| G(q) \| \leq c_g + c'_g \| q \| \tag{7}$$

where c_g, c'_g are two positive scalars, with the latter being equal to zero if no elongation is present. The friction losses are usually modeled as a possibly nonlinear damping action $D(q)\dot{q}$, with $D \succ 0$. The input field $A(q) \in \mathbb{R}^{n \times m}$ is the transpose of the Jacobian mapping the $m \leq n$ actuation forces from their point of application to the configuration space. Indeed, control actions are often not directly colocated on the states [35]. Without loss of generality, assume A to be full-rank columns. Some representative examples of actuation matrices are provided in Figure 3.

Piecewise Constant Strain Approximations

This family of discretization methods works by assuming that the strain ξ is piecewise constant in s, with discontinuities happening at fixed points along the rod, called nodes. Figure 1(b) gives an example of one such a model. The most straightforward implementation of this principle is planar PCC models. Here, all strains but one curvature

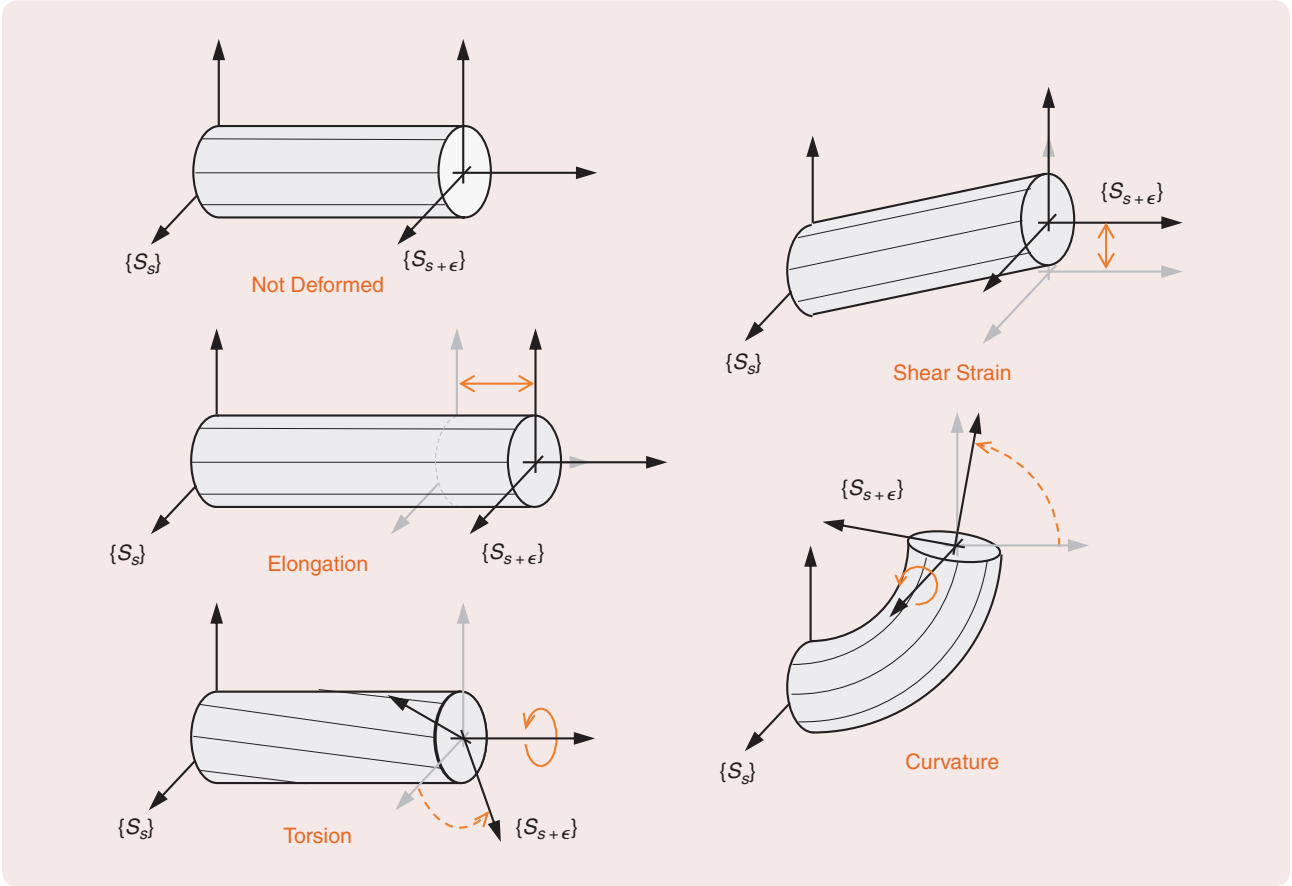

FIGURE 2 The six pure strains corresponding to a $\xi(s) \in \mathbb{R}^6$ with all elements but one equal to zero. Each one is associated with either a pure translation or rotation along with one of the three local axes of the reference frame S_s. Infinitesimal translations are referred to as elongation when occurring along the axis tangent to the backbone and as shear strain if happening along with the directions orthogonal to the backbone (only one is shown). Similarly, infinitesimal rotations are referred to as torsion when happening along the axis tangent to the backbone and as curvature if occurring in the direction of the two orthogonal directions (only one is shown).

are neglected. The curvature itself is assumed to be piecewise constant. The resulting shape is a sequence of arcs connected in such a way that x is everywhere differentiable, as shown in Figure 1. The vector $q \in \mathbb{R}^n$ collecting all the local curvatures (one per CC segment) is the finite-dimensional configuration of a PCC robot. Thus, a PCC robot has as many degrees of freedom n as the number of considered segments n_S. Soft robots under PCC approximation can be seen as a direct extension of serial manipulators with revolute joints to the continuum domain. Instead of being localized to one point (the joint), the change in angle here is homogeneously distributed along the segment. Note, indeed, that the curvature is equivalent to the angle subtended by the CC arc—also called the bending angle—since it is defined with respect to a normalized arc length. The kinematics and dynamics of a single CC segment are analyzed in "Dynamics of a Constant Curvature Segment."

The kinematic description (1) of PCC robots has been intensively used for more than a decade in continuum robotics, as proved by the seminal review article [36], published in 2010. The simplicity of the kinematics has played a major role in fostering this success, together with the effectiveness in describing real systems. Note, indeed, that a PCC is the exact steady-state solution of the infinite-dimensional model when only pure torques are applied

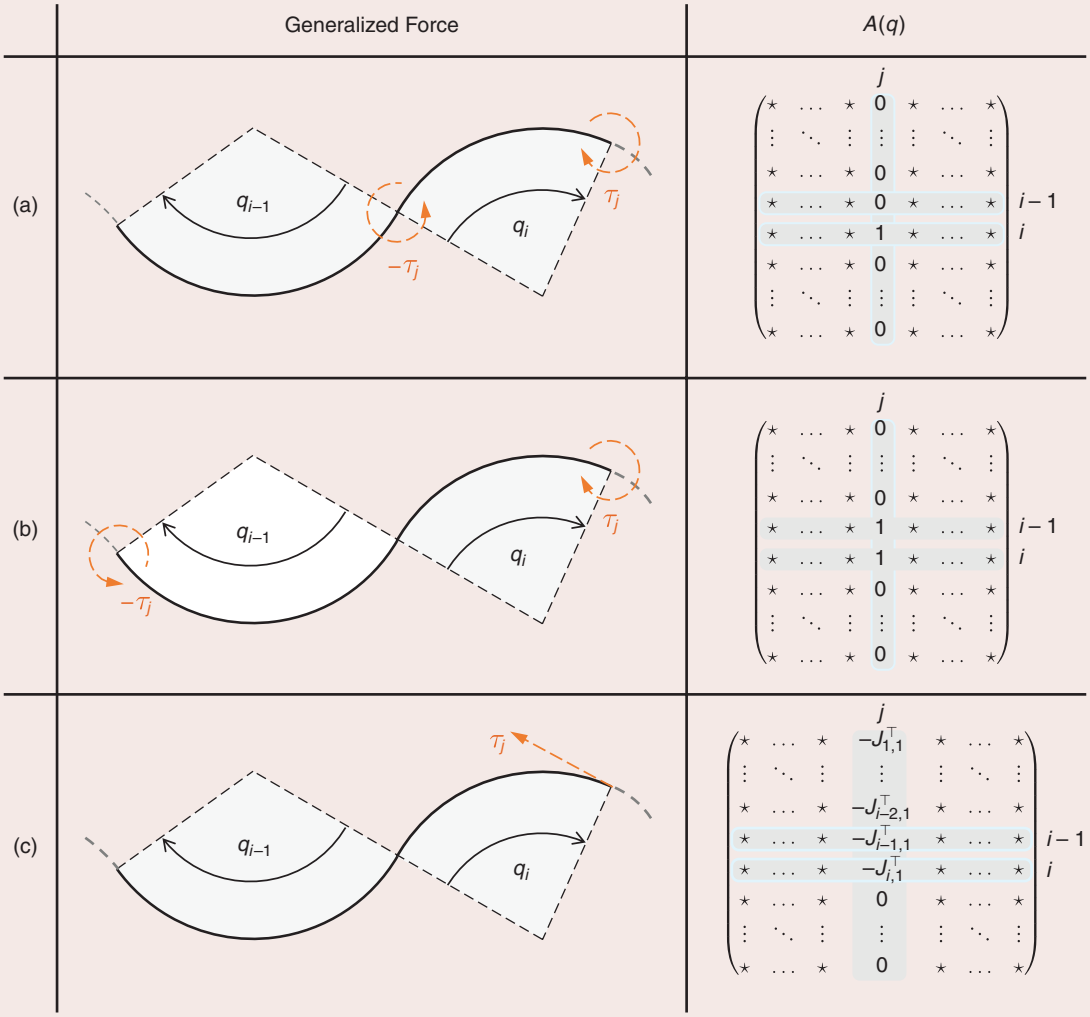

FIGURE 3 Actuation patterns resulting in different elements of the matrix $A(q)$. The examples are focused on how a generalized force τ_j that is applied to the ith segment is mapped in the configuration space. CC discretization is used for illustrative purposes. One actuated segment is represented with one or two CC segments: (a) coarse internal discretization and (b) finer internal discretization. The actuator produces an internal pair of opposite torques. This is the case of a pair of pressurized chambers and of a tendon-driven system with motors placed at the base of the segment. (c) τ_j is a force applied tangentially to the tip of the ith segment. Here, $J_{k,1}$ is the kth element of the Jacobian mapping $\dot{q}$ in the first linear velocity of the tip of segment i.

Dynamics of a Constant Curvature Segment

The goal of this sidebar is to help a novice in soft robotics become familiar with the topic by concisely presenting the derivation of the main ingredients of what is arguably the simplest soft robot: a constant curvature (CC) segment. Regardless of its simplicity, this case already allows for many intuitions that can be directly transferred to more complex and general cases. Consider a single planar segment, as in Figure S1, which is an arc with fixed length L and curvature possibly varying in time. The scalar curvature $q \in \mathbb{R}$ is sufficient to describe its full configuration. Note that since the curvature is defined here with respect to the normalized arc length, q is the angle subtended by the arc, which is also called the bending angle. The two concepts are used interchangeably in this article. As a comparison, Figure S1 also reports the noncontinuum element of which a CC segment can be considered the direct extension: a revolute joint connecting two rigid links of length $L/2$. This can be seen as a rigid link lumped approximation of the CC segment.

The shape $x(s, t)$ of the soft robot can be expressed by collecting the position and orientation of all the reference frames S_s connected to the coordinate $s \in [0, 1]$. These quantities can be retrieved via simple geometrical arguments, as visually illustrated by Figure S1. The result is

$$x(s,t) = h(s, q(t)) = L\begin{bmatrix} \dfrac{\sin sq(t)}{q(t)} & \dfrac{1-\cos sq(t)}{q(t)} & \dfrac{s}{L}q(t) \end{bmatrix}^\top. \quad \text{(S1)}$$

Thus, q can also be defined as the angle between the base frame and tip frame. Note that $x(s, t)$ has no singularity point since its limit in the straight configuration ($q = 0$) is well defined and equal to $[L\ 0\ 0]^\top$. However, the division by zero can generate numerical instabilities in practice. Figure S2 compares how the shape of a CC segment changes compared to that of its lumped discrete approximation. The two models get progressively more different with the increase of $|q|$, with one reason being that the length arc to which both links of the rigid model are tangent shrinks by a factor $(q/2)\cot(q/2)$.

According to (1), the Jacobian matrix mapping the time derivative of the curvature $\dot{q}(t) \in \mathbb{R}$ to $\dot{x}(s,t) \in \mathbb{R}^3$ is

$$J(s,q) = L\begin{bmatrix} \dfrac{sq\cos(sq) - \sin(sq)}{q^2} \\ \dfrac{(\cos(sq)-1) + sq\sin(sq)}{q^2} \\ \dfrac{s}{L} \end{bmatrix}^\top. \quad \text{(S2)}$$

This kinematic description is sufficient to express the inertia according to (3). If a uniform distribution of mass [$m(s) = m$] and a very thin rod ($\mathcal{J} \simeq 0$) are assumed, then the configuration-dependent inertia is

$$M(q) = \frac{mL^2}{20}\underbrace{\left(\frac{20}{3}\frac{q^3 + 6q - 12\sin(q) + 6q\cos(q)}{q^5}\right)}_{\lim_{q\to 0} * = 1} > 0. \quad \text{(S3)}$$

Note that similar closed-form solutions for M can be found for different mass distributions and nonnull inertia. These assumptions are introduced here for the sake of conciseness. Figure S3 shows a plot of $M(q)$ for all the curvatures in $[-2\pi, 2\pi]$. The inertia decreases with the increase of $|q|$, following a bell curve that

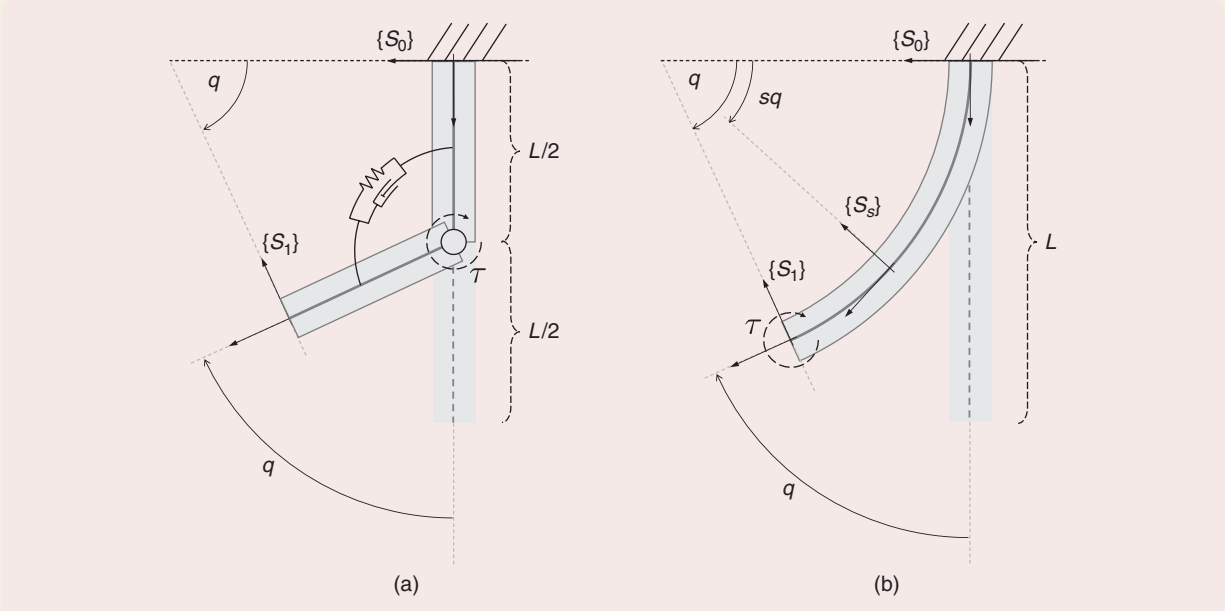

FIGURE S1 A CC segment together with a lumped rigid link model serving as its first-order approximation. The two resulting dynamics have equivalent structural properties but are described by substantially different dynamic equations. (a) R-PEA. (b) CC segment.

goes to zero when $|q| \to \infty$. This is because changes in q are reflected in progressively smaller changes in the shape of the soft robot when the curvature is larger; that is, $\|x(s, q+\delta_q) - x(s, q)\|_2^2$ decreases with the increase of $|q|$ for all fixed $\delta_q > 0$. It is also worth noticing that the inertia of the lumped model with a homogeneous distribution of mass is $(m/2)(L/2)^2/3 = mL^2/24$, which is smaller than $M(0)$ despite the two systems being perfectly superimposed in the straight configuration. This can be explained by considering that the rigid model neglects the motion of the lower half of the robot, so an actuation torque sees only the inertia produced by half of the robot's body.

Since M is not constant, this formulation of the CC segment dynamics is affected by the following centrifugal force:

$$C(q, \dot{q})\dot{q} = \frac{1}{2}\frac{\mathrm{d}M}{\mathrm{d}t}\dot{q} = -\frac{mL^2}{3}\frac{12q - 30\sin(q) + 3q^2\sin(q) + 18q\cos(q) + q^3}{q^6}\dot{q}^2. \tag{S4}$$

Note that we could evaluate C by direct differentiation of M since both are scalar. Figure S3 reports the evolution of this force when q changes. As expected from a centrifugal action, $-C(q, \dot{q})\dot{q}$ tends to increase with $|q|$ for all $\dot{q} \neq 0$.

Consider the base of the robot being oriented with a generic angle ϕ with respect to a gravity acceleration of intensity g. The gravity potential can be calculated by summing the contributions of each infinitesimal element:

$$U_G(q, \phi) = \underbrace{\int_0^1 mg(x(s,0) - x(s,q))^\top \begin{bmatrix}\cos(\phi)\\ \sin(\phi)\\ 0\end{bmatrix} \mathrm{d}s}_{\text{Infinitesimal contribution of element } s} \tag{S5}$$

which is the variation of the center of mass location with respect to the straight configuration, projected to the direction of the gravity acceleration and multiplied for mg. According to (5), direct differentiation of the associated potential yields the gravitational torque

$$G(q, \phi) = -mg\left(\int_0^1 J(s, q)\mathrm{d}s\right)^\top \begin{bmatrix}\cos(\phi)\\ \sin(\phi)\\ 0\end{bmatrix} = -mgL\left(2\frac{\cos(q-\phi) - \cos(\phi)}{q^3} + \frac{\sin(q-\phi) - \sin(\phi)}{q^2}\right). \tag{S6}$$

Figure S3 depicts the case of $\phi = 0$, corresponding to a gravity field aligned with the straight configuration of the robot (pointing downward in Figure S2). Two relevant symmetries that may help with thinking about how G changes with ϕ are $G(q, \phi) = -G(q, \phi + \pi)$ and $G(q, \phi) = -G(-q, -\phi)$. The flexural rigidity can be modeled as a torque proportional to the local bending of the robot, which is the curvature q. Thus, the elastic force is

$$K(q) = \frac{\partial}{\partial q}\overbrace{\int_0^1 \underbrace{\frac{1}{2}k(s)\,q^2}_{\text{Infinitesimal contribution}}\mathrm{d}s}^{U_K(q)} = \underbrace{\left(\int_0^1 k(s)\,\mathrm{d}s\right)}_{\text{Average stiffness}} q \tag{S7}$$

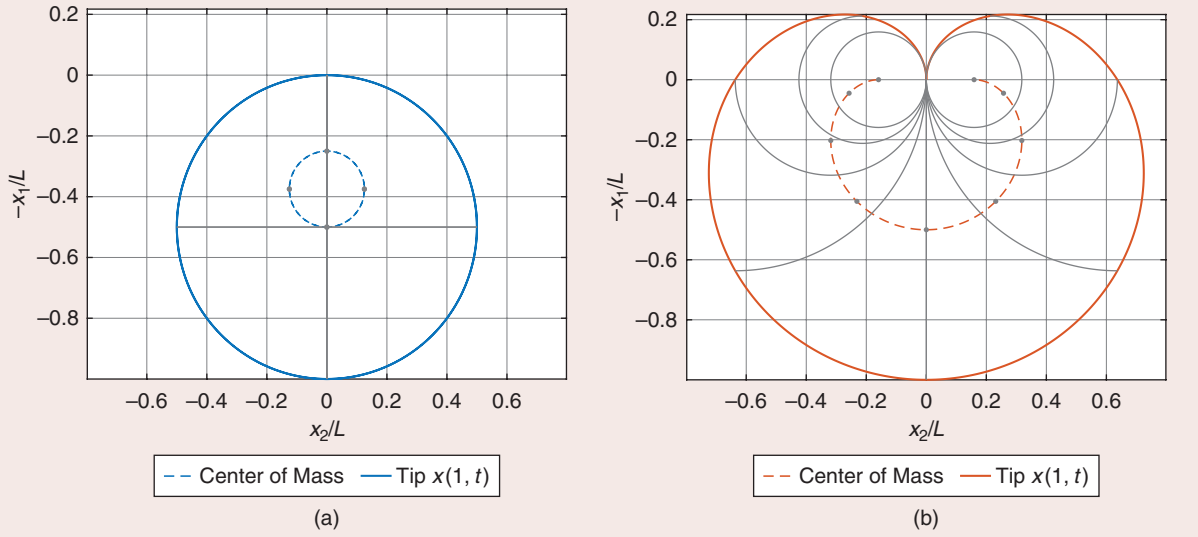

FIGURE S2 The geometrical characterization of (a) a rigid robot with a single revolute joint and (b) a CC robot. The behaviors are similar to the straight configuration, but they strongly depart from one another when the angle $|q|$ increases. The configurations corresponding to $q \in \{-2\pi, -3\pi/2, \ldots, 3\pi/2, 2\pi\}$ are shown with thin gray lines. The corresponding centers of mass are also reported as gray dots. Note that this range of angles corresponds to two full rotations for the rigid links case.

(*Continued*)

Dynamics of a Constant Curvature Segment (*Continued*)

where $k(s) \in \mathbb{R}$ is the local stiffness in s, which is assumed to be almost constant for the CC assumption to hold. Similarly, the damping torque can be evaluated by assuming local dissipation proportional to the variation of curvature. The torque then needs to be mapped in q, leveraging the kinetostatic duality:

$$D(q)\dot{q} = \int_0^1 \underbrace{J(s,q)^\top \begin{bmatrix} 0 \\ 0 \\ d(s)\dot{q} \end{bmatrix}}_{\text{Infinitesimal contribution}} \mathrm{d}s = \underbrace{\left(\int_0^1 s\, d(s)\, \mathrm{d}s\right)}_{\text{Equivalent damping}} q \tag{S8}$$

where $d(s) \in \mathbb{R}$ is the local damping in s. Thus, both the elastic and damping forces are linear under the discussed assumptions. Equivalent results are also obtained when infinitesimal springs and dampers proportional to the elongation are assumed to be distributed along the thickness of the robot [48]. Finally, consider the robot to be actuated with a pure torque applied at the tip, resulting in

$$A(q)\tau = J(1,q)^\top \begin{bmatrix} 0 \\ 0 \\ \tau \end{bmatrix} = \tau. \tag{S9}$$

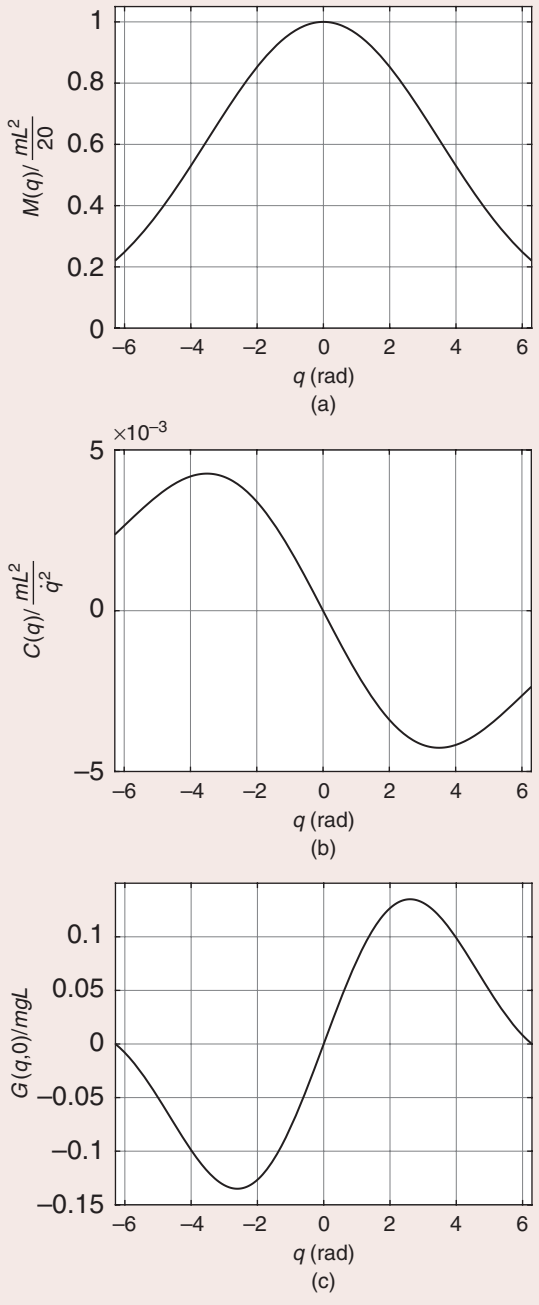

FIGURE S3 The evolutions of (a) (S3), (b) (S4), and (c) (S6), all normalized with respect to the quantities that appear linearly in their expression. A change in those quantities results in a linear scaling of the plots along the vertical axis.

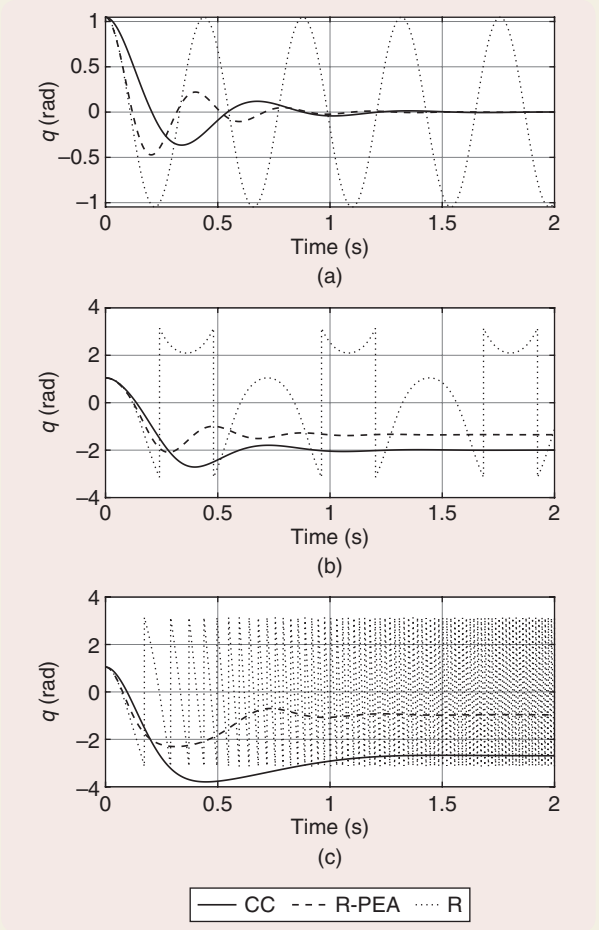

FIGURE S4 The evolution of a CC segment and its lumped rigid link approximation with parallel springs (R-PEA) and without parallel springs (R). The CC dynamics are described by (S3)–(S9). The parameters considered here are $m = 0.5\,\mathrm{Kg}$, $L = 0.25\,\mathrm{m}$, $\int_0^1 k = 0.05\,\mathrm{N\cdot m}$, $\int_0^1 sd = 0.01\,\mathrm{N\cdot ms}$, and $(q(0), \dot{q}(0)) = (\pi/3, 0)$. The three plots show the evolutions for (τ, ϕ) equal to (a) $(0\,\mathrm{N\cdot m}, 0)$, (b) $(-0.3\,\mathrm{N\cdot m}, 0)$, and (c) $(0\,\mathrm{N\cdot m}, -\pi/2)$. In all the three cases, CC and R-PEA are qualitatively similar and both different from R.

(*Continued*)

Dynamics of a Constant Curvature Segment (*Continued*)

Equations (S3)–(S9) can be combined using (2), yielding a scalar second-order dynamic for q that has the same structure and structural properties of a lumped joint model with parallel impedance but with different and more complex expressions. Examples of the resulting evolutions are shown in Figure S4.

along the structure of a homogeneous planar soft element. When moving to a 3D space, the geometrical characterization of a PCC robot as a sequence of arcs remains unvaried, but the plane of bending can change. This effectively introduces two degrees of freedom per segment; that is, $n = 2n_S$. The usual way in which this motion is represented in the literature is by including in q the orientation of the n relative orientations of the planes of bending. Although intuitive, this representation introduces singularities and discontinuities [37], which can be avoided with alternative parameterizations [38], [39], [40], [41]. Occasionally, piecewise constant elongation is also considered, with discontinuity points coincident to the curvature ones, thus leading to $n = 2n_S$ for the planar case and $n = 3n_S$ for the 3D one. An extension of the PCC framework to include deformable cross sections is proposed in [42].

As discussed for the general case, the dynamic model (2) of a PCC robot is obtained by combining (1) with the physical characteristics of the system through standard Lagrangian formalism [43]. Yet, deriving closed-form expressions of M and G is unpractical when considering multiple segments without relying on recursive formulations. Approximations of the mass distribution are thus often imposed to simplify the model derivations. Models having the mass of each segment lumped into a single point along the rod are discussed in [44] and [45]. Alternatively, a lumped mass and inertia can be placed at the center of mass [46], [47], therefore neglecting only the change in rotational inertia. Under this hypothesis, the soft robot can be represented through an augmented rigid robot model, therefore enabling the use of standard tools for calculating the expression of dynamic forces [48], [49].

A simpler alternative to PCC that can be used to model robots bending and elongating are rigid link approximations [50], [51]. The rod here is approximated through a sequence of links connected with standard independent joints. This is equivalent to considering a ξ that is null everywhere except for a finite set of points where it assumes the value of a Dirac's delta. Lumped springs are added in parallel to each joint to describe the robot's impedance. The resulting structure is a standard rigid robot with parallel elasticity, and it is therefore described by a set of ODEs as (2). Kinematic models of parallel soft manipulators based on these strategies are discussed in [52], [53], and [54].

PCC models can be extended further by also adding piecewise constant shear deformation and twist. This is done by the piecewise constant strain models proposed in [55] and [56], which define procedures for extracting models in the form of (2), where $q \in \mathbb{R}^{6n_s}$. The inertia matrix $M(q)$ implements a full dynamic coupling within the six strains. On the contrary, the elastic part of the potential forces $K(q)$ is usually either diagonal or block diagonal. Thanks to their capability of describing complex strain conditions naturally arising in closed kinematic chains, these models can be used to describe soft parallel structures [57].

How Fine Should the Discretization Be?

For a given soft robot to be modeled under a piecewise constant strain approximation, the number of segments n_s to be considered is up to the designer of the model to decide as a result of application-specific considerations. First, the mechanics of the robot impose a lower bound in case the robot is obtained as a sequence of actuated modules since considering fewer than one constant strain segment for each actuated one would generate incoherent behaviors (for example, actuating one segment would result in a motion in the following one). Also, it is, in general, inconvenient to have constant strain segments shared among more than one actuated segment. If the robot is used for simulation, then a tradeoff between accuracy and simplicity must be established. For $n_s \to \infty$, the model converges to the exact continuum representation, but the computational cost for the simulation will increase as $O(n_s^2)$ at best [58]. In case the model is used for control design, then the number and the location of the segments may change the structural properties of (2). It is common to place segments in such a way that the resulting model is fully actuated; that is, $A(q)$ is square and full rank. For planar PCC models, if τ are torques applied at the tip of each CC segment, then $A(q) = I$, therefore further strengthening the parallelism with standard serial rigid robots. Most of existing actuation technologies will satisfy this hypothesis (for example, tendons and fluids).

Functional Parameterizations

Instead of discretizing along the arc length, the finite-dimensional parameterization can happen by projecting onto a low-dimensional functional subspace. In the case of strain parameterizations, this is done as follows:

$$\xi(s,t) = \sum_{i=1}^{n} \pi_i(s) q_i(t) \tag{8}$$

where $\{\pi_1(s), \ldots, \pi_n(s)\}$ is a base of the subspace and the weights $q_i(t)$ can be taken as the configuration of the robot.

One simple way of selecting $\pi_i : [0, 1] \to \mathbb{R}^6$ is to truncate an infinite-dimensional basis of a regular enough functional space. This choice ensures that the approximation converges to the exact model for $n \to \infty$. It is also convenient to include constant functions so that the model is a proper extension of the CC or constant strain one. For example, in the case of inextensible planar soft robots (that is, ξ contains only the curvature), polynomials $\pi_i(s) = s^{i-1}$ are a basis that satisfies both conditions.

Functional parameterizations are widely used in modeling flexible link robots [59] to represent infinitesimal vibrations of the link from its nominal configuration and not strains. In this context, the base functions $\pi_i(s)$ are usually selected as the n slowest modes of the Euler-Bernoulli beam modeling the link [60], [61]. Early works in hyperredundant robotics [62] pioneered the application of functional expansion to the large deformations of rod-like structures that are now being proposed for soft robotics. The latter include projections in polynomial spaces [63], [64] and on a base derived as the truncated Taylor expansion of the forward kinematics [65], [66]. This strategy is also investigated in [67], [68], and [69] when modeling deformable objects. Functional expansions are also used in continuum mechanics to approximate the equilibria of rods and beams [70], [71]. Note that, contrary to (8), all these works focus on functional expansions of the shape expressed as the Cartesian configurations $x(\cdot, t)$.

The use of the strain-level expansions (8) is a more recent result. The dynamics of planar soft robots with polynomial curvature are discussed in [72] and [73]. A general formulation for a generic choice of π_i is proposed in [31] and [74], and its application to parallel structures is discussed in [75]. Note that this framework naturally includes rigid link and piecewise constant strain approximations when considering Dirac's deltas and rectangular functions as π_i. No matter the choice of π_i, the robot's dynamics can still be formulated as (2). However, a full dynamic and potential coupling among all the degrees of freedom exists in general, even when relying on a strain-based parameterization.

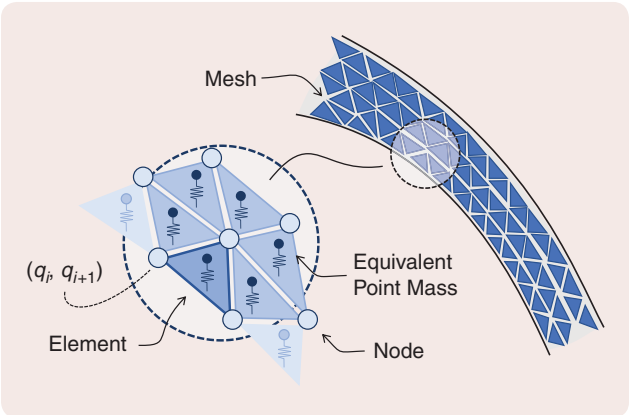

FIGURE 4 The dynamics of the planar portion of a soft robot are approximated using FEMs as a network interconnection of triangular elements. A mesh defines the topology of this interconnection. The mechanical properties (stiffness, damping, and mass) are computed on elements based on the constitutive law of the material. These properties are then assembled in large vectors and sparse matrices, using the connectivity of the mesh. The configuration q of the robot is defined as the collection of the Cartesian positions of the mesh nodes. Dissipative elements are not shown for the sake of space.

Volumetric Models

Despite also applying to the discretization of rods, finite-element models (FEMs) are the way to go when it comes to modeling nonslender robots. In FEMs (also called finite-element methods) of deformable solids [76], the geometric shape is described by identifying a mesh, which is a set of nodes together with the information about neighboring nodes (Figure 4). If the position of the nodes is known, an approximation of the entire volume results from interpolation. FEM is, therefore, the preferred solution whenever the changes in the 3D structure of the robot are not negligible compared to the structure's virtual backbone. In their general definition, FEMs are formulated as ways of approximating solutions of PDEs. Thus, FEMs can be used to discretize rod models of soft robots [56]. Furthermore, this framework naturally extends to modeling systems encompassing multiple continuous behaviors, for example, magnetic, thermal, and fluid [77].

The discussed space interpolation naturally leads to a kinematic description in the form of (1). The configuration $q \in \mathbb{R}^n$ is the collection of the nodes' location in the space. So, n is, in general, three times the number of nodes. Since the full volume is explicitly considered, the forward kinematics $h(s, q)$ are to be parameterized with $s \in \mathbb{R}^3$ rather than a scalar. Similar to rod models, FEMs have the advantageous property of converging to the exact model when n tends to infinity. Using several thousand nodes, in general, produces a very accurate model at the cost of a quite large configuration space. Note, however, that measuring and observing the whole state of a FEM model are not always needed when implementing closed-loop controls. Dynamic equations in the form of (2) result from the application of Lagrangian machinery to (1) in a similar fashion as the rod case. The discretizations in strain space ξ discussed in the previous sections usually result in a linear $K(q)$ and constant $D(q)$ at the cost of a configuration-dependent inertia matrix $M(q)$. On the contrary, FEM analysis resulting in the following simplifications is introduced whenever the mass is assumed to be concentrated to the nodes: $\partial M(q)/\partial q = 0$, $C(q, \dot{q}) = 0$, and $\partial G(q)/\partial q = 0$. Thus, the multibody dynamic part of (2) simplifies into $M\ddot{q} + G$. Furthermore, M is sparse if q represents the nodes' configuration in the space. On the downside, $K(q)$ is usually nonlinear, and $D(q)$ and $A(q)$ are rarely constant.

Model Order Reduction

The high-dimensional configuration space of a FEM model can be compressed by selecting a set of $n_\mathrm{r} << n$ directions of interest [78]. In practice, n_r is usually on the order of a few dozens, and thus, $n/n_\mathrm{r} \gtrsim 10^2$. The reduced order configuration is defined as $q_\mathrm{r} = \Phi q$, where, for simplicity, it is assumed that the configuration q is defined such that $q = 0$ is the system equilibrium for $\tau = 0$. This projection is conceptually similar to the functional parameterizations discussed in the preceding for rod dynamics. The resulting dynamics in q_r space are

$$(\Phi^\top M\Phi)\ddot{q}_\mathrm{r} + \Phi^\top G + (\Phi^\top D(\Phi q_\mathrm{r})\Phi)\dot{q}_\mathrm{r} + \Phi^\top K(\Phi q_\mathrm{r}) = \Phi^\top A(\Phi q_\mathrm{r})\tau \tag{9}$$

which is again in the general form of (2). Note that $\Phi^\top M\Phi$ is diagonal if M is diagonal and if Φ is orthogonal. The matrix Φ should be selected in such a way that the solution of (9) is representative of the evolution of (2) for the full FEM model as soon as the initial condition satisfies $(q_\mathrm{r}(0), \dot{q}_\mathrm{r}(0)) = (\Phi q(0), \Phi\dot{q}(0))$. Modal analysis is a well-known tool in FEM theory to achieve this goal [78, Ch. 12]. The linear modes of the linearized system about the equilibrium configuration are calculated. The eigenvectors associated with the smallest eigenvalues (slowest modes) are used to build Φ. The value of n_R can be defined according to the frequency range of vibrations that the designer is interested in capturing. This procedure implicitly operates a regularization of the FEM model, getting rid of many numerical vibrations happening at high frequency, which can be assimilated to numerical noise. Alternatively, the columns of Φ can be evaluated from the singular value decomposition of a dataset of representative evolutions of the system [79]. Following a similar philosophy as the functional expansions discussed for rod models, model order reduction of FEMs can also be extended to nonlinear deformations [80], [81], [82]. Primitives that are intrinsically volume preserving are proposed in [83]. The extension to the modeling of soft robots with self-contact forces is discussed in [84]. One reason for n to reach high values—up to hundreds of thousands—is that the robot geometry has many details (thinned areas, holes, and small grooves). This issue can be tamed through several methods, as, for example, extended FEM [85], [86], which does not radically reduce the size of the models. Condensation is another widely used approach. It operates model reduction by partitioning the configuration space in loaded—directly actuated—and unloaded variables. The loading conditions are modeled as holonomic constraints and solved with Lagrangian multipliers [78], [87], [88]. Condensation has also been used to connect FEM and rod models in [89]. A recent review article on model reduction techniques is also available [90].

Existence of Equilibria

The equilibrium configurations of (2) associated with a control input $\bar{\tau}$ are all the $\bar{q} \in \mathbb{R}^n$ such that

$$K(\bar{q}) + G(\bar{q}) = A(\bar{q})\bar{\tau}. \tag{10}$$

Due to the many nonlinearities involved, the solutions of (10) cannot be expressed in closed form, in general. An exception is when $K + G$ is monotone (for example, high enough stiffness) and the input field A is configuration independent. In this case, the solution of (10) is

$$\bar{q} = (K + G)^{-1}(A\bar{\tau}). \tag{11}$$

A single equilibrium always exists for any choice of actuation. If $K + G$ is not monotone or the actuation field A is configuration dependent, the existence of at least one equilibrium for any given $\bar{\tau}$ is to be expected if $K(q)$ is radially unbounded (that is, the stiffness is not vanishing). Several solutions to this equation may, in general, exist. Consider, for example, the case of $n = 1$ and $c_\mathrm{a}^- < A < c_\mathrm{a}^+$. Thus, if $K(q)$ is radially unbounded and $G(q)$ is limited, then K/A and G/A are also. Thus, $(K + G)/A$ is radially unbounded even if, in general, not monotonic. It is also a continuous function. As a consequence, there is always at least one equilibrium configuration, that is, a configuration $\bar{q}$ that verifies $(K(\bar{q}) + G(\bar{q}))/A(\bar{q}) = \tau$. This sketch of proof is represented by Figure 5. The existence of at least one equilibrium for any constant actuation is in sharp contrast with classic rigid robots, for which a constant actuation can never result in an equilibrium configuration unless gravity is involved.

Actuators Dynamics

A wide variety of strategies can serve as actuation sources for soft robots, including pneumatic actuation, tendon-driven systems, and electroactive materials [1]. Yet, relatively

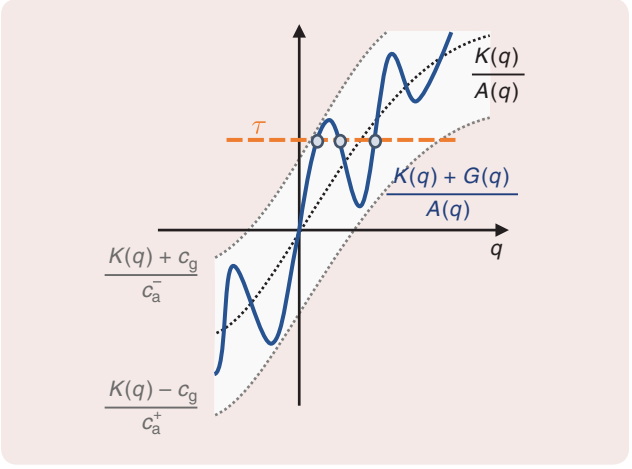

FIGURE 5 In the scalar case, (10) always has at least one solution for unbounded K and bounded A and G. This figure reports a representation of the reasoning behind the proof of this statement.

little attention has been devoted, so far, to incorporating the dynamics of actuators (for example, pistons, valves, and motors) in dynamic models used for control. Nonetheless, we can still provide a model based on similar formulations from classic robotics [91], [92], which holds for actuation strategies where the main function components of the actuators are themselves mechanical (for example, tendons actuated through electric motors and fluids pressurized through pistons):

$$M(q)\ddot{q} + C(q,\dot{q})\dot{q} + D(q)\dot{q} + K(q) + G(q) + \frac{\partial U_c}{\partial q}(q,\eta) = 0 \quad (12)$$

$$B(\eta)\ddot{\eta} + H(\eta,\dot{\eta})\dot{\eta} + \frac{\partial U_c}{\partial \eta}(q,\eta) = \tau \quad (13)$$

where we do not include dissipation in the actuation and transmission systems for the sake of simplicity. Here, (12) is a modified version of (2), thus describing the soft robot's dynamics. Instead of assuming that the control input can be directly exerted on the robot, we introduce (13) governing the actuators' dynamics. The configuration of all the actuators is collected in $\eta \in \mathbb{R}^m$ as, for example, motor angles and piston motions. Here, $B, H \in \mathbb{R}^{m\times m}$ are the associated inertia and Coriolis matrices. The former is usually diagonal and configuration independent, and, in turn, $H = 0$. This is, however, not always the case, an exception being magnetically actuated soft robots with magnets moved by a rigid robot [93]. In this case, η are the joint configurations of the rigid robot.

The coupling between the dynamics (12) and (13) is purely mediated by the potential field U_c, which models elasticity of tendons, molecular interactions in compressible fluids, and electromagnetic fields, just to cite a few. Thus, through this formulation, we render explicit that the control action $\tau \in \mathbb{R}^m$ influences the behavior of the actuators (13), which, in turn, modifies the behavior of the robot (12) via the coupling $\partial U_c / \partial q$.

One way to connect (12) to the original (2) is to consider the case in which the dynamics of η are fast compared to q as well as globally stable. Then, (13) can be approximated by its steady-state behavior $\eta \simeq \bar{\eta}(q,\tau)$. In this case, $-\partial U_c(q,\bar{\eta}(q,\tau))/\partial q$ serves as a generalization of the input field $A(q)\tau$ appearing in (2). Alternatively, singular perturbation theory can be used to separate the fast actuator dynamics from the slow soft robot one without applying quasi-static approximations [94].

Simulators

A bottleneck to entering the field of soft robots control has been the need to implement the simulator of the soft robot. This is especially troublesome when considering that the models used for simulation are typically more sophisticated than the ones used for control. Luckily, several simulators are being developed, of which many are already available as open source projects: SOFA [95], [96], DiffAqua [97], and ChainQueen [98] use velumetric FEM techniques, while Elastica [99], TMTDyn [100], SimSOFT [56], Viper [101], and SoRoSim [102] implement discretizations of rod models. More details on simulators for soft robots can be found in [103, Sec. VII]. Still, selecting the right model among all the available ones is a task with no clear solution. Experimental comparisons, such as the ones provided in [104] and [105], can be a useful tool in this context.

SHAPE CONTROL IN THE FULLY ACTUATED APPROXIMATION

The primary task of control architectures in classic robotics is to accurately manage the posture of the robot, that is, configuration space control. In the case of soft robots, this translates into devising strategies to control the whole shape of the system, that is, controlling q (see "Model-Based Perception of Shape and Forces"). Depending on the model used for control design, this task may translate into different goals—for example, curvature, strain, and volume control—that share a set of characteristics. The importance of carefully selecting the model used for control design therefore becomes apparent. Indeed, applying the same control solution with different models will produce substantially different closed-loop behaviors, both in terms of the transient and steady states. We start in this section with robots that can be effectively modeled as fully actuated; that is, $m = n$, and, without loss of generality, $A(q) = I$. It is shown how this approximation allows for acquiring important insight on the behavior of soft robots.

Posture Regulation

Posture regulation is defined as follows. Given a desired constant configuration $\bar{q} \in \mathbb{R}^n$, find a control action $\tau \in \mathbb{R}^m$ such that the configuration of the soft robot $q \in \mathbb{R}^n$ eventually converges to the desired one; that is,

$$\lim_{t\to\infty} q(t) = \bar{q}. \quad (14)$$

As discussed in the previous section, an equilibrium is always associated to any constant control input, as exemplified by (11). This equilibrium is also asymptotically stable under opportune conditions on the mechanical impedance of the robot. Consider the following purely feedforward controller (see Figure 6):

$$\tau(\bar{q}) = K(\bar{q}) + G(\bar{q}) \quad (15)$$

where K and G are the elastic and gravitational fields with potentials U_K and U_G, respectively, as defined in (5). Substituting (15) in (2) and rearranging terms yields

$$M(q)\ddot{q} + C(q,\dot{q})\dot{q} = \underbrace{(K(\bar{q}) + G(\bar{q})) - (K(q) + G(q))}_{\text{Physical P loop}} + \underbrace{D(q)(-\dot{q})}_{\text{Physical D loop}} \quad (16)$$

Model-Based Perception of Shape and Forces

Despite the many advances in designing and fabricating soft sensors [9], the perception problem remains an open one in soft robotics. The use of models can help connect a finite number of sensor measurements to the virtually infinite degrees of freedom. Yet, for most existing models, there exists no sensor capable of directly measuring the configuration space q. At best, a nonlinear combination of the state variables $h(q)$ can be measured, where h is the forward kinematics of the sensor location. This is the dual to the colocation problem in control. Indeed, retrieving a configuration q compatible with the measurements $\bar{x} = h(q)$ is formally equivalent to the task space regulation (34), and thus, it can be solved by using (35). Alternative kinematic inversion solutions can also be used. For example, constant curvature models admit closed-form inverse kinematics [S42]. Nonlinear constrained optimization is used in [S43] for soft robots with lumped joints. Knowledge of the robot dynamics can also be taken into account when using nonlinear observers, as in the extended Kalman filter [S44], [S45].

The persistence of the potential field $K(q) + G(q)$ connects forces and configurations, especially at the steady state, as described by (10). The static inversion of a rigid link approximation of a soft rod is used in [S46] to extract posture information from a six-axis force/torque sensor plate placed at its base. Yet, this relationship is most often used in the other direction: from posture measurements to force sensing. Static models can be used to regress an equivalent wrench applied at the end effector from posture information [S47], [S48] under the hypothesis that the robot is lightweight. Disturbance observers can be used to detect interactions when the robot mass is not negligible [S49]. The location and intensity of the external force can be simultaneously regressed when enough information on the current shape of the robot is available. This is achieved in [S50] by using a piecewise constant curvature model and in [S51] through modal expansion. Numerical inversion of a static Cosserat model can provide an estimation of the whole force distribution through functional expansion of the force profile [S52]. Static finite-element model inversion is used in [S53] to detect and characterize contacts integrating capacitive and pneumatic sensing. The method can also be applied to soft surfaces. Tip forces and a robot's shape can also be estimated simultaneously by integrating measurements of the base load with a static Cosserat model [S54].

REFERENCES

[S42] S. Neppalli, M. A. Csencsits, B. A. Jones, and I. D. Walker, "Closed-form inverse kinematics for continuum manipulators," *Adv. Robot.*, vol. 23, no. 15, pp. 2077–2091, Apr. 2012, doi: 10.1163/016918609X12529299964101.

[S43] P. Hyatt, D. Kraus, V. Sherrod, L. Rupert, N. Day, and M. D. Killpack, "Configuration estimation for accurate position control of large-scale soft robots," *IEEE/ASME Trans. Mechatronics*, vol. 24, no. 1, pp. 88–99, Feb. 2019, doi: 10.1109/TMECH.2018.2878228.

[S44] D. Lunni, G. Giordano, E. Sinibaldi, M. Cianchetti, and B. Mazzolai, "Shape estimation based on kalman filtering: Towards fully soft proprioception," in *Proc. IEEE Int. Conf. Soft Robot. (RoboSoft)*, 2018, pp. 541–546, doi: 10.1109/ROBOSOFT.2018.8405382.

[S45] J. Y. Loo, C. P. Tan, and S. G. Nurzaman, "H-infinity based extended kalman filter for state estimation in highly non-linear soft robotic system," in *Proc. IEEE Amer. Contr. Conf. (ACC)*, 2019, pp. 5154–5160, doi: 10.23919/ACC.2019.8814869.

[S46] R. Takano, H. Mochiyama, and N. Takesue, "Real-time shape estimation of Kirchhoff elastic rod based on force/torque sensor," in *Proc. IEEE Int. Conf. Robot. Automat. (ICRA)*, 2017, pp. 2508–2515, doi: 10.1109/ICRA.2017.7989292.

[S47] D. C. Rucker and R. J. Webster, "Deflection-based force sensing for continuum robots: A probabilistic approach," in *Proc. IEEE/RSJ Int. Conf. Intell. Robots Syst.*, 2011, pp. 3764–3769, doi: 10.1109/IROS.2011.6094526.

[S48] F. Campisano et al., "Online disturbance estimation for improving kinematic accuracy in continuum manipulators," *IEEE Robot. Autom. Lett.*, vol. 5, no. 2, pp. 2642–2649, Apr. 2020, doi: 10.1109/LRA.2020.2972880.

[S49] C. Della Santina, R. L. Truby, and D. Rus, "Data–driven disturbance observers for estimating external forces on soft robots," *IEEE Robot. Autom. Lett.*, vol. 5, no. 4, pp. 5717–5724, Oct. 2020, doi: 10.1109/LRA.2020.3010738.

[S50] A. Bajo and N. Simaan, "Kinematics-based detection and localization of contacts along multisegment continuum robots," *IEEE Trans. Robot.*, vol. 28, no. 2, pp. 291–302, Apr. 2012, doi: 10.1109/TRO.2011.2175761.

[S51] Y. Chen, L. Wang, K. Galloway, I. Godage, N. Simaan, and E. Barth, "Modal-based kinematics and contact detection of soft robots," *Soft Robot.*, vol. 8, no. 3, pp. 298–309, Jun. 2021, doi: 10.1089/soro.2019.0095.

[S52] V. A. Aloi and D. C. Rucker, "Estimating loads along elastic rods," in *Proc. IEEE Int. Conf. Robot. Automat. (ICRA)*, 2019, pp. 2867–2873, doi: 10.1109/ICRA.2019.8794301.

[S53] S. E. Navarro et al., "A model-based sensor fusion approach for force and shape estimation in soft robotics," *IEEE Robot. Autom. Lett.*, vol. 5, no. 4, pp. 5621–5628, Oct. 2020, doi: 10.1109/LRA.2020.3008120.

[S54] S. H. Sadati et al., "Stiffness imaging with a continuum appendage: Real-time shape and tip force estimation from base load readings," *IEEE Robot. Autom. Lett.*, vol. 5, no. 2, pp. 2824–2831, Apr. 2020, doi: 10.1109/LRA.2020.2972790.

where we can recognize the same mathematical structure of a classic robot (the left-hand side) controlled through a nonlinear proportional derivative (PD) regulator (the right-hand side). Note that the reference is constant, and thus, $\dot{\bar{q}} = 0$. It is worth stressing that the physical system is excited with a simple feedforward at this stage, which behaves as a PD regulator only when combined with part of the robot's dynamics.

The control community has devoted much attention to (nonlinear) PD controllers [106], which has produced a thriving literature that soft roboticists can borrow from [107], [108], [109] by relying on (16), as done in the following theorem.

Theorem 1

The state $(\bar{q}, 0) \in \mathbb{R}^{2n}$ is an asymptotically stable equilibrium of system (2) subject to the constant control action (15) if an open neighborhood $\mathcal{N}(\bar{q}) \subseteq \mathbb{R}^n$ of $\bar{q}$ exists such that $\forall q \in \mathcal{N}(\bar{q})/\{\bar{q}\}$:

$$(U_G(q) + U_K(q)) > (U_G(\bar{q}) + U_K(\bar{q})) + \left(\frac{\partial}{\partial q}(U_G(q) + U_K(q))\right)\Big|_{q=\bar{q}}^{\top} (q - \bar{q}) \quad (17)$$

and

$$G(q) + K(q) \neq G(\bar{q}) + K(\bar{q}). \tag{18}$$

Proof

Consider as a Lyapunov candidate the following generalization of the energy of the robot:

$$V(q,\dot{q}) = \underbrace{\frac{1}{2}\dot{q}^\top M(q)\dot{q}}_{\text{Kinetic energy}} + \underbrace{U_G(q) - U_G(\bar{q}) + U_K(q) - U_K(\bar{q})}_{\text{Centered potential energy}} + \underbrace{(G(\bar{q}) + K(\bar{q}))^\top(\bar{q} - q)}_{\text{Correction term}}. \tag{19}$$

The kinetic energy is always strictly positive definite in $\dot{q}$ since $M \succ 0$. Thus, a necessary and sufficient condition for V to be positive definite in $(q,\dot{q})$ is that $V - \dot{q}^\top M(q)\dot{q}/2$ is positive definite in q, which is equivalent to (17). The next step is to study the sign of the time derivative of (19), which is

$$\begin{aligned}\dot{V}(q,\dot{q}) &= \dot{q}^\top M(q)\ddot{q} + \frac{1}{2}\dot{q}^\top \dot{M}(q)\dot{q} \\ &\quad - \dot{q}^\top((K(\bar{q}) + G(\bar{q})) - (K(q) + G(q))) \\ &= -\dot{q}^\top C(q,\dot{q})\dot{q} + \dot{q}^\top D(q)(-\dot{q}) + \frac{1}{2}\dot{q}^\top \dot{M}(q)\dot{q} \\ &= -\dot{q}^\top D(q)\dot{q}\end{aligned} \tag{20}$$

where the first step exploits (16) to express $M\ddot{q}$ and the second step exploits the passivity of the system $\dot{q}^\top(\dot{M}(q) - 2C(q,\dot{q}))\dot{q} = 0$. Equation (20) is only positive semidefinite despite $D(q)$ being a strictly positive matrix since $\dot{V}(q,0) = 0$ for all q. Thanks to LaSalle's principle, the system converges to the set of $(q,0)$ such that $\ddot{q} = 0$. Thus, we can prove the asymptotic stability of $(\bar{q},0)$ by showing that the desired equilibrium configuration $\bar{q}$ is the only configuration in $\mathcal{N}(\bar{q})$ such that $\ddot{q} = 0$ for $\dot{q} = 0$. Combining these conditions with (2) results in

$$G(q) + K(q) \neq \bar{\tau} \tag{21}$$

for all $q \in \mathcal{N}(\bar{q})$. Plugging the $\bar{\tau}$ from (15) into (21) yields hypothesis (18), thus concluding the proof. □

If the level curves of the potential energy $U_G(q) + U_K(q)$ are closed in $\mathcal{N}(q_0)$, then we can rely on the proof of Theorem 1 to introduce a lower bound for the region of asymptotic stability associated to $\bar{q}$ as the set $S = \{(q,\dot{q}) \in \mathbb{R}^{2n}$ s.t. $V(q,\dot{q}) < c\}$, with c being the maximum value such that $S \subseteq \mathcal{N}(q_0) \times \mathbb{R}^n$.

Equation (17) is a convexity condition on the total potential energy $U_G(q) + U_K(q)$. Thus, it can be locally checked by looking at the sign of the Hessian matrix. This results in the condition

$$\left(\frac{\partial K(q)}{\partial q} + \frac{\partial G(q)}{\partial q}\right)\Big|_{q=\bar{q}} \succ 0 \tag{22}$$

which means that the force field linearized at the desired equilibrium is attractive. In turn, this also implies that the potential force field is locally not constant, therefore also implying that hypothesis (18) is true at least in an infinitesimal neighborhood of $\bar{q}$. Additionally, (22) becomes a necessary condition for (17) when $\succeq$ is used instead of $\succ$. The two terms in (22) are the stiffness matrices associated with elastic and potential fields. While the first is always positive definite [see (6)], the second is not definite in sign. Gravity may serve either as a destabilizing ($\partial G(q)/\partial q \preceq 0$)

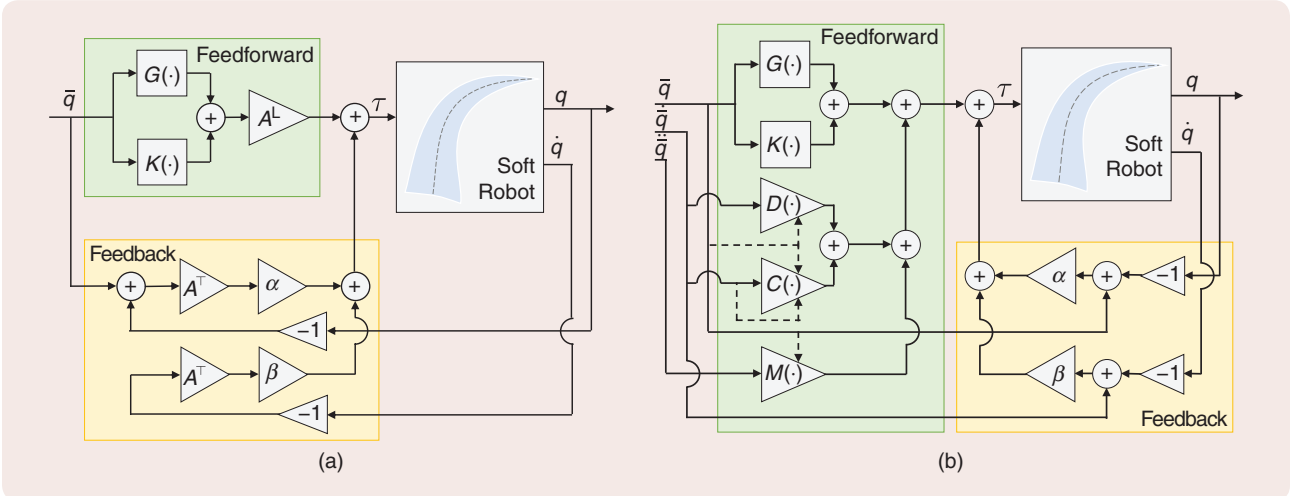

FIGURE 6 Block schemes of PD-like controllers for shape regulation and tracking. (a) The regulator (30) [which corresponds to (23) when $A = I$] compared to (29) when α, β are null and to the pure feedforward action (15) when $A = I$ and α, β are null. (b) The high-gain PD controller with feedforward compensation (28) for trajectory tracking under fully actuated approximations. If the dashed lines are connected to q and $\dot{q}$ instead of the reference, the controller directly extends the classic PD+. Feedforward and feedback components are highlighted.

or as stabilizing force ($\partial G(q)/\partial q \succeq 0$). For the CC segment described in "Dynamics of a Constant Curvature Segment," these two conditions correspond, respectively, to the robot pointing upward ($\phi = \pi$) or downward ($\phi = 0$) when in a straight configuration ($q = 0$).

Thus, as already pointed out for the analysis of equilibria, the presence of an elastic field makes the control problem simpler to solve compared to the standard rigid case. This can be regarded as an instance of the so-called self-stabilization property of soft robots, which has been recognized by several works in the literature [110], [111]. However, even if a feedforward action has proved to be sufficient for stiff enough systems, it is still interesting to consider what happens when a further feedback loop is introduced. This may serve several purposes: enlarge the basin of attraction, shape the transient, and reject disturbances. In the latter case, stability can still be verified in a similar fashion provided that some conditions on the disturbance are met (for example, boundedness).

Further following the analogy with nonlinear PDs, (15) can be extended as follows for the fully actuated case (Figure 6):

$$\tau(\bar{q},q,\dot{q}) = \underbrace{K(\bar{q}) + G(\bar{q})}_{\text{Feedforward}} + \underbrace{\alpha(\bar{q}-q) - \beta\dot{q}}_{\text{PD}}. \tag{23}$$

Here, $\alpha, \beta \in \mathbb{R}^{n\times n}$ are two gain matrices weighting the proportional and derivative actions, respectively.

Corollary 1

The state $(\bar{q},0) \in \mathbb{R}^{2n}$ is an asymptotically stable equilibrium of the closed loop (2)–(23) if $D(q) \succ -\beta$ and an open neighborhood $\mathcal{N}(\bar{q}) \subseteq \mathbb{R}^n$ of $\bar{q}$ exists such that $\forall q \in \mathcal{N}(\bar{q})/\{\bar{q}\}$:

$$\begin{aligned}&(U_G(q) + U_K(q)) + \frac{1}{2}(q-\bar{q})^\top \alpha (q-\bar{q}) \\ &\quad > (U_G(\bar{q}) + U_K(\bar{q})) + \left(\frac{\partial}{\partial q}(U_G(q) + U_K(q))\right)\Big|_{q=\bar{q}}^\top (q-\bar{q})\end{aligned} \tag{24}$$

and

$$G(q) + K(q) + \alpha(\bar{q}-q) \neq G(\bar{q}) + K(\bar{q}). \tag{25}$$

Proof

The closed-loop dynamics are $M(q)\ddot{q} + C(q,\dot{q})\dot{q} = (K(\bar{q}) - K(q)) + (G(\bar{q}) - G(q)) + \alpha(\bar{q}-q) - (D(q)+\beta)\dot{q}$. The previously discussed proof generalizes to this case by adding $(\bar{q}-q)^\top \alpha(\bar{q}-q)/2$ to (19). The time derivative of this new Lyapunov candidate is $\dot{V} = -\dot{q}^\top (D(q)+\beta)\dot{q}$, which is semi-negative definite if $D(q) + \beta \succ 0$. Thus, any $\beta \succeq 0$ implements a damping injection that does not destabilize the closed loop. The rest of the proof follows as in the feedforward case. □

Similar considerations on the region of asymptotic stability to the ones made for Theorem 1 apply here. The sufficient condition for local asymptotic stability is

$$\left(\frac{\partial K(q)}{\partial q} + \frac{\partial G(q)}{\partial q}\right)\Big|_{q=\bar{q}} + \alpha \succ 0 \tag{26}$$

which becomes necessary when only semipositiveness is required. Note that (26) can always be fulfilled through a large enough proportional gain α. Yet, large gains may result in a stiffening of the soft robot [112] and amplification of the noise and excitation of neglected dynamics.

Figure 7 provides a comparison of (15) and (23) in regulating the shape of a fully actuated model of a soft robot. The desired

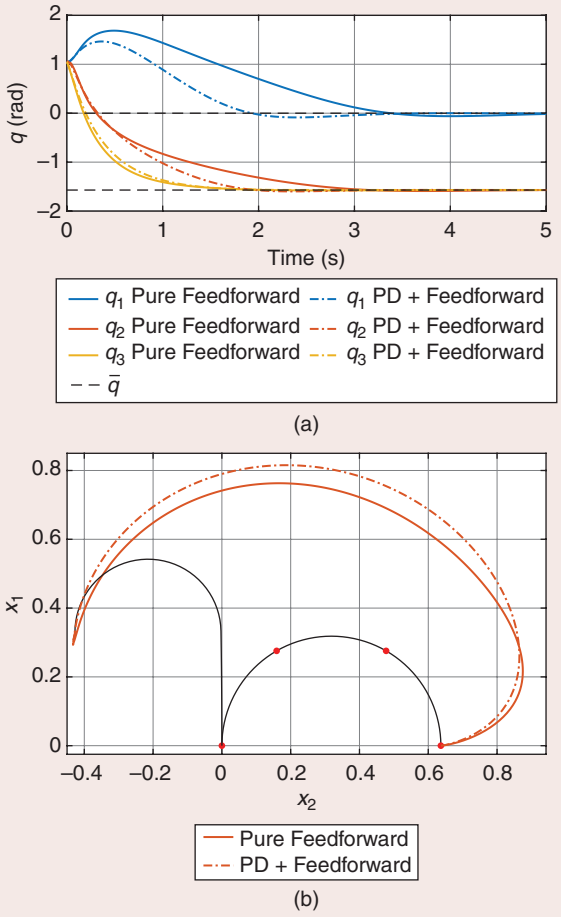

FIGURE 7 The pure feedforward controller (15) and the PD with feedforward controller (23), regulating the shape of a planar soft robot. (a) The evolution of configurations in time. (b) The evolution of the tip in space. The robot shape is described by three CC segments, each independently actuated (that is, $A = I$). The segments are 0.33 m long and 0.33 Kg heavy. Gravity is aligned with the base, and it points downward. The elastic forces and dissipative forces are $K(q) = q$ and $D(q) = q/3$. The initial condition is $q(0) = (\pi/3, \pi/3, \pi/3)$ and $\dot{q} = 0$. The desired configuration is $\bar{q} = (0, -\pi/2, -\pi/2)$. Both corresponding shapes in the bottom plot are shown as solid black lines. The initial shape also has red dots marking each segment's beginning and end. The control gains are $\alpha = I$ and $\beta = I/2$.

configuration is already stable in the open loop, with the eigenvalues of the right-hand side of (22) being approximately $(1.01, 2.96, 3.19)$. Note that a softer robot requiring a feedback to converge as $\partial G(q)/\partial q$ has two negative eigenvalues in $\bar{q}$. Nonetheless, the feedback action also proves beneficial in this case in speeding up the convergence.

Possibly nonlinear integral actions can also be added to (23) for compensating steady-state errors and achieving global stabilization, as discussed in [109]. In this case, we can drop the model-based component $K(\bar{q}) + G(\bar{q})$ and entirely rely on the integral action to compensate for it. The result is a model-free version of (23), extensively tested experimentally in [113]. A bilinear extension has been proposed and tested in [114].

Trajectory Tracking

In trajectory tracking, the desired behavior is specified as an evolution of the full robot shape in time. Consider a twice-differentiable function of time $\bar{q}: \mathbb{R} \to \mathbb{R}^n$. Then, the control goal is to find a control strategy τ such that

$$\lim_{t \to \infty} (q(t), \dot{q}(t)) - (\bar{q}(t), \dot{\bar{q}}(t)) = 0. \tag{27}$$

Usually, the reference is considered bounded in norm $\|(\bar{q}(t), \dot{\bar{q}}(t))\| < c_t$ for some positive c_t. In theory, under the fully actuated approximation $n = m$, (2) can be completely feedback linearized with a computed torque scheme. However, such a strategy would be hardly applicable on a real system. This section focuses on controllers achieving the trajectory tracking goal by relying minimally on direct model cancellations. For the sake of space, proof of convergence is not provided. All the controllers can be obtained by adapting proofs from the nonlinear PD literature to work for a system such as (16), as in Theorem 1.

If the reference trajectory is slowly varying (that is, $\|\dot{\bar{q}}\|$ is small enough), then (15) and (23) can still be applied as they are, possibly with the inclusion of damping feedforward compensation terms, that is, $D(\bar{q})\dot{\bar{q}}$ and $(D(\bar{q}) + \beta)\dot{\bar{q}}$, respectively. The state will not converge to $(\bar{q}, \dot{\bar{q}})$ at the steady state but to a neighborhood of it [115], [116]. The higher the gains and the slower the reference, the smaller the neighborhood.

Explicit compensation of dynamic forces is needed to achieve null steady-state error. Again, this can happen by largely relying on feedforward actions (Figure 6):

$$\begin{aligned}\tau(\bar{q}, \dot{\bar{q}}, \ddot{\bar{q}}, q, \dot{q}) = &\underbrace{M(\bar{q})\ddot{\bar{q}} + C(\bar{q}, \dot{\bar{q}})\dot{\bar{q}} + D(q)\dot{\bar{q}} + K(\bar{q}) + G(\bar{q})}_{\text{Feedforward}} \\ &+ \underbrace{\alpha(\bar{q} - q) + \beta(\dot{\bar{q}} - \dot{q})}_{\text{PD}}.\end{aligned} \tag{28}$$

By adapting the results in [117], we can prove that (28) leads to local exponential stabilization of the desired

Robust Control

Models for soft robots always come with some degree of uncertainty. The nature of the materials used and the manufacturing process are such that the mechanical characteristics of soft systems can vary dramatically, even when starting from a similar original design. Moreover, the state discretization that is at the base of all the discussed control strategies implies that part of the dynamics is ignored. Both sources of uncertainty will likely be mitigated by advancements in material science and modeling. Yet, these improvements will hardly be sufficient to completely eliminate the issue, which must be taken into account while devising model-based strategies. One way of achieving this goal is to integrate learning loops into the controller. Alternatively, control loops can be devised in such a way that they are intrinsically robust to uncertainties. This is often done implicitly in soft robotics by avoiding strong reliance on feedback model cancellations and high gains. These are indeed characteristics shared by almost all the techniques discussed in this article. Alternatively, robustness to uncertainties can be implemented by explicitly relying on robust control design [S55]. For example, linear robust H_∞ control is used in [S56], [S57], and [S58] for controlling a soft actuator, a single segment, and a planar soft robot, respectively. Interval arithmetic is used in [S59] to design a nonlinear model-based controller that can achieve prescribed tracking performance in the presence of uncertainties. Robust sliding mode control is considered in [S60], [121], and [181]. Fractional order control is used in [14] and [S62]. The latter is discussed in detail by [S62], part of the same special issue.

REFERENCES

[S55] C. Abdallah, D. M. Dawson, P. Dorato, and M. Jamshidi, "Survey of robust control for rigid robots," *IEEE Control Syst. Mag.*, vol. 11, no. 2, pp. 24–30, Feb. 1991, doi: 10.1109/37.67672.

[S56] A. Hunt, Z. Chen, X. Tan, and M. Kruusmaa, "An integrated electroactive polymer sensor–actuator: Design, model-based control, and performance characterization," *Smart Mater. Struct.*, vol. 25, no. 3, Feb. 2016, Art. no. 035016, doi: 10.1088/0964-1726/25/3/035016.

[S57] A. Shu, B. Deutschmann, A. Dietrich, C. Ott, and A. Albu-Schäffer, "Robust h^∞ control of a tendon–driven elastic continuum mechanism via a systematic description of nonlinearities," *IFAC-PapersOnLine*, vol. 51, no. 22, pp. 386–392, Dec. 2018, doi: 10.1016/j.ifacol.2018.11.572.

[S58] A. Doroudchi et al., "Decentralized control of distributed actuation in a segmented soft robot arm," in *Proc. IEEE Conf. Decis. Contr. (CDC)*, 2018, pp. 7002–7009, doi: 10.1109/CDC.2018.8619036.

[S59] F. Hisch, A. Giusti, and M. Althoff, "Robust control of continuum robots using interval arithmetic," *IFAC-PapersOnLine*, vol. 50, no. 1, pp. 5660–5665, Jul. 2017, doi: 10.1016/j.ifacol.2017.08.1115.

[S60] A. A. Alqumsan, S. Khoo, and M. Norton, "Multi-surface sliding mode control of continuum robots with mismatched uncertainties," *Meccanica*, vol. 54, no. 14, pp. 2307–2316, Nov. 2019, doi: 10.1007/s11012-019-01072-6.

[S61] B. Deutschmann, C. Ott, C. A. Monje, and C. Balaguer, "Robust motion control of a soft robotic system using fractional order control," in *Proc. Int. Conf. Robot. Alpe-Adria Danube Region*, C. Ferraresi and G. Quaglia, Eds. Cham, Switzerland: Springer, 2017, pp. 147–155.

[S62] C. A. Monje et al., "A survey on fractional order control in soft robots (Provisional Title)," *IEEE Control Mag.*, to be published

trajectory if $\alpha + \partial K/\partial q$ and $\beta + D$ are larger than two bounds that increase with the increase of $\| \partial G/\partial q \|, \| \dot{\tilde{q}} \|$, and $\| \ddot{\tilde{q}} \|$. Purely feedforward dynamic controllers for soft robots are experimentally validated in [118] and [119]. Thus, if the reference is slowly varying or the natural impedance is high enough, then the feedback gains α, β can be selected null, and the controller is once more purely feedforward. For generic trajectories, the discussed condition will be hardly verified by the physical properties, and the extra feedback will be necessary. As an alternative to high gains, (28) can be further evolved into a partially nonlinear closed loop (Figure 6). This is done by evaluating M, C, and G on the measured state $(q, \dot{q})$ rather than on the reference $(\tilde{q}, \dot{\tilde{q}})$. This produces a closed loop that is equivalent to a rigid robot controlled through a PD+ controller [120], where the plus refers to the mixed feedforward-feedback compensation of dynamic forces. In this case, we can achieve perfect tracking even when $\alpha = 0$ and $\beta = 0$. This control strategy is discussed and experimentally validated on a soft robotic platform in [48]. A version of this controller that is robust to system uncertainties and does not require direct measurement of $\dot{q}$ is proposed and tested in [121], which is close to the robust PD controller proposed in [122]. Thanks to (16), the latest advancements in PD control of mechanical systems [123], [124], [125] can also be adapted to further improve performances and robustness to uncertainties (see "Robust Control").

Figure 8 compares the performance of three of the controllers introduced in the preceding in tracking a sinusoidal

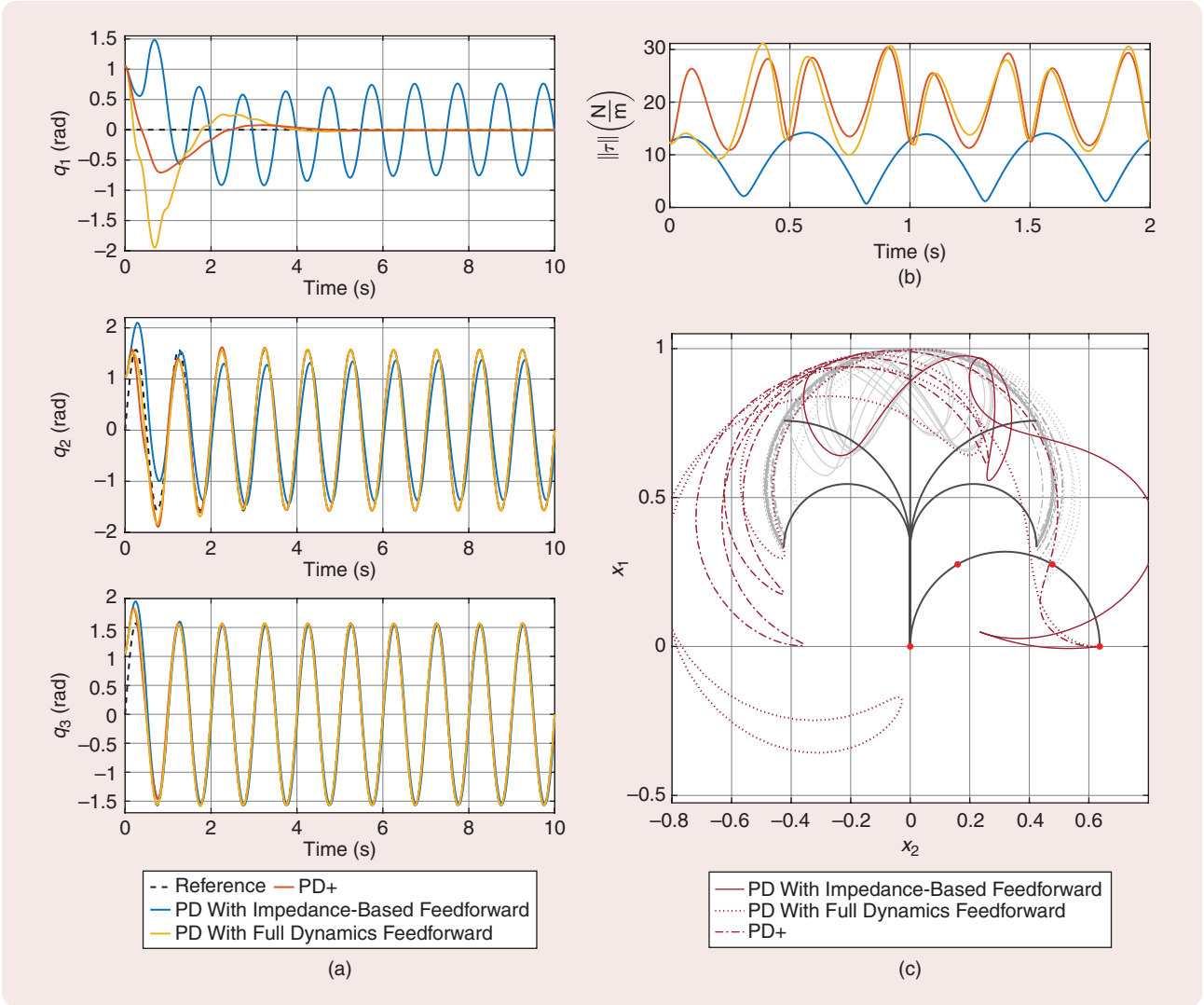

FIGURE 8 A comparison of the shape tracking performance of PD-like controllers with impedance-only feedforward compensation, feedforward including dynamic forces (28), and mixed feedback-feedforward compensation in the fashion of the PD+ controller. The robot is the same one discussed in Figure 7. This time, the reference is the trajectory $\tilde{q}(t) = (0, \pi/2, \pi/2)\sin(2\pi t)$. (a) The curvature evolution in time per segment for each of the three controllers. (b) The evolution of the control action two-norm. (c) The evolution of the tip in space. The first two seconds are red, and the rest of the evolution is gray. The initial condition and five configurations that are part of the desired evolution appear as solid black lines. The former also has red dots indicating each segment's start and end. The control gains are the same for all controllers and equal to $\alpha = I$ an $\beta = I/10$.

evolution of curvature. Tracking performance increases with the complexity of the controller. However, when applying these controllers to physical systems, it should be kept in mind that more complex controllers can result in less robust performance when the model is inaccurate.

Several other works in the soft robotics literature deal with the trajectory tracking challenge by relying on fully actuated approximations. A computed torque controller built on a planar PCC model and sliding mode variation is experimentally tested in [126]. A model-based decentralized controller is proposed in [127] and applied to a fully actuated discretization of the Cosserat model. Finally, [128] derives model-based controllers under a first-order approximation, that is, when $\| D(q)\dot{q} \| >> \| M(q)\ddot{q} + C(q,\dot{q})\dot{q} \|$. This is the case for lightweight soft robots moving in viscous fluids [129].

ADVANCED CONTROL CHALLENGES: UNDERACTUATION, ACTUATORS DYNAMICS, AND TASK EXECUTION

This section discusses challenges that are largely unexplored and still in need of general solutions and formulations.

Dealing With Underactuation in Shape Control

Fully actuated approximations have proved to be effective in practice despite being a clear oversimplification of the control problem. By bringing underactuation into the picture, the degrees of freedom not directly affected by the control action can be analyzed and potentially used in the design of the controller toward solutions with improved performance and certifiable reliability. Indeed, using a rough approximation during control design may often lead to performance degradation (see Figure 9) and even instability. Thus, consider a nonsquare actuation matrix $A(q)$, with $m < n$. The first difficulty that arises is that the desired shape $\bar{q}$ may not be an attainable equilibrium of the system; that is, $K(\bar{q}) + G(\bar{q}) \notin \text{Span}(A(\bar{q}))$. In other terms, there does not necessarily exist a control action $\bar{\tau}$ that renders a generic given shape $\bar{q}$ an equilibrium. Similarly, a control input evolution $\tau(t)$ may not exist such that a generic state $(\bar{q}, \dot{\bar{q}})$ can be reached from any initial condition. The authors of [130] discuss how different actuation patterns may affect the accessible set [131] of a soft robot.

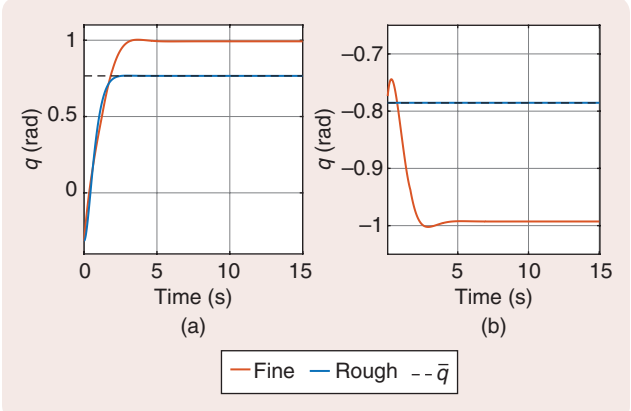

FIGURE 9 Performance degradation due to a rough discretization during control design. A slender soft robot is actuated through a torque applied at its tip. Controller (23) is designed leveraging a single CC segment approximation. The performance on the nominal system (rough) and on a more precise approximation obtained by discretizing the robot with four CC segments (finer) is shown. The relevant parameters are $L = 1$ m, $m = 1$ Kg, $\phi = \pi$ $\alpha = 0.5$(N · m/rad) and $\beta = 1$(N · ms/rad). For the single CC model, the impedance is $K(q) = q$ and $D = 0.3$ N · ms/rad. (a) Example 1. (b) Example 2.

Assume that the equilibrium $\bar{q}$ is attainable with the given underactuation matrix $A(q)$. Under this assumption, (15) can be generalized in (see Figure 6)

$$\tau = A^{\mathrm{L}}(\bar{q})(K(\bar{q}) + G(\bar{q})) \tag{29}$$

with A^{L} the left inverse of A, as in the Moore-Penrose pseudoinverse $(A^{\top}A)^{-1}A^{\top}$. If A is configuration independent, this leads to the same closed loop (16). Thus, the physical impedance acts as a stabilizing action not only on the colocated part but also on the variables that are not directly reached by the actuation. If A is configuration dependent, then its local changes may have destabilizing effects that must be considered in a modified (22), as discussed in [132, Appendix]. When dealing with slowly varying trajectories, similar considerations can be applied to the trajectory tracking problem. However, extending the results involving feedback actions, as, for example, (28), is a substantially more complex challenge that is still to be addressed. Relying on linearized models can be a practically effective alternative, either when linearizing around the equilibrium [133] or around the desired trajectory [134].

Control design and analysis get substantially more complex when it comes to stabilizing unstable equilibria of underactuated models. In this case, (22) is not verified, and feedback actions must be involved. Discussion and experimental validation of combining local linear control, an accurate FEM model, and a Luenberger observer for designing a damping injection loop are provided in [135] and [136]. A FEM-based gain scheduling controller is used in [137] to cover the state space of the robot with linear setpoint regulators, including integral actions. Moving a step toward the nonlinear domain, the simple controller (23) can be extended to the following PD+FF (Figure 6)

$$\tau(\bar{q}, q, \dot{q}) = A^{\mathrm{L}}(K(\bar{q}) + G(\bar{q})) + \alpha A^{\top}(\bar{q} - q) - \beta A^{\top}\dot{q} \tag{30}$$

which is a generalization of (23) to the underactuated domain. Note that the two gains α, β are still elements of $\mathbb{R}^{m\times m}$, and thus, they weight the involvement of the actuators into the control loop.

Corollary 2

The thesis of Corollary 1 is verified for the closed loop (2)–(30), with constant A, under the same set of hypotheses when switching α and β with $A\alpha A^{\top}$ and $A\beta A^{\top}$, respectively, and if

$$(I - AA^{\mathrm{L}})(K(\bar{q}) + G(\bar{q})) = 0. \tag{31}$$

Proof

Under hypothesis (31), the following holds: $AA^{\mathrm{L}}(K(\bar{q})+G(\bar{q}))=K(\bar{q})+G(\bar{q})$. The closed-loop dynamics are thus structurally equivalent to those one in Corollary 1; that is, $M(q)\ddot{q}+C(q,\dot{q})\dot{q}=(K(\bar{q})-K(q))+(G(\bar{q})-G(q))+A\alpha A^{\top}(\bar{q}-q)-(D(q)+A\beta A^{\top})\dot{q}$. Thus, the rest of the proof follows as in the fully actuated case. □

Per the fully actuated case, an integral action could be incorporated in (30), possibly dropping the feedforward

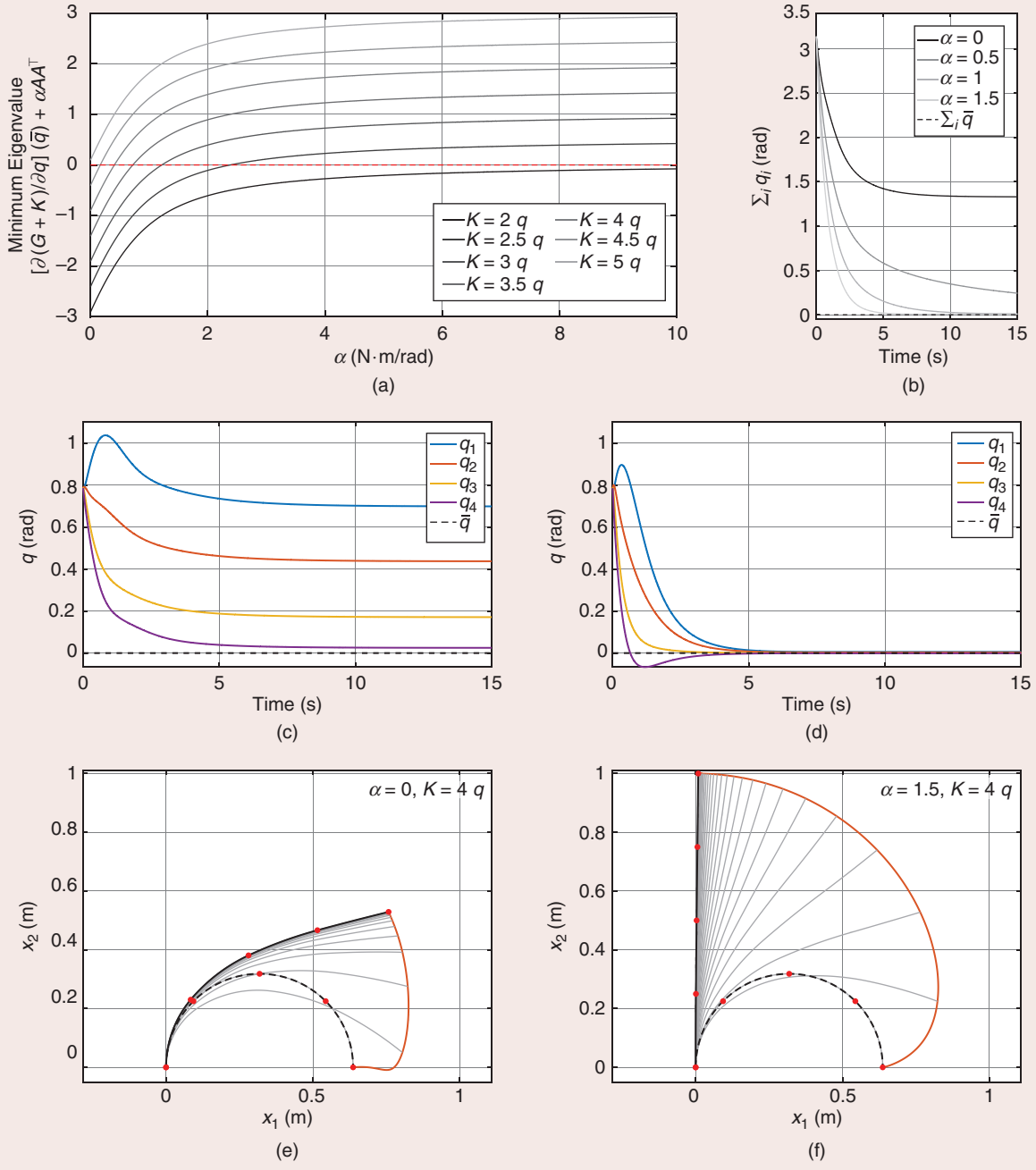

FIGURE 10 Examples of (33) controlling a slender planar soft segment actuated through a torque at its tip. The robot is modeled with four CC segments ($n = 4$) of equal mass ($m = 0.25$ Kg), length ($L = 0.25$ m), and homogeneous impedance ($K(q) = 4q$, $D(q)\dot{q} = 1.2\dot{q}$). Gravity is pointing downward ($\phi = \pi$). We aim for stabilizing the robot's straight configuration $\bar{q} = [0,0,0,0]^{\top}$ rad. (a) Changing the gain α and the stiffness K affects the stability, measured as the minimum eigenvalue of (32). The red dashed line highlights the threshold above which the robot is locally stable. Closed-loop evolutions appear in (b)–(f). (b) The evolution of $A^{\top}q$ for different choices of α and $\beta = 1$(N · ms/rad). The gains are $(\alpha, \beta) = (0$(N · m/rad), 1(N · ms/rad)) in (c) and (e) and $(\alpha, \beta) = (0$(N · m/rad), 1(N · ms/rad)) in (d) and (f). The robot starts at rest from the configuration $q(0) = [\pi/4, \pi/4, \pi/4, \pi/4]^{\top}$ rad. (c) and (d) The evolution in time of the four curvatures. (e) and (f) The evolution of the robot's shape. The initial condition is a black dashed line, the final condition is a black solid line, and the ends of the segments are highlighted with red dots.

compensation of potential forces. However, the preceding proof of stability does not trivially extend to cover this controller variation.

The sufficient convergence condition (26) for the local convexity of the modified potential becomes

$$\left(\frac{\partial K(q)}{\partial q}+\frac{\partial G(q)}{\partial q}+A\alpha A^{\top}\right)\Big|_{q=\bar{q}} \succ 0 \tag{32}$$

where if $\alpha \succ 0$, then $A\alpha A^{\top} \succeq 0$ but $\operatorname{Rank}(A\alpha A^{\top}) \leq m < n$. Thus, the equilibrium $\bar{q}$ can be stabilized using (30) only if the actuation is colocated on the directions in which the effective stiffness loses rank. This can be interpreted as the controller working to stabilize the actuated coordinates $A^{\top}q$ while relying on the soft robot's physical elasticity $K(q)$ to stabilize the unactuated coordinates.

To get a better sense of how this controller is acting, consider the example of a planar inextensible soft robot

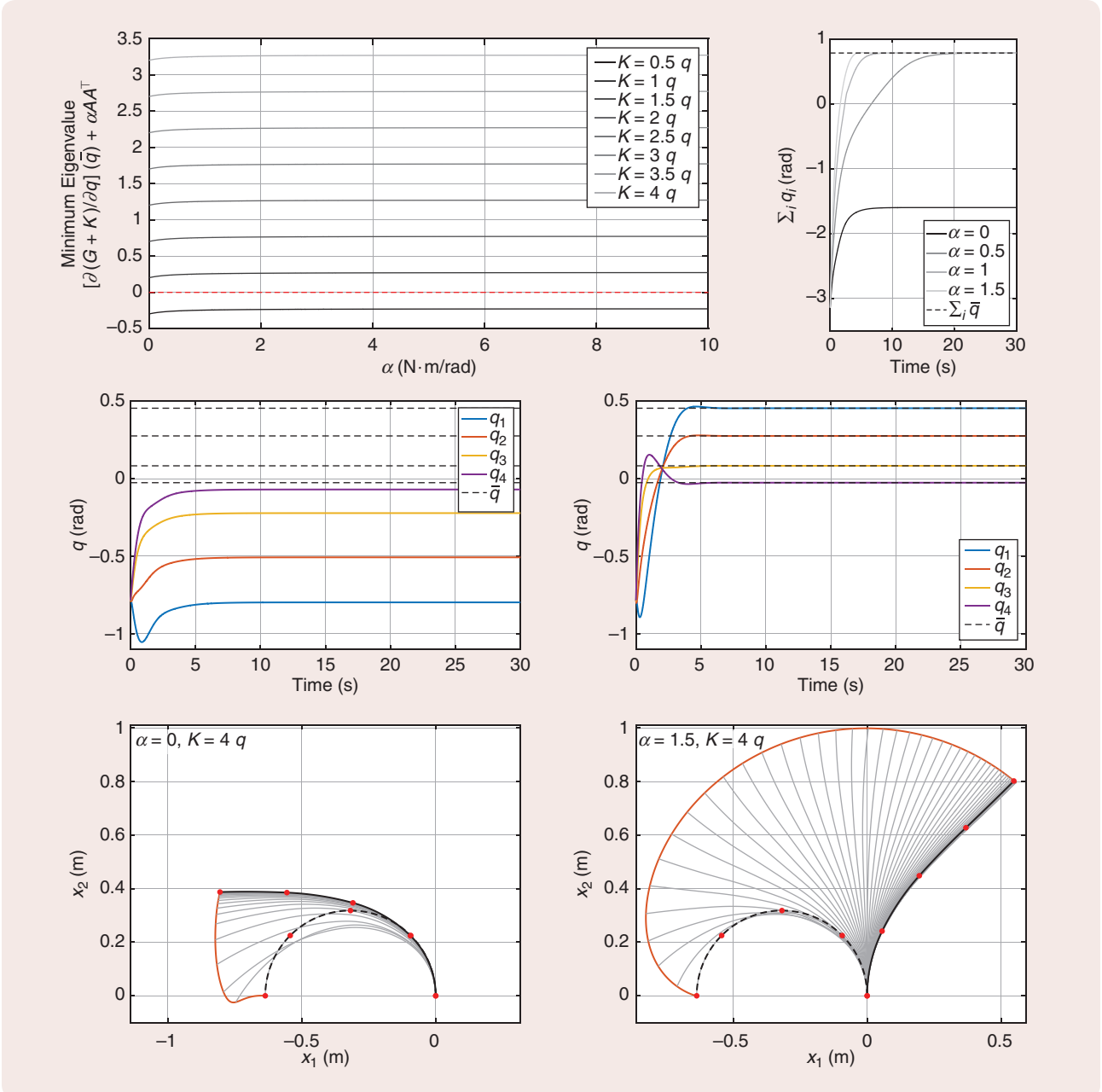

FIGURE 11 Examples of (33) controlling a slender planar soft segment actuated through a torque at its tip. Everything is as in Figure 10 except for the initial and desired configurations, which are $q(0) = [-\pi/4, -\pi/4, -\pi/4, -\pi/4]^{\top}$ rad and $\bar{q} = [0.4413, 0.2720, 0.0872 - 0.0179]^{\top}$ rad, respectively. The latter is such that $\Sigma_i \bar{q}_i = \pi/4$. Note that even if $\alpha = 0$ results in local asymptotic stability of $\bar{q}$ [see (a)], it is not sufficient to enlarge the region of asymptotic stability enough to include $q(0)$.

actuated with a pure torque at its tip that we model as a sequence of n CC segments, not necessarily of the same length. The actuation matrix of this system is $A = [1 \dots 1]^\top$. Thus, (30) becomes

$$\tau = \underbrace{\frac{\sum_{i=1}^{n} (K_i(\bar{q}) + G_i(\bar{q}))}{n}}_{\text{Average potential force}} + \alpha \underbrace{\left[\left(\sum_{i=1}^{n} \bar{q}_i \right) - \left(\sum_{i=1}^{n} q_i \right) \right]}_{\text{Error on tip's orientation}} - \beta \underbrace{\left(\sum_{i=1}^{n} \dot{q}_i \right)}_{\text{Tip's angular velocity}} \quad (33)$$

where we used the Moore-Penrose pseudoinverse as the left inverse of A, with K_i and G_i being the ith elements of K and G. The feedback action is translated into a PD of the angular component of the tip configuration $x(1, t)$. The interpretation of the actuated variables $A^\top q$ as portions of $x(s, t)$ always holds whenever A is constant because this matrix is the transpose Jacobian of the coordinates on which the generalized forces are applied. Instead, the feedforward action being the average of the local potential forces is peculiar to this actuation modality. Finally, $A\alpha A^\top$ in (32) is an $n \times n$ matrix, with each element being α. Figures 10(a) and 11(a) outline how the smallest eigenvalue of the left-hand side of (32) changes with the robot's stiffness and the proportional gain α. For large stiffnesses, the equilibrium is always stable; for small stiffnesses, the equilibrium is always unstable; and in between, it depends on the value of α. Note that this is quite different from the result we would have obtained with a CC approximation of the segment ($n = 1$), for which an α large enough always exists such that (26) holds. Figures 10(b)–(f) and 11(b)–(f) report the closed-loop behavior.

Some recent works deal with the regulation of equilibria under similar colocated conditions. In [138], an energy shaping controller is proposed for setpoint posture regulation of a planar segment modeled as a sequence of rigid links, with the same torque applied to all links. The authors extend the strategy by including an integral action in [139] to compensate for time-varying external disturbances. Moving to more general systems, [74] tests, in simulation, the use of computed torque plus zero-dynamics damping injection in a geometrical exact discrete Cosserat model. This technique was already used for controlling an eel-like hyperredundant robot in [140]. No proof of convergence is provided, but the simulations show good performance. Finally, [141] generalizes (30) to nonlinear proportional and derivative actions and provides a proof of convergence by relying on potential energy shaping control and damping injection.

If (32) and its nonlocal version cannot be verified for any α, then the potential field $K(q) + G(q)$ is repulsive in one or more of the directions orthogonal to $A^\top$. This is an essentially more challenging scenario compared to the elastically dominated alternative, and it can happen when the robot is very soft compared to its weight. Recently, [142] showed that adding online gravity compensation to (30) is enough to tackle this challenge whenever actuated and unactuated variables are not elastically coupled. In the preceding n–CC example, this happens if the stiffness distribution is homogenous: $(K_i(q) = K_j(q), \forall i, j \in \{1 \dots n\})$. An alternative is to focus on specific systems. For example, [73] and [143] propose two inverted pendula (the former continuum, the latter hybrid) as soft extensions of the acrobot [144]. Both works discuss analytically the stabilization of an unstable equilibrium. Interestingly, [73] shows that a range of low stiffnesses exists for which the robot can be stabilized only by means of noncolocated feedback.

Finally, tracking control in the underactuated case has received minimal attention. One interesting example is [145], which derives a nominal tracking controller under a linear approximation and uses a disturbance observer to compensate for mismatches.

Actuators Dynamics and Constraints

Actuators dynamics plays an important role in shaping the soft robot behavior, especially if compared to classic rigid robots. Nonetheless, few works have explicitly taken into account a dynamics formulation, such as (13), in the design of the controller. Some actuation technologies require accurately considering the control problem for a single isolated actuator. This is the case for electrothermally active materials [114], [146], [147], [148] and magnetic actuation of micro- and nanorobots [149], [150]. An extensive comparison of feedback control strategies applied to a pneumatically actuated soft segment is available in [151].

If a clear separation exists between the response time of actuators (13) and the robot (12), then a singular perturbation approach [152] could be used to improve the performance of the model-based controllers introduced in the preceding. Alternatively, a backstepping design achieves the same goal without any assumption on the relative timescales [153], at the cost of a more complex control architecture. Both techniques have been extensively used to control flexible robots actuated with similar modalities as typically found in soft robotics as tendon driven [154], pistons [155], and artificial muscles [156], [157]. Only recently have works in soft robotics investigated the application of backstepping techniques [158], [159], [160], focusing exclusively on pneumatically actuated robots. A linear model of the robot and the airflow is considered in [158], while [159] and [160] tackle the nonlinear case. We are not aware of any examples of the application of singular perturbation in soft robotics.

In soft robotic actuation, it is often the case that the input space can take values only in a subset of $\mathbb{R}^m$. This may be due to upper bounds to the maximum force and unilateral constraints induced by tendons that can only pull and pressure chambers that can only push. These constraints are usually addressed by heuristics that mask their existence to

controllers carefully tuned to not exceed the limits of actuation. As an alternative to heuristics, the masking can also be devised through model-based techniques, such as the closed-form solution of optimal control allocation problems [161]. Alternatively, model predictive controllers (MPCs) can generate control actions that inherently verify the constraints. In [162], a linear MPC is used to control a pneumatically actuated humanoid robot with joint-like localized bending and under a decentralized approximation. In [163], the strategy is extended to a nonlinear MPC, and evolutionary algorithms are used to solve the nonlinear optimization. In [164], nonlinear order reduction techniques are used to generate accurate relaxations of a nonlinear finite-horizon optimal control problem (including state and input constraints) and formulated on nonlinear FEM models.

Task Space Regulation and Tracking

The task space of a robot is usually identified with the configuration of its end effector. In soft robots, this corresponds to the configuration of the tip $x(1,t)=h(1,q(t))$. For simplicity of notation, we drop the s coordinate in this section. This emphasizes that the results discussed in the following are general for any s and any smooth function h of the configuration q. Examples are the potential energy and the distance of the soft robot from an obstacle. Thus, a task is fulfilled if

$$\lim_{t\to\infty} h(q(t)) - \bar{x}(t) = 0 \tag{34}$$

where the desired task coordinates $\bar{x}$ can be either a constant value (regulation) or a function of time (tracking).

A substantial body of literature [36], [165], [166], [167], [168], [169], [170] deals with the problem under the kinematic approximation. For a fully actuated model, this means assuming that the robot evolution is described by (1), with $\dot{q}$ being the control input. This is a well-known problem in robotics [171], [172], [173], which can be solved with the control loop

$$\dot{q} = J^{+}(q)(K_e(\bar{x} - h(q)) + \dot{\bar{x}}) \tag{35}$$

with J^{+} being the Moore-Penrose pseudoinverse of J. Indeed, combining (1) and (35) yields the closed-loop dynamics $\mathrm{d}(x-\bar{x})/\mathrm{d}t = K_e(x-\bar{x})$ that fulfill (34) exponentially fast for all $K_e \succ 0$. Note that for $\dot{\bar{x}} = 0$, the time discretization [174], [175] of (35) is equivalent to applying the Newton-Raphson method to solve the following quadratic programming problem:

$$\min_{q\in\mathbb{R}^n} \|h(q) - \bar{x}\|_2^2. \tag{36}$$

Soft and hard constraints can be explicitly included in (36) and possibly reflected in (35), using multitask prioritization. In practice, (35) is integrated numerically, and the result serves as reference $\bar{q}$ for a low-level controller that regulates q. This can happen entirely in feedforward or as a high-level feedback loop. In the latter case, q and $h(q)$ are directly measured. Alternatively, the kinematic behavior

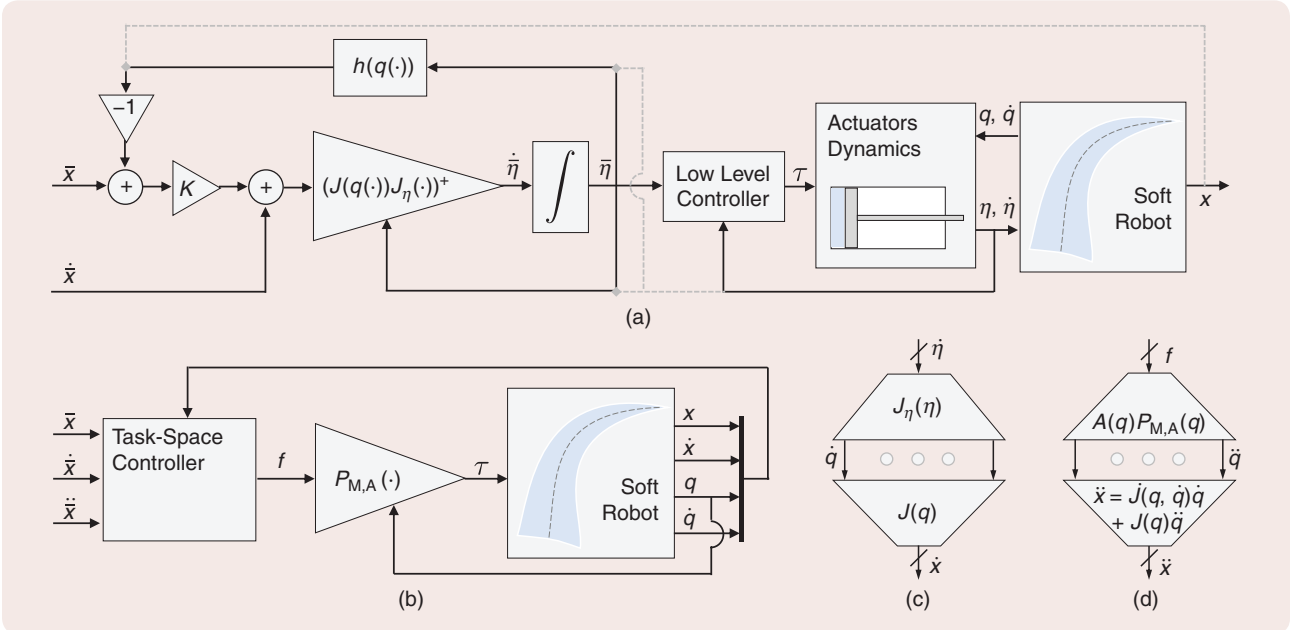

FIGURE 12 Task space controllers in the underactuated case. (a) The standard approach (37), which deals with the problem under quasi-static and actuator dominance approximations. (b) A theoretically attractive but potentially not robust alternative, which acts directly in task space (39). Both solutions deal with configuration space underactuation by constructing control spaces that are at least as large as the output but, in general, smaller than the configuration. These are (c) actuator-side velocities $\dot{\eta}$ for the first strategy and (d) task-level forces f for the second.

can be forced on the system using model based cancellations [176]. Therefore, the use of a kinematic controller implicitly lies on the assumption that all configurations q are attainable through a low-level controller, such as the ones discussed in previous sections.

To extend (35) to the underactuated case, one has to introduce extra assumptions. First, it must be assumed that a low-level feedback loop $\tau(\bar{\eta}, \eta, \dot{\eta}, q, \dot{q})$ is available such that if applied to (13), then η converges to $\bar{\eta}$ fast enough. Under this assumption, η and $\bar{\eta}$ can be used interchangeably. This is a strong assumption, in general. However, if the robot dynamics are negligible compared to the actuators one—for example, a lightweight robot with strongly reduced actuation—standard actuator-side regulation $\tau(\bar{\eta}, \eta, \dot{\eta})$ is sufficient. This is the case for lightweight continuum medical devices [177], [178]. Second, it has to be assumed that the robot is drawn to a stable equilibrium $\bar{q}$ whenever a constant $\bar{\eta}$ is imposed. More precisely, $\bar{q}$ is defined as one of the possibly many solutions of the equilibrium equation of (12) for a fixed actuator's state; that is, $-\partial U_{\mathrm{c}}(\bar{q}, \bar{\eta})/\partial q = K(\bar{q}) + G(\bar{q})$. This equilibrium configuration is not necessarily attractive. However, this condition can be checked by seeing whether the feedforward action (29) generates an asymptotically stable equilibrium. See the "Dealing With Underactuation in Shape Control" section and Corollary 2 therein for more discussion on the topic. Third, a function $q : \mathbb{R}^m \to \mathbb{R}^n$ must exist and map every $\bar{\eta}$ to a unique equilibrium $\bar{q}$. We define $J_\eta(\eta)$ as the Jacobian of this map.

If these three hypotheses are simultaneously verified, then a differential kinematic model can be constructed, which goes directly from actuators space η to task space x:

$$\dot{x} = \overbrace{J(q(\eta))\underbrace{J_\eta(\eta)\dot{\eta}}_{\dot{q}}}^{\text{End-to-end Jacobian}}. \tag{37}$$

This is formally equivalent to (1) from a mathematical standpoint. Thus, a kinematic controller can be constructed by following the same line of reasoning of (35), resulting in the control action [Figure 12(a)]

$$\dot{\eta} = (J(q(\eta))J_\eta(\eta))^{+}(K_{\mathrm{e}}(\bar{x} - h(q(\eta))) + \dot{\bar{x}}). \tag{38}$$

This formulation is quite powerful since $J_\eta(q(\eta))J(\eta)$ is, in general, full rows rank as soon as the dimension of x is smaller than or equal to m. This property holds even if the soft robot's model is strongly underactuated ($n >> m$). This condition is visually represented by Figure 12(c). Consider, as an example, the case of a long soft tentacle, as in Figure 1, being actuated with three tendons and controlled to reach a goal location with the tip. A tentacle that is very soft or long can arguably require n to be much larger than three to be modeled correctly. Thus, in this example, $J(\eta) \in \mathbb{R}^{n\times 3}$ and $J_\eta(q(\eta)) \in \mathbb{R}^{3\times n}$ are strongly higher and lower rectangular matrices, respectively. Nevertheless, the end-to-end Jacobian in (37) is a 3×3 matrix, no matter the level of discretization n. Finally, it is worth noting that similar steps can be followed by bypassing the model of the actuator and directly reasoning on (2). This can be achieved by focusing on τ rather than on η. In this case, J_{a} can be derived from (11). A similar loop as (38) can thus be used to evaluate the control action in (29).

Several variations on the kinematic inversion strategies have been proposed in the literature. The Cosserat kinematic model is combined with linearized task space control in [179] and with sliding mode control in [180] and [181]. A visual servoing-based kinematic PCC model, where the camera looks at the robot, is used to devise the closed loop [182]. The inverse kinematics problem is tackled for parallel soft robots by relying on rigid link discretization in [52], on FEM models in [183], and on Cosserat parallel kinematics in [29] and [184].

As an alternative to the many assumptions required by the kinematic approximation, task space control of underactuated dynamic models can be directly embedded in the dynamic controller by relying on the operational space formulation [132], [185]. For classic rigid robots, this can be done by differentiating, one more time, (35) and combining the result with (16). Algebraic manipulations yield the operational, or task space, dynamics:

$$\underbrace{\Lambda(q)\ddot{x} + \eta(q, \dot{q}) + J_M^{+\mathsf{T}}(q)(G(q)}_{\text{Terms commonly found in rigid robots}} + K(q) + D(q)\dot{q}) = J_M^{+\mathsf{T}}(q)A(q)\tau \tag{39}$$

where the inertia matrix in the task space is $\Lambda = (JM^{-1}J^{\mathsf{T}})^{-1} \in \mathbb{R}^{m\times m}$, Coriolis and centrifugal terms are collected in $\eta(q, \dot{q}) = \Lambda(JM^{-1}C - \dot{J})\dot{q}$, and $J_M^{+} = M^{-1}J^{\mathsf{T}}\Lambda \in \mathbb{R}^{n\times m}$ is the dynamically consistent pseudoinverse. Equation (39) resembles the task space dynamics of a rigid robot, with two differences: the robot's impedance $K(q) + D(q)\dot{q}$ and the task space input field $J_M^{+\mathsf{T}}(q)A(q)$. The former does not introduce major differences since, in any case, the integrability of the potential field is lost in task coordinates. The latter can be solved in general since it admits the right-hand-side inverse

$$P_{\mathrm{M,A}}(q) = (J(q)M^{-1}(q)A(q))^{-1}J(q)M^{-1}(q) \tag{40}$$

for all configurations q such that $J(q)M^{-1}(q)A(q)$ is full rank [132]. As a result, $\tau = P_{\mathrm{M,A}}(q)J^{\mathsf{T}}(q)f$ generates fully actuated task space dynamics. Thus, direct extensions of standard operational space controllers [186] can be used to ensure that (34) holds for the full dynamic model (2) and possibly in the presence of strong underactuation ($m << n$). This control strategy is depicted in Figure 12(b) and (d). Note, however, that this is not sufficient to ensure that the full state $(q, \dot{q})$ converges to a steady state. How to design a provably stable task space dynamic controller in the presence of underaction remains an open problem. This is also a

challenge that is far from being solved for classic articulated robots [187].

Interaction With the Environment

Due to their inherent compliance, soft robots promise to revolutionize how robotic systems interact with the environment by bringing into the picture a new level of safety and robustness to unmodeled interactions when compared to standard rigid robots. Yet, most of the works on soft robot control deal with soft robots moving in free space. Moreover, planning algorithms are usually devised to explicitly avoid any interaction with the environment [51], [161], [188], [189], [190]. In practice, the controllers discussed in the preceding appear to work well when interactions with a passive environment occur. Yet, the literature analyzing interactions between the robot and an unstructured environment from a model-based perspective is limited.

Assume that the soft robot is interacting with the environment through a contact area, as in Figure 13. Then, a single point c can be identified as the contact centroid [191] such that the net effect of the contact pressure distributions is an equivalent wrench $f_{\text{ext}}, \tau_{\text{ext}} \in \mathbb{R}^3$ in c. This can be included in (2) as

$$M(q)\ddot{q} + C(q,\dot{q})\dot{q} + G(q) + D(q)\dot{q} + K(q) = \begin{bmatrix} A(q) & J_c^{\top}(q) \end{bmatrix} \begin{bmatrix} \tau \\ f_{\text{ext}} \\ \tau_{\text{ext}} \end{bmatrix} \tag{41}$$

where $J_c(q) \in \mathbb{R}^{6\times n}$ is the Jacobian mapping $\dot{q}$ to the linear and angular velocities of the robot in c. A way of characterizing interactions is to look at the Cartesian stiffness matrix, which quantifies the change of reaction forces as a result of a perturbation of the contact location. In unloaded conditions [192], [193], the physical Cartesian stiffness generated by the robot's softness is

$$K_x^{-1}(q) = J_c(q)\underbrace{\left(\frac{\partial K(q)}{\partial q} + \frac{\partial G(q)}{\partial q}\right)^{-1}}_{\substack{\text{Inverse of stiffness in} \\ \text{configuration space}}} J_c^{\top}(q) \in \mathbb{R}^{6\times 6} \tag{42}$$

with assumed constant A and constant τ. Note that (26) requires that the stiffness in q space is as high as possible for maximum open-loop stability. On the contrary, (42) requires the stiffness to remain small if the robot is required to behave compliantly in interactions with the environment. There is, therefore, a tradeoff between softness and stability that must be carefully considered during the robot's design phase. One way to resolve it is to consider ways of changing joint stiffness in time. Configuration space stiffness can be varied actively by relying on feedback control [112], [194] and passively by changing physical properties of the system [195], [196], [197]. The inversion of (42) is investigated in [198], [199], and [200]. The first two discuss how to prescribe stiffness in configuration space to achieve a desired Cartesian stiffness, while the third is the configuration q to be optimized. Direct Cartesian impedance control schemes have been proposed and experimentally validated by relying on the kinematic approximation (38) in [201] and the task space dynamic formulation (39) in [48]. An in-depth introduction to Cartesian impedance control for flexible systems is provided in [202]. As an alternative, the wrench f_{ext}, τ_{ext} can be directly regulated using Cartesian force control loops. This is achieved in [203] and [204] under the kinematic approximation (38). In [205], control inputs are numerically evaluated as the ones minimizing a weighted sum of interaction forces and error at the end effector and relying on a quasi-static FEM model. A similar strategy has been used to implement whole body manipulation [206] when a model of the environment is available.

Contrary to standard robots, soft robots may need to actively seek interactions with the environment (Figure 13). Indeed, external wrenches may be seen as an extra actuation source, as appears evident from (41). Thus, interactions can be used to overcome the limitations imposed by underactuation ($\text{Span}(A) \subset \mathbb{R}^n$) and input saturations ($\|\tau\| < c_\tau$). The use of external wrenches to sustain the robot's body is called bracing [207], and it is demonstrated with a soft robot in [118]. Alternatively, environmental interactions can be used to enlarge the accessible space. A planning method for vine robots that finds the sequence of interactions necessary to reach the desired locations is discussed in [208].

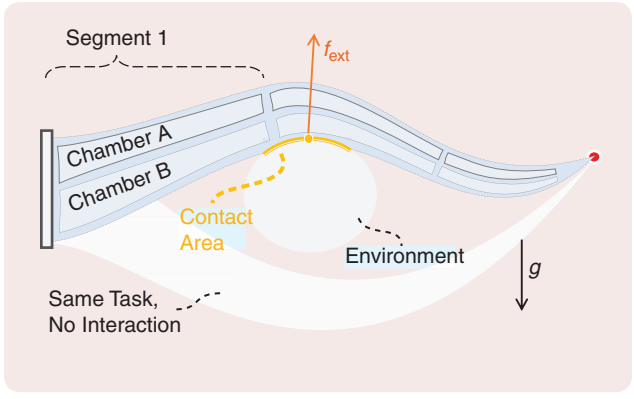

FIGURE 13 A soft robot composed of three pneumatically actuated segments and its relation with a simplified environment. The robot can achieve its tip positioning goal in two ways (the desired configuration is shown in red). It can plan its actions to avoid the environment altogether, or it can exploit the environment. In the latter case, the control design is more complex since it deals with parallel and possibly hybrid dynamics. On the other hand, the force f_{ext} exerted by the environment at the centroid of contact (shown as a yellow circle) relieves chambers A and B from the burden of sustaining the robot against gravity. If the contact is correctly preserved, it will also increase the stability margins of the system.

WHEN FIRST PRINCIPLE MODELS ALONE ARE NOT ENOUGH: LEVERAGING DATA AND MACHINE LEARNING IN MODEL-BASED CONTROL

As mentioned in the introduction, machine learning has been intensively used in the control of soft robots. Although many advancements have been made in model-based formulations, the importance of integrating data into a model-based perspective cannot be understated, especially in the soft robotics context. At this point of the survey, it will probably not come as a surprise that the main reasons are 1) difficulties in obtaining a complete model (for example, the actuators cannot be modeled from first principles, an accurate discretization would be too computationally expensive, and the environment cannot be known in advance) and 2) uncertainties are inherent in any soft robotic application (for example, unreliability of sensors and actuators as well as changes of physical parameters over time and over several iterations of the same device).

This section focuses on how learning can be integrated into a model-based framework to tackle the control of soft robots. Combining models with data is quite an active topic in the control community, and many solutions are currently being developed that will most likely find useful application in the soft robotic field [209], [210], [211], [212], [213]. It is beyond the scope of this work to discuss these new advancements. More details on the topic can be found in another survey article entirely focused on machine learning strategies for soft robots [214], which is contained in the same special issue of the present work.

Using Models to Drive Learning

The acquisition of new information and its transformation into a control action can be driven by the knowledge of (an approximation of) the model itself. This can be done while learning a feedback control as well as a feedforward action and by serving as a source of synthetic data for more standard machine learning approaches.

Adaptive Control

Adaptive control [Figure 14(a)] is an established technique in control theory [215] that augments feedback controllers with an online learning loop. The typical structure of an adaptive controller is

$$\dot{p} = \mathcal{L}(p, \tau, q, \dot{q}), \quad \tau = \tau_p(\bar{q}, \dot{\bar{q}}, \ddot{\bar{q}}, q, \dot{q}). \tag{43}$$

The uncertainty is represented as a set of unknown parameters $p \in \mathbb{R}^o$ appearing linearly in (1) or (2). The control action τ is generated through a model-based controller τ_p parameterized in p. For example, the dynamics of a CC segment, as discussed in "Dynamics of a Constant Curvature Segment," can be linearly parameterized in mL^2, mgL, $\int_0^1 k(s)\,ds$, and $\int_0^1 s\,d(s)\,ds$. These parameters and any of their subsets would create the vector p and thus appear in an adaptive version of (23). The model structure can guide the design of a learning rule $\mathcal{L}$ such that p is moved toward values that better explain the data. If $\mathcal{L}$ learns the parameters p that describe the real system, then from there, $\dot{p} = 0$, and τ_p behaves as a standard model-based controller.

Classic results in adaptive PD [216] and PD+ [217] control can be potentially applied to the soft robotic case by leveraging the equivalence exemplified by (16). Yet, the transfer is less direct than for the nonadaptive case. An adaptive visual servoing scheme is proposed in [218] by

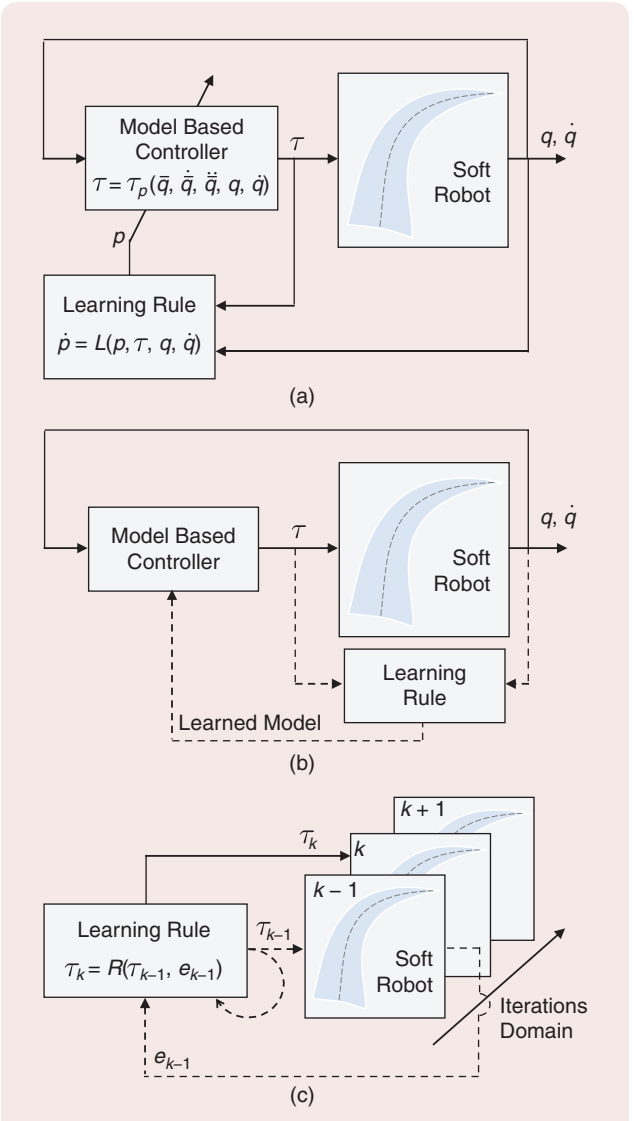

FIGURE 14 Three standard integration solutions between model-based controllers and learning rules. Dashed lines represent a transfer of information that happens on a different timescale. (a) An adaptive control architecture, where a learning loop L continuously updates a model-based controller. (b) A model is learned beforehand. The controller is designed once and for all based on the learned model. (c) A standard iterative learning control loop, where a feedforward action is updated by iteration. Here, the learning rule R itself is designed through model-based techniques.

relying on a kinematic PCC approximation. Linear adaptive control is used in [219] to control a single bending actuator. A similar strategy is applied to the control of a soft hand exoskeleton in [220] and [221], where the parameters of the human fingers are learned. An adaptive version of the MPC is discussed in [222] and [223] and experimentally validated against a nonadaptive MPC. A nonlinear adaptive controller originally developed for rigid robots is applied to soft robots in [224] and [225] by relying on an augmented rigid robot approximation. Adaptive schemes can also serve as a way of extending the effectiveness of linear controllers to changes in the operative point, as discussed in [14]. Adaptive control can be extended beyond known–unknowns by including p generic disturbances acting on the system. High-gain observers are used in [226] to estimate and compensate for the mismatch between a simplified linear model of a parallel soft robot and the real system. Also, [227] discusses the position regulation in Cartesian space for a soft robot with discretized but uncertain kinematics, including adaptive compensation of disturbances. An adaptive loop that learns the gains of a sliding mode controller is proposed in [228]. In classic robotics, this concept has been pushed even further by adding nonlinear black-box approximators borrowed from machine learning to the original dynamics and including their weights in the p vector [229], [230], [231].

Iterative Learning Control

As an alternative to learning the feedback loop, models can be used to guide the learning of a feedforward action [Figure 14(c)]. This can be done under the hypothesis that a same task can be tried out multiple times by the robot using iterative learning control (ILC) [232]. Define $k \in \mathbb{N}$ as the iteration index, which captures how many times the robot has attempted the execution of the task. Then, in this context, a learning rule R is a way of updating the feedforward action:

$$\tau_k(t) = R\left(\tau_{k-1}([0, t_f]), e_{k-1}([0, t_f])\right) \tag{44}$$

where $e(t)$ is a measure of how well the task has been executed at time t. Note that the learning rule R can, in general, combine information from the whole error and control evolution at step $k-1$. The design of R is driven by the knowledge of the nominal model, and it is defined in such a way that the robot learns a feedforward action $\tau_\infty(t)$ implementing a perfect execution of the task ($\|e_\infty\| = 0$). ILC is particularly suited for soft robots since 1) the learning process is robust to uncertainties in the model, 2) purely feedforward actions do not disrupt the physical softness of the system [112], and 3) the actions are inherently stable if the robot is not too soft. The actuation patterns necessary to track an optimal trajectory are learned using this technique in [118]. Crawling motions of soft worms have been improved via ILC in [233] and [234]. A linear discrete learning rule is used in [235] and [236] to control a soft spherical joint. Nonlinear ILC is used in [237] to control a soft finger. ILC is combined with an MPC in [238] and used to control a soft bending actuator mounted on a human finger. A continuous feedback-feedforward rule is proposed in [239] and applied to the swing up of a soft inverted pendulum.

Simulators as Virtual Environments

A more indirect way of using models to drive learning is by building simulators. Models developed from first principles can be used to create virtual environments where robots can evolve [240], [241] and learn new skills [99], [242], [243], [244]. Differentiable simulators are particularly suited to be used in this context, as discussed in [245].

Control Loops Based on Learned Models

Directly learning an end-to-end controller using standard machine learning techniques can present several disadvantages, such as limited explainability [246] and difficulties in ensuring performance and the stability of the closed loop. Moreover, the learning process may be ill conditioned due to the highly redundant nature of soft robots. An alternative to learning the controller is to learn the model and then use it within a model-based control framework.

Learning the Model by Using the Model

Approximation of dynamical systems is discussed in [247] and [248], and model learning for robot control is surveyed in [249]. When using fully black-box approximators, first principle models can still be used to generate a warm start for the learning process. For example, [250] uses a linear model of a pneumatic actuator for pretraining a neural network, which is then fine-tuned with experimental data. A nonlinear model of a multisegment soft robot is used in [251] to train a recurrent neural network. Even when a good model is already available, it can still be the case that learning strategies are used to better its performance. A method for learning only the nonlinear stiffness characteristics of a soft robot is discussed in [252]. The acquisition of data is driven by a FEM model of the elastic part. An optimal estimation strategy of geometrical quantities describing the robot kinematics is discussed in [253].

Closing the Loop

Once learned, the models can be used as a base for model-based control loops [Figure 14(b)]. In [254], a shallow neural network is used to learn the forward kinematics of a soft robot. Then, (38) is used to solve the inverse problem. Neural networks can be fully differentiable, and their Jacobian can be easily calculated. This is advantageous if compared to directly learning the inverse kinematics since (38) resolves automatically those redundancies that would make the direct learning of inverse kinematics ill posed.

Visual servoing under kinematic approximation for controlling the shape of a soft object is extended in [255] to the case where the Jacobian is estimated online. Similar strategies can also be employed in a dynamic setting. Whenever (22) is verified, learned models can be used to produce open-loop control actions that are ineherently stable [110], [256], [257]. Learned models can also be used when feedback is needed to stabilize the desired behavior. For example, a neural network is trained to approximate the update function of a soft segment in [258], and its input-output gradient is used to run a linear MPC algorithm. A similar strategy is used in [250]. However, the neural network is directly incorporated into an MPC control loop. Alternatively, Koopman theory enables directly learning linear dynamics evolving within a high-dimensional lifted space [259], [260], [261]. The resulting model has been used as a base for linear quadratic regulator [262] and linear MPC [221].

CONCLUSIONS

This article has surveyed control strategies for soft robots that rely on model-based formulations. Special attention has been devoted to organizing this large body of literature within a coherent framework and with a common terminology inspired by articulated robotics and robot control. Thanks to the latter, once the discretization of the infinite-dimensional space is introduced, the similarities among rigid, flexible, and soft robots become apparent. Connections with existing results developed outside soft robotics could therefore be drawn, and controllers could be ported from the articulated to the soft continuum world. On the other hand, using a common language pinpoints the fundamental differences between soft robotics and other related fields. The most apparent one is numerous degrees of freedom, making soft robots intrinsically underactuated, which makes control much more challenging than in other kinds of robotics. On the other hand, the positive definite elastic potential and the strictly dissipative force field are always present, no matter the level of discretization. These two actions behave as a physical control loop stabilizing the system and, thus, simplify the control problem enormously.

Notwithstanding the significant advancements achieved so far, the research community has barely scratched the model-based view's surface in soft robotics (see "Better Than Rigid Robots: Exploiting Softness in Model-Based Control"). Many are the challenges that remain open and the questions unanswered. How should underactuation be taken into account? To which extent can the nonactuated dynamics be neglected (or not)? Can generic unstable equilibria be stabilized? How can we implement motions that are simultaneously compliant, fast, and precise? How can we execute controlled movements involving continuous interactions with an unstructured environment? Can a complete integration of embodied intelligence and control design be reached within the model-based framework?

Finally, it should not be forgotten that soft robotics was born as an experimental discipline that aims to revolutionize how robots are entering our lives. Thus, all these theoretical advancements should contribute to realizing this grand vision by endowing real soft robots with unmatched motor capabilities.

ACKNOWLEDGMENT

The authors would like to thank Pietro Pustina, Hadi Sadati, Brandon Caasenbrood, Gregory Chirikjian, Lucas Ribeiro, Enrico Franco, Pablo Borja Rosales, and Audrey Sedal for their help in improving the quality and correctness of the manuscript. We are deeply grateful for the time they took from their busy schedules to work on it and for their many insightful comments. The work was in part supported under the European Union's Horizon Europe Program from Project EMERGE—Grant Agreement No. 101070918.

AUTHOR INFORMATION

Cosimo Della Santina (c.dellasantina@tudelft.nl) is an assistant professor at TU Delft, 2628 CD Delft, The Netherlands, and a research scientist at the German Aerospace Institute. He received the Ph.D. degree in robotics (cum laude, 2019) from the University of Pisa. He was a visiting Ph.D. student and a postdoc (2017 to 2019) at the Computer Science and Artificial Intelligence Laboratory, Massachusetts Institute of Technology. He was a senior postdoc (2020) and guest lecturer (2021) in the Department of Informatics, Technical University of Munich. He has been awarded the euRobotics Georges Giralt Ph.D. Award (2020) and the IEEE Robotics and Automation Society Fabrizio Flacco Young Author Award (2019), and he has been a finalist for the European Embedded Control Institute Ph.D. Award (2020). In 2023, he received the IEEE RAS Early Academic Career Award in Robotics and Automation. His research interests include the motor intelligence of physical systems, with a focus on elastic and soft robots.

Christian Duriez received an engineering degree from the Institut Catholique d'Arts et Métiers, Lille, France, and the Ph.D. degree in robotics from the University of Evry, France. His thesis was realized at CEA/Robotics and Interactive Systems Technologies, followed by a postdoctoral position at the CIMIT SimGroup, Boston, MA, USA. He arrived at the National Institute for Research in Digital Science and Technology (INRIA), 59000 Lille, France, in 2006, joining the ALCOVE team to work on the interactive simulation of deformable objects and haptic rendering. In 2009, he was the vice-head of the Simulation in Healthcare Using Computer Research Advances team and focused on medical simulation. He is now the head of the Deformable Robotic Software team, created in January 2015. His research interests include soft robot models and control, fast finite-element methods, simulation of contact response, and other complex mechanical

interactions. All his research results are developed in Simulation Open Framework Architecture, a framework that he codevelops with other INRIA teams. He was also one of the founders of the startup company InSimo.

Daniela Rus is the Andrew (1956) and Erna Viterbi Professor of Electrical Engineering and Computer Science, and director of the Computer Science and Artificial Intelligence Laboratory, at the Massachusetts Institute of Technology (MIT), Cambridge, MA 02139 USA. Her research interests include robotics and artificial intelligence. The key focus of her research is to develop the science and engineering of autonomy. She is a senior visiting fellow at MITRE Corporation. She currently serves as a U.S. expert for Global Partnerships in AI, a member of the board of trustees of Mohamed Bin Zayed University of Artificial Intelligence, a member of the British Telecom Technology Advisory Board, and a member of the board of directors of Mass Robotics. She also served as deputy dean of research in the Schwarzman College of Computing, MIT, from 2019 to 2022. She is a MacArthur Fellow; a Fellow of IEEE, the Association for Computing Machinery, the Association for the Advancement of Artificial Intelligence, and the American Association for the Advancement of Science; and a member of the National Academy of Engineering and the American Academy of Arts and Sciences. She is the recipient of the Engelberger Award for Robotics, IEEE Robotics and Automation Society (RAS) Pioneer Award, RAS Technical Award, Mass Technology Leadership Council Innovation Catalyst Award, and International Joint Conferences on Artificial Intelligence John McCarthy Award. She earned the Ph.D. degree in computer science from Cornell University.

REFERENCES

[1] C. Della Santina, M. G. Catalano, and A. Bicchi, "Soft robots," in *Encyclopedia of Robotics*, M. H. Ang, O. Khatib, and B. Siciliano, Eds. Berlin, Germany: Springer-Verlag, 2021, pp. 1–15.

[2] D. Trivedi, C. D. Rahn, W. M. Kier, and I. D. Walker, "Soft robotics: Biological inspiration, state of the art, and future research," *Appl. Bionics Biomechanics*, vol. 5, no. 3, pp. 99–117, Jan. 2008, doi: 10.1155/2008/520417.

[3] R. Pfeifer, M. Lungarella, and F. Iida, "The challenges ahead for bio-inspired 'soft' robotics," *Commun. ACM*, vol. 55, no. 11, pp. 76–87, Nov. 2012, doi: 10.1145/2366316.2366335.

[4] S. Kim, C. Laschi, and B. Trimmer, "Soft robotics: A bioinspired evolution in robotics," *Trends Biotechnol.*, vol. 31, no. 5, pp. 287–294, May 2013, doi: 10.1016/j.tibtech.2013.03.002.

[5] D. Rus and M. T. Tolley, "Design, fabrication and control of soft robots," *Nature*, vol. 521, no. 7553, pp. 467–475, May 2015, doi: 10.1038/nature14543.

[6] C. Laschi, B. Mazzolai, and M. Cianchetti, "Soft robotics: Technologies and systems pushing the boundaries of robot abilities," *Sci. Robot.*, vol. 1, no. 1, Dec. 2016, Art. no. eaah3690, doi: 10.1126/scirobotics.aah3690.

[7] M. Calisti, G. Picardi, and C. Laschi, "Fundamentals of soft robot locomotion," *J. Roy. Soc. Interface*, vol. 14, no. 130, May 2017, Art. no. 20170101, doi: 10.1098/rsif.2017.0101.

[8] M. Cianchetti, C. Laschi, A. Menciassi, and P. Dario, "Biomedical applications of soft robotics," *Nature Rev. Mater.*, vol. 3, no. 6, pp. 143–153, Jun. 2018, doi: 10.1038/s41578-018-0022-y.

[9] H. Wang, M. Totaro, and L. Beccai, "Toward perceptive soft robots: Progress and challenges," *Adv. Sci.*, vol. 5, no. 9, Sep. 2018, Art. no. 1800541, doi: 10.1002/advs.201800541.

[10] F. Chen and M. Y. Wang, "Design optimization of soft robots: A review of the state of the art," *IEEE Robot. Autom. Mag.*, vol. 27, no. 4, pp. 27–43, Dec. 2020, doi: 10.1109/MRA.2020.3024280.

[11] T. G. Thuruthel, Y. Ansari, E. Falotico, and C. Laschi, "Control strategies for soft robotic manipulators: A survey," *Soft Robot.*, vol. 5, no. 2, pp. 149–163, Apr. 2018, doi: 10.1089/soro.2017.0007.

[12] C. Armanini, C. Messer, A. T. Mathew, F. Boyer, C. Duriez, and F. Renda, "Soft robots modeling: A literature unwinding," 2021, *arXiv:2112.03645*.

[13] B. Deutschmann, A. Dietrich, and C. Ott, "Position control of an underactuated continuum mechanism using a reduced nonlinear model," in *Proc. IEEE 56th Annu. Conf. Decis. Control (CDC)*, 2017, pp. 5223–5230, doi: 10.1109/CDC.2017.8264433.

[14] J. Muñoz, D. S. Copaci, C. A. Monje, D. Blanco, and C. Balaguer, "Isom based adaptive fractional order control with application to a soft robotic neck," *IEEE Access*, vol. 8, pp. 198,964–198,976, Nov. 2020, doi: 10.1109/ACCESS.2020.3035450.

[15] R. Niiyama, A. Nagakubo, and Y. Kuniyoshi, "Mowgli: A bipedal jumping and landing robot with an artificial musculoskeletal system," in *Proc. IEEE Int. Conf. Robot. Automat.*, 2007, pp. 2546–2551, doi: 10.1109/ROBOT.2007.363848.

[16] P. Brochu and Q. Pei, "Dielectric elastomers for actuators and artificial muscles," in *Electroactivity Polymeric Materials*, L. Rasmussen, Ed. Boston, MA, USA: Springer-Verlag, 2012, pp. 1–56.

[17] N. Kellaris et al., "Spider-inspired electrohydraulic actuators for fast, soft-actuated joints," *Adv. Sci.*, vol. 8, no. 14, Jul. 2021, Art. no. 2100916, doi: 10.1002/advs.202100916.

[18] G. S. Chirikjian, "Theory and applications of hyper-redundant robotic manipulators," Ph.D. dissertation, California Institute of Technology, Pasadena, CA, USA, 1992.

[19] G. S. Chirikjian, "Conformational modeling of continuum structures in robotics and structural biology: A review," *Adv. Robot.*, vol. 29, no. 13, pp. 817–829, Jul. 2015, doi: 10.1080/01691864.2015.1052848.

[20] H. Mochiyama and H. Kobayashi, "The shape Jacobian of a manipulator with hyper degrees of freedom," in *Proc. IEEE Int. Conf. Robot. Automat. (Cat. No. 99CH36288C)*, 1999, vol. 4, pp. 2837–2842, doi: 10.1109/ROBOT.1999.774027.

[21] B. D. Coleman, E. H. Dill, M. Lembo, Z. Lu, and I. Tobias, "On the dynamics of rods in the theory of Kirchhoff and Clebsch," *Arch. Rational Mech. Anal.*, vol. 121, no. 4, pp. 339–359, Dec. 1993, doi: 10.1007/BF00375625.

[22] J. Spillmann and M. Teschner, "Corde: Cosserat rod elements for the dynamic simulation of one-dimensional elastic objects," in *Proc. ACM SIGGRAPH/Eurogr. Symp. Comput. Animation*, 2007, pp. 63–72.

[23] H. Lang, J. Linn, and M. Arnold, "Multi-body dynamics simulation of geometrically exact cosserat rods," *Multibody Syst. Dyn.*, vol. 25, no. 3, pp. 285–312, Mar. 2011, doi: 10.1007/s11044-010-9223-x.

[24] M. Gazzola, L. Dudte, A. McCormick, and L. Mahadevan, "Forward and inverse problems in the mechanics of soft filaments," *Roy. Soc. Open Sci.*, vol. 5, no. 6, Jun. 2018, Art. no. 171628, doi: 10.1098/rsos.171628.

[25] D. Trivedi, A. Lotfi, and C. D. Rahn, "Geometrically exact models for soft robotic manipulators," *IEEE Trans. Robot.*, vol. 24, no. 4, pp. 773–780, Aug. 2008, doi: 10.1109/TRO.2008.924923.

[26] D. C. Rucker and R. J. Webster III, "Statics and dynamics of continuum robots with general tendon routing and external loading," *IEEE Trans. Robot.*, vol. 27, no. 6, pp. 1033–1044, Dec. 2011, doi: 10.1109/TRO.2011.2160469.

[27] F. Renda, M. Giorelli, M. Calisti, M. Cianchetti, and C. Laschi, "Dynamic model of a multibending soft robot arm driven by cables," *IEEE Trans. Robot.*, vol. 30, no. 5, pp. 1109–1122, Oct. 2014, doi: 10.1109/TRO.2014.2325992.

[28] C. E. Bryson and D. C. Rucker, "Toward parallel continuum manipulators," in *Proc. IEEE Int. Conf. Robot. Automat. (ICRA)*, 2014, pp. 778–785, doi: 10.1109/ICRA.2014.6906943.

[29] C. B. Black, J. Till, and D. C. Rucker, "Parallel continuum robots: Modeling, analysis, and actuation-based force sensing," *IEEE Trans. Robot.*, vol. 34, no. 1, pp. 29–47, Feb. 2018, doi: 10.1109/TRO.2017.2753829.

[30] F. Janabi-Sharifi, A. Jalali, and I. Walker, "Cosserat rod-based dynamic modeling of tendon-driven continuum robots: A tutorial," *IEEE Access*, vol. 9, pp. 68,703–68,719, May 2021, doi: 10.1109/ACCESS.2021.3077186.

[31] F. Renda, C. Armanini, V. Lebastard, F. Candelier, and F. Boyer, "A geometric variable-strain approach for static modeling of soft manipulators with tendon and fluidic actuation," *IEEE Robot. Autom. Lett.*, vol. 5, no. 3, pp. 4006–4013, Jul. 2020, doi: 10.1109/LRA.2020.2985620.

[32] A. L. Orekhov and N. Simaan, "Solving cosserat rod models via collocation and the magnus expansion," 2020, *arXiv:2008.01054*.

[33] J. Till, V. Aloi, and C. Rucker, "Real-time dynamics of soft and continuum robots based on cosserat rod models," *Int. J. Robot. Res.*, vol. 38, no. 6, pp. 723–746, May 2019, doi: 10.1177/0278364919842269.

[34] B. Thamo, K. Dhaliwal, and M. Khadem, "Rapid solution of cosserat rod equations via a nonlinear partial observer," in *Proc. IEEE Int. Conf. Robot. Automat. (ICRA)*, 2021, pp. 9433–9438, doi: 10.1109/ICRA48506.2021.95C61588.
[35] S. Zaidi, M. Maselli, C. Laschi, and M. Cianchetti, "Actuation technologies for soft robot grippers and manipulators: A review," *Current Robot. Rep.*, vol. 2, no. 3, pp. 355–369, Sep. 2021, doi: 10.1007/s43154-021-00054-5.
[36] R. J. Webster III and B. A. Jones, "Design and kinematic modeling of constant curvature continuum robots: A review," *Int. J. Robot. Res.*, vol. 29, no. 13, pp. 1661–1683, Nov. 2010, doi: 10.1177/0278364910368147.
[37] B. A. Jones and I. D. Walker, "Limiting-case analysis of continuum trunk kinematics," in *Proc. IEEE Int. Conf. Robot. Automat.*, 2007, pp. 1363–1368, doi: 10.1109/ROBOT.2007.363174.
[38] A. Chawla, C. Frazelle, and I. Walker, "A comparison of constant curvature forward kinematics for multisection continuum manipulators," in *Proc. 2nd IEEE Int. Conf. Robot. Comput. (IRC)*, 2018, pp. 217–223, doi: 10.1109/IRC.2018.00046.
[39] W. Felt et al., "An inductance-based sensing system for bellows-driven continuum joints in soft robots," *Auton. Robots*, vol. 43, no. 2, pp. 435–448, Feb. 2019, doi: 10.1007/s10514-018-9769-7.
[40] T. F. Allen, L. Rupert, T. R. Duggan, G. Hein, and K. Albert, "Closed-form non-singular constant-curvature continuum manipulator kinematics," in *Proc. 3rd IEEE Int. Conf. Soft Robot. (RoboSoft)*, 2020, pp. 410–416, doi: 10.1109/RoboSoft48309.2020.9116015.
[41] C. D. Santina, A. Bicchi, and D. Rus, "On an improved state parametrization for soft robots with piecewise constant curvature and its use in model based control," *IEEE Robot. Autom. Lett.*, vol. 5, no. 2, pp. 1001–1008, Apr. 2020, doi: 10.1109/LRA.2020.2967269.
[42] S. Sadati et al., "A geometry deformation model for braided continuum manipulators," *Front. Robot. AI*, vol. 4, Jun. 2017, Art. no. 22, doi: 10.3389/frobt.2017.00022.
[43] I. S. Godage, G. A. Medrano-Cerda, D. T. Branson, E. Guglielmino, and D. G. Caldwell, "Dynamics for variable length multisection continuum arms," *Int. J. Robot. Res.*, vol. 35, no. 6, pp. 695–722, May 2016, doi: 10.1177/0278364915596450.
[44] V. Falkenhahn, T. Mahl, A. Hildebrandt, R. Neumann, and O. Sawodny, "Dynamic modeling of bellows-actuated continuum robots using the Euler–Lagrange formalism," *IEEE Trans. Robot.*, vol. 31, no. 6, pp. 1483–1496, Dec. 2015, doi: 10.1109/TRO.2015.2496826.
[45] H. Wang, C. Wang, W. Chen, X. Liang, and Y. Liu, "Three-dimensional dynamics for cable-driven soft manipulator," *IEEE/ASME Trans. Mechatron.*, vol. 22, no. 1, pp. 18–28, Feb. 2017, doi: 10.1109/TMECH.2016.2606547.
[46] I. S. Godage, R. Wirz, I. D. Walker, and R. J. Webster III, "Accurate and efficient dynamics for variable-length continuum arms: A center of gravity approach," *Soft Robot.*, vol. 2, no. 3, pp. 96–106, Sep. 2015, doi: 10.1089/soro.2015.0006.
[47] I. S. Godage, R. J. Webster, and I. D. Walker, "Center-of-gravity-based approach for modeling dynamics of multisection continuum arms," *IEEE Trans. Robot.*, vol. 35, no. 5, pp. 1097–1108, Oct. 2019, doi: 10.1109/TRO.2019.2921153.
[48] C. Della Santina, R. K. Katzschmann, A. Bicchi, and D. Rus, "Model-based dynamic feedback control of a planar soft robot: Trajectory tracking and interaction with the environment," *Int. J. Robot. Res.*, vol. 39, no. 4, pp. 490–513, Mar. 2020, doi: 10.1177/0278364919897292.
[49] R. K. Katzschmann, C. Della Santina, Y. Toshimitsu, A. Bicchi, and D. Rus, "Dynamic motion control of multi-segment soft robots using piecewise constant curvature matched with an augmented rigid body model," in *Proc. 2nd IEEE Int. Conf. Soft Robot. (RoboSoft)*, 2019, pp. 454–461, doi: 10.1109/ROBOSOFT.2019.8722799.
[50] R. Kang, D. T. Branson, E. Guglielmino, and D. G. Caldwell, "Dynamic modeling and control of an octopus inspired multiple continuum arm robot," *Comput. Math. Appl.*, vol. 64, no. 5, pp. 1004–1016, Sep. 2012, doi: 10.1016/j.camwa.2012.03.018.
[51] R. J. Roesthuis and S. Misra, "Steering of multisegment continuum manipulators using rigid-link modeling and FBG-based shape sensing," *IEEE Trans. Robot.*, vol. 32, no. 2, pp. 372–382, Apr. 2016, doi: 10.1109/TRO.2016.2527047.
[52] O. Altuzarra, D. Caballero, F. J. Campa, and C. Pinto, "Position analysis in planar parallel continuum mechanisms," *Mechanism Mach. Theory*, vol. 132, pp. 13–29, Feb. 2019, doi: 10.1016/j.mechmachtheory.2018.10.014.
[53] K. Nuelle, T. Sterneck, S. Lilge, D. Xiong, J. Burgner-Kahrs, and T. Ortmaier, "Modeling, calibration, and evaluation of a tendon-actuated planar parallel continuum robot," *IEEE Robot. Autom. Lett.*, vol. 5, no. 4, pp. 5811–5818, Jul. 2020, doi: 10.1109/LRA.2020.3010213.
[54] G. Chen, Y. Kang, Z. Liang, Z. Zhang, and H. Wang, "Kinetostatics modeling and analysis of parallel continuum manipulators," *Mechanism Mach. Theory*, vol. 163, Sep. 2021, Art. no. 104380, doi: 10.1016/j.mechmachtheory.2021.104380.
[55] F. Renda, F. Boyer, J. Dias, and L. Seneviratne, "Discrete cosserat approach for multisection soft manipulator dynamics," *IEEE Trans. Robot.*, vol. 34, no. 6, pp. 1518–1533, Dec. 2018, doi: 10.1109/TRO.2018.2868815.
[56] S. Grazioso, G. Di Gironimo, and B. Siciliano, "A geometrically exact model for soft continuum robots: The finite element deformation space formulation," *Soft Robot.*, vol. 6, no. 6, pp. 790–811, Dec. 2019, doi: 10.1089/soro.2018.0047.
[57] C. Armanini, I. Hussain, M. Z. Iqbal, D. Gan, D. Prattichizzo, and F. Renda, "Discrete cosserat approach for closed-chain soft robots: Application to the finray finger," *IEEE Trans. Robot.*, vol. 37, no. 6, pp. 2083–2098, Dec. 2021, doi: 10.1109/TRO.2021.3075643.
[58] R. Featherstone, *Rigid Body Dynamics Algorithms*. New York, NY, USA: Springer-Verlag, 2014.
[59] A. De Luca and W. J. Book, "Robots with flexible elements," in *Springer Handbook of Robotics*, B. Siciliano and O. Khatib, Eds. Berlin, Germany: Springer-Verlag, 2016, pp. 243–282.
[60] W. J. Book, "Recursive lagrangian dynamics of flexible manipulator arms," *Int. J. Robot. Res.*, vol. 3, no. 3, pp. 87–101, Sep. 1984, doi: 10.1177/027836498400300305.
[61] A. De Luca and B. Siciliano, "Inversion-based nonlinear control of robot arms with flexible links," *J. Guid., Control, Dyn.*, vol. 16, no. 6, pp. 1169–1176, Nov. 1993, doi: 10.2514/3.21142.
[62] G. S. Chirikjian and J. W. Burdick, "A modal approach to hyper-redundant manipulator kinematics," *IEEE Trans. Robot. Autom. (1989–June 2004)*, vol. 10, no. 3, pp. 343–354, Jun. 1994, doi: 10.1109/70.294209.
[63] S. H. Sadati, S. E. Naghibi, I. D. Walker, K. Althoefer, and T. Nanayakkara, "Control space reduction and real-time accurate modeling of continuum manipulators using ritz and ritz–galerkin methods," *IEEE Robot. Autom. Lett.*, vol. 3, no. 1, pp. 328–335, Jan. 2018, doi: 10.1109/LRA.2017.2743100.
[64] I. Singh, Y. Amara, A. Melingui, P. M. Pathak, and R. Merzouki, "Modeling of continuum manipulators using pythagorean hodograph curves," *Soft Robot.*, vol. 5, no. 4, pp. 425–442, Aug. 2018, doi: 10.1089/soro.2017.0111.
[65] I. S. Godage, D. T. Branson, E. Guglielmino, G. A. Medrano-Cerda, and D. G. Caldwell, "Shape function-based kinematics and dynamics for variable length continuum robotic arms," in *Proc. IEEE Int. Conf. Robot. Automat.*, 2011, pp. 452–457, doi: 10.1109/ICRA.2011.5979607.
[66] I. S. Godage, E. Guglielmino, D. T. Branson, G. A. Medrano-Cerda, and D. G. Caldwell, "Novel modal approach for kinematics of multisection continuum arms," in *Proc. IEEE/RSJ Int. Conf. Intell. Robots Syst.*, 2011, pp. 1093–1098, doi: 10.1109/IROS.2011.6094477.
[67] D. Navarro-Alarcon and Y.-H. Liu, "Fourier-based shape servoing: A new feedback method to actively deform soft objects into desired 2-d image contours," *IEEE Trans. Robot.*, vol. 34, no. 1, pp. 272–279, Feb. 2018, doi: 10.1109/TRO.2017.2765333.
[68] J. Qi, W. Ma, D. Navarro-Alarcon, H. Gao, and G. Ma, "Adaptive shape servoing of elastic rods using parameterized regression features and auto-tuning motion controls," 2020, *arXiv:2008.06896*.
[69] G. Palli, "Model-based manipulation of deformable linear objects by multivariate dynamic splines," in *Proc. IEEE Conf. Ind. Cyberphysical Syst. (ICPS)*, 2020, vol. 1, pp. 520–525, doi: 10.1109/ICPS48405.2020.9274730.
[70] R. Echter and M. Bischoff, "Numerical efficiency, locking and unlocking of NURBS finite elements," *Comput. Methods Appl. Mech. Eng.*, vol. 199, nos. 5–8, pp. 374–382, Jan. 2010, doi: 10.1016/j.cma.2009.02.035.
[71] L. Greco and M. Cuomo, "B-Spline interpolation of Kirchhoff-Love space rods," *Comput. Methods Appl. Mech. Eng.*, vol. 256, pp. 251–269, Apr. 2013, doi: 10.1016/j.cma.2012.11.017.
[72] C. Della Santina and D. Rus, "Control oriented modeling of soft robots: The polynomial curvature case," *IEEE Robot. Autom. Lett.*, vol. 5, no. 2, pp. 290–298, Apr. 2020, doi: 10.1109/LRA.2019.2955936.
[73] C. Della Santina, "The soft inverted pendulum with affine curvature," in *Proc. 59th IEEE Conf. Decis. Control (CDC)*, 2020, pp. 4135–4142, doi: 10.1109/CDC42340.2020.9303976.
[74] F. Boyer, V. Lebastard, F. Candelier, and F. Renda, "Dynamics of continuum and soft robots: A strain parameterization based approach," *IEEE Trans. Robot.*, vol. 37, no. 3, pp. 847–863, Jun. 2021, doi: 10.1109/TRO.2020.3036618.
[75] S. Briot and F. Boyer, "A geometrically exact assumed strain modes approach for the geometrico- and kinemato-static modelings of continuum parallel robots," *IEEE Trans. Robot.*, early access, 2022, doi: 10.1109/TRO.2022.3219777.
[76] W. Rust, *Non-Linear Finite Element Analysis in Structural Mechanics*. Cham, Switzerland: Springer-Verlag, 2015.
[77] W. B. Zimmerman, *Multiphysics Modeling with Finite Element Methods*, vol. 18. Singapore: World Scientific, 2006.
[78] Z.-Q. Qu, *Model Order Reduction Techniques with Applications in Finite Element Analysis: With Applications in Finite Element Analysis*. London, U.K.: Springer-Verlag, 2004.
[79] O. Goury and C. Duriez, "Fast, generic, and reliable control and simulation of soft robots using model order reduction," *IEEE Trans. Robot.*, vol. 34, no. 6, pp. 1565–1576, Dec. 2018, doi: 10.1109/TRO.2018.2861900.

[80] G. Kerschen, M. Peeters, J.-C. Golinval, and A. F. Vakakis, "Nonlinear normal modes, Part I: A useful framework for the structural dynamicist," *Mech. Syst. Signal Process.*, vol. 23, no. 1, pp. 170–194, Jan. 2009, doi: 10.1016/j.ymssp.2008.04.002.
[81] F. S. Sin, D. Schroeder, and J. Barbič, "Vega: Non-linear FEM deformable object simulator," in *Computer Graphics Forum*, vol. 32. Oxford, U.K.: Blackwell, 2013, pp. 36–48.
[82] J. Chenevier, D. González, J. V. Aguado, F. Chinesta, and E. Cueto, "Reduced-order modeling of soft robots," *PLoS One*, vol. 13, no. 2, Feb. 2018, Art. no. e0192052, doi: 10.1371/journal.pone.0192052.
[83] X. Yi and G. S. Chirikjian, "When kinematics dominates mechanics: Locally volume-preserving primitives for model reduction in finite elasticity," 2022, *arXiv:2202.09270*.
[84] O. Goury, B. Carrez, and C. Duriez, "Real-time simulation for control of soft robots with self-collisions using model order reduction for contact forces," *IEEE Robot. Autom. Lett.*, vol. 6, no. 2, pp. 3752–3759, Mar. 2021, doi: 10.1109/LRA.2021.3064247.
[85] J. Oliver, A. E. Huespe, and P. J. Sánchez, "A comparative study on finite elements for capturing strong discontinuities: E-FEM vs x-FEM," *Comput. Methods Appl. Mech. Eng.*, vol. 195, nos. 37–40, pp. 4732–4752, Jul. 2006, doi: 10.1016/j.cma.2005.09.020.
[86] A. Yazid, N. Abdelkader, and H. Abdelmadjid, "A state-of-the-art review of the x-FEM for computational fracture mechanics," *Appl. Math. Modelling*, vol. 33, no. 12, pp. 4269–4282, Dec. 2009, doi: 10.1016/j.apm.2009.02.010.
[87] M. Paz, "Dynamic condensation," *AIAA J.*, vol. 22, no. 5, pp. 724–727, May 1984, doi: 10.2514/3.48498.
[88] C. Duriez, "Control of elastic soft robots based on real-time finite element method," in *Proc. IEEE Int. Conf. Robot. Automat.*, 2013, pp. 3982–3987, doi: 10.1109/ICRA.2013.6631138.
[89] Y. Adagolodjo, F. Renda, and C. Duriez, "Coupling numerical deformable models in global and reduced coordinates for the simulation of the direct and the inverse kinematics of soft robots," *IEEE Robot. Autom. Lett.*, vol. 6, no. 2, pp. 3910–3917, Apr. 2021, doi: 10.1109/LRA.2021.3061977.
[90] S. Sadati, S. E. Naghibi, L. Da Cruz, and C. Bergeles, "Reduced-order modeling and model order reduction for soft robots," *Front. Robot.* AI, to be published. [Online]. Available:https://www.researchgate.net/publication/346038019_Reduced-Order_Modeling_and_Model_Order_Reduction_for_Soft_Robots
[91] M. W. Spong, "Modeling and control of elastic joint robots," *J. Dyn. Syst., Meas., Control*, vol. 109, no. 4, pp. 310–318, Dec. 1987, doi: 10.1115/1.3143860.
[92] C. D. Santina, "Flexible manipulators," in *Encyclopedia of Robotics*, M. H. Ang, O. Khatib, and B. Siciliano, Eds. Berlin, Germany: Springer-Verlag, 2021, pp. 1–15.
[93] G. Pittiglio et al., "Magnetic levitation for soft-tethered capsule colonoscopy actuated with a single permanent magnet: A dynamic control approach," *IEEE Robot. Autom. Lett.*, vol. 4, no. 2, pp. 1224–1231, Apr. 2019, doi: 10.1109/LRA.2019.2894907.
[94] P. V. Kokotovic, R. E. O'Malley Jr., and P. Sannuti, "Singular perturbations and order reduction in control theory—An overview," *Automatica*, vol. 12, no. 2, pp. 123–132, Mar. 1976, doi: 10.1016/0005-1098(76)90076-5.
[95] J. Allard et al., "SOFA – An open source framework for medical simulation," in *Proc. Med. Meets Virtual Reality (MMVR)*, Bristol, U.K.: IOP Press, 2007, vol. 125, pp. 13–18.
[96] E. Coevoet et al., "Software toolkit for modeling, simulation, and control of soft robots," *Adv. Robot.*, vol. 31, no. 22, pp. 1208–1224, Nov. 2017, doi: 10.1080/01691864.2017.1395362.
[97] P. Ma et al., "Diffaqua: A differentiable computational design pipeline for soft underwater swimmers with shape interpolation," *ACM Trans. Graph.*, vol. 40, no. 4, pp. 1–14, Jul. 2021, doi: 10.1145/3450626.3459832.
[98] Y. Hu et al., "ChainQueen: A real-time differentiable physical simulator for soft robotics," in *Proc. IEEE Int. Conf. Robot. Automat. (ICRA)*, 2019, pp. 6265–6271, doi: 10.1109/ICRA.2019.8794333.
[99] N. Naughton, J. Sun, A. Tekinalp, T. Parthasarathy, G. Chowdhary, and M. Gazzola, "Elastica: A compliant mechanics environment for soft robotic control," *IEEE Robot. Autom. Lett.*, vol. 6, no. 2, pp. 3389–3396, Apr. 2021, doi: 10.1109/LRA.2021.3063698.
[100] S. H. Sadati et al., "TMTDyn: A Matlab package for modeling and control of hybrid rigid–continuum robots based on discretized lumped systems and reduced-order models," *Int. J. Robot. Res.*, vol. 40, no. 1, pp. 296–347, Jan. 2021, doi: 10.1177/0278364919881685.
[101] B. Angles et al., "Viper: Volume invariant position-based elastic rods," in *Proc. ACM Comput. Graph. Interactive Techn.*, 2019, vol. 2, no. 2, pp. 1–26, doi: 10.1145/3340260.
[102] A. T. Mathew, I. B. Hmida, C. Armanini, F. Boyer, and F. Renda, "A MATLAB toolbox for hybrid rigid soft robots based on the geometric variable strain approach," 2021, *arXiv:2107.05494*.
[103] J. Collins, S. Chand, A. Vanderkop, and D. Howard, "A review of physics simulators for robotic applications," *IEEE Access*, vol. 9, pp. 51,416–51,431, Mar. 2021, doi: 10.1109/ACCESS.2021.3068769.
[104] M. T. Chikhaoui, S. Lilge, S. Kleinschmidt, and J. Burgner-Kahrs, "Comparison of modeling approaches for a tendon actuated continuum robot with three extensible segments," *IEEE Robot. Autom. Lett.*, vol. 4, no. 2, pp. 989–996, Apr. 2019, doi: 10.1109/LRA.2019.2893610.
[105] P. Rao, Q. Peyron, S. Lilge, and J. Burgner-Kahrs, "How to model tendon-driven continuum robots and benchmark modelling performance," *Frontiers Robot. AI*, vol. 7, Feb. 2021, Art. no. 223, doi: 10.3389/frobt.2020.630245.
[106] K. J. Åström and T. Hägglund, "The future of PID control," *Control Eng. Pract.*, vol. 9, no. 11, pp. 1163–1175, Nov. 2001, doi: 10.1016/S0967-0661(01)00062-4.
[107] R. Kelly and R. Carelli, "A class of nonlinear PD-type controllers for robot manipulators," *J. Robot. Syst.*, vol. 13, no. 12, pp. 793–802, Dec. 1996, doi: 10.1002/(SICI)1097-4563(199612)13:12<793::AID-ROB2>3.0.CO;2-Q.
[108] R. Kelly, "PD control with desired gravity compensation of robotic manipulators: A review," *Int. J. Robot. Res.*, vol. 16, no. 5, pp. 660–672, Oct. 1997, doi: 10.1177/027836499701600505.
[109] R. Kelly, "Global positioning of robot manipulators via PD control plus a class of nonlinear integral actions," *IEEE Trans. Autom. Control*, vol. 43, no. 7, pp. 934–938, Jul. 1998, doi: 10.1109/9.701091.
[110] T. G. Thuruthel, E. Falotico, M. Manti, and C. Laschi, "Stable open loop control of soft robotic manipulators," *IEEE Robot. Autom. Lett.*, vol. 3, no. 2, pp. 1292–1298, Apr. 2018, doi: 10.1109/LRA.2018.2797241.
[111] F. Bosi, D. Misseroni, F. Dal Corso, S. Neukirch, and D. Bigoni, "Asymptotic self-restabilization of a continuous elastic structure," *Physical Rev. E*, vol. 94, no. 6, Dec. 2016, Art. no. 063005, doi: 10.1103/PhysRevE.94.063005.
[112] C. D. Santina et al., "Controlling soft robots: Balancing feedback and feedforward elements," *IEEE Robot. Autom. Mag.*, vol. 24, no. 3, pp. 75–83, Sep. 2017, doi: 10.1109/MRA.2016.2636360.
[113] A. H. Khan, Z. Shao, S. Li, Q. Wang, and N. Guan, "Which is the best PID variant for pneumatic soft robots? An experimental study," *IEEE/CAA J. Autom. Sin.*, vol. 7, no. 2, pp. 451–460, Mar. 2020, doi: 10.1109/JAS.2020.1003045.
[114] D. Copaci, J. Muñoz, I. González, C. A. Monje, and L. Moreno, "SMA-driven soft robotic neck: Design, control and validation," *IEEE Access*, vol. 8, pp. 199,492–199,502, Nov. 2020, doi: 10.1109/ACCESS.2020.3035510.
[115] S. Kawamura, F. Miyazaki, and S. Arimoto, "Is a local linear PD feedback control law effective for trajectory tracking of robot motion?" in *Proc. IEEE Int. Conf. Robot. Automat.*, 1988, pp. 1335–1340, doi: 10.1109/ROBOT.1988.12253.
[116] I. Cervantes and J. Alvarez-Ramirez, "On the PID tracking control of robot manipulators," *Syst. Control Lett.*, vol. 42, no. 1, pp. 37–46, Jan. 2001, doi: 10.1016/S0167-6911(00)00077-3.
[117] R. Kelly and R. Salgado, "PD control with computed feedforward of robot manipulators: A design procedure," *IEEE Trans. Robot. Autom. (1989–June 2004)*, vol. 10, no. 4, pp. 566–571, Aug. 1994, doi: 10.1109/70.313108.
[118] A. D. Marchese, R. Tedrake, and D. Rus, "Dynamics and trajectory optimization for a soft spatial fluidic elastomer manipulator," *Int. J. Robot. Res.*, vol. 35, no. 8, pp. 1000–1019, Jul. 2016, doi: 10.1177/0278364915587926.
[119] V. Falkenhahn, A. Hildebrandt, R. Neumann, and O. Sawodny, "Model-based feedforward position control of constant curvature continuum robots using feedback linearization," in *Proc. IEEE Int. Conf. Robot. Automat. (ICRA)*, 2015, pp. 762–767, doi: 10.1109/ICRA.2015.7139264.
[120] B. Paden and R. Panja, "Globally asymptotically stable 'PD+' controller for robot manipulator," *Int. J. Control*, vol. 47, no. 6, pp. 1697–1712, 1988, doi: 10.1080/00207178808906130.
[121] G. Cao, B. Huo, L. Yang, F. Zhang, Y. Liu, and G.-B. Bian, "Model-based robust tracking control without observers for soft bending actuators," *IEEE Robot. Autom. Lett.*, vol. 6, no. 3, pp. 5175–5182, Jul. 2021, doi: 10.1109/LRA.2021.3071952.
[122] P. Ouyang, J. Acob, and V. Pano, "PD with sliding mode control for trajectory tracking of robotic system," *Robot. Comput.-Integr. Manuf.*, vol. 30, no. 2, pp. 189–200, Apr. 2014, doi: 10.1016/j.rcim.2013.09.009.
[123] Y. Su, "Global continuous finite-time tracking of robot manipulators," *Int. J. Robust Nonlinear Control*, vol. 19, no. 17, pp. 1871–1885, Nov. 2009, doi: 10.1002/rnc.1406.
[124] Y. Su and J. Swevers, "Finite-time tracking control for robot manipulators with actuator saturation," *Robot. Comput.-Integr. Manuf.*, vol. 30, no. 2, pp. 91–98, Apr. 2014, doi: 10.1016/j.rcim.2013.09.005.
[125] M. Zhang, P. Borja, R. Ortega, Z. Liu, and H. Su, "PID passivity-based control of port-Hamiltonian systems," *IEEE Trans. Autom. Control*, vol. 63, no. 4, pp. 1032–1044, Apr. 2018, doi: 10.1109/TAC.2017.2732283.
[126] A. D. Kapadia, K. E. Fry, and I. D. Walker, "Empirical investigation of closed-loop control of extensible continuum manipulators," in *Proc. IEEE/RSJ Int. Conf. Intell. Robots Syst.*, 2014, pp. 329–335, doi: 10.1109/IROS.2014.6942580.
[127] A. Doroudchi and S. Berman, "Configuration tracking for soft continuum robotic arms using inverse dynamic control of a cosserat rod model,"

in *Proc. IEEE Int. Conf. Soft Robot. (RoboSoft)*, 2021, pp. 207–214, doi: 10.1109/RoboSoft51838.2021.9479223.
[128] T. G. Thuruthel, F. Renda, and F. Iida, "First-order dynamic modeling and control of soft robots," *Frontiers Robot. AI*, vol. 7, Jul. 2020, Art. no. 95, doi: 10.3389/frobt.2020.00095.
[129] E. Milana, B. Gorissen, S. Peerlinck, M. De Volder, and D. Reynaerts, "Artificial soft cilia with asymmetric beating patterns for biomimetic low-reynolds-number fluid propulsion," *Adv. Functional Mater.*, vol. 29, no. 22, May 2019, Art. no. 1900462, doi: 10.1002/adfm.201900462.
[130] G. Zheng, O. Goury, M. Thieffry, A. Kruszewski, and C. Duriez, "Controllability pre-verification of silicone soft robots based on finite-element method," in *Proc. Int. Conf. Robot. Automat. (ICRA)*, 2019, pp. 7395–7400, doi: 10.1109/ICRA.2019.8794370.
[131] E. Sontag, "From linear to nonlinear: Some complexity comparisons," in *Proc. 34th IEEE Conf. Decis. Control*, 1995, vol. 3, pp. 2916–2920, doi: 10.1109/CDC.1995.478585.
[132] C. Della Santina, L. Pallottino, D. Rus, and A. Bicchi, "Exact task execution in highly under-actuated soft limbs: An operational space based approach," *IEEE Robot. Autom. Lett.*, vol. 4, no. 3, pp. 2508–2515, Jul. 2019, doi: 10.1109/LRA.2019.2907412.
[133] M. Thieffry, A. Kruszewski, T.-M. Guerra, and C. Duriez, "Trajectory tracking control design for large-scale linear dynamical systems with applications to soft robotics," *IEEE Trans. Control Syst. Technol.*, vol. 29, no. 2, pp. 556–566, Mar. 2021, doi: 10.1109/TCST.2019.2953624.
[134] M. Thieffry, A. Kruszewski, T.-M. Guerra, and C. Duriez, "LPV framework for non-linear dynamic control of soft robots using finite element model," *IFAC-PapersOnLine*, vol. 53, no. 2, pp. 7312–7318, Jan. 2020, doi: 10.1016/j.ifacol.2020.12.984.
[135] M. Thieffry, A. Kruszewski, T.-M. Guerra, and C. Duriez, "Reduced order control of soft robots with guaranteed stability," in *Proc. Eur. Control Conf. (ECC)*, 2018, pp. 635–640, doi: 10.23919/ECC.2018.8550298.
[136] M. Thieffry, A. Kruszewski, C. Duriez, and T.-M. Guerra, "Control design for soft robots based on reduced-order model," *IEEE Robot. Autom. Lett.*, vol. 4, no. 1, pp. 25–32, Jan. 2019, doi: 10.1109/LRA.2018.2876734.
[137] K. Wu and G. Zheng, "FEM-based gain-scheduling control of a soft trunk robot," *IEEE Robot. Autom. Lett.*, vol. 6, no. 2, pp. 3081–3088, Apr. 2021, doi: 10.1109/LRA.2021.3061311.
[138] E. Franco and A. Garriga-Casanovas, "Energy-shaping control of soft continuum manipulators with in-plane disturbances," *Int. J. Robot. Res.*, vol. 40, no. 1, pp. 236–255, Jan. 2021, doi: 10.1177/0278364920907679.
[139] E. Franco, A. G. Casanovas, and A. Donaire, "Energy shaping control with integral action for soft continuum manipulators," *Mechanism Mach. Theory*, vol. 158, Apr. 2021, Art. no. 104250, doi: 10.1016/j.mechmachtheory.2021.104250.
[140] F. Boyer, M. Porez, and W. Khalil, "Macro-continuous computed torque algorithm for a three-dimensional eel-like robot," *IEEE Trans. Robot.*, vol. 22, no. 4, pp. 763–775, Aug. 2006, doi: 10.1109/TRO.2006.875492.
[141] P. Borja, A. Dabiri, and C. Della Santina, "Energy-based shape regulation of soft robots with unactuated dynamics dominated by elasticity," in *Proc. IEEE 5th Int. Conf. Soft Robot. (RoboSoft)*, 2022, pp. 396–402, doi: 10.1109/RoboSoft54090.2022.9762071.
[142] P. Pustina, C. Della Santina, and A. De Luca, "Feedback regulation of elastically decoupled underactuated soft robots," *IEEE Robot. Autom. Lett.*, vol. 7, no. 2, pp. 4512–4519, Apr. 2022, doi: 10.1109/LRA.2022.3150829.
[143] L. Weerakoon and N. Chopra, "Swing up control of a soft inverted pendulum with revolute base," in *Proc. 60th IEEE Conf. Decis. Control (CDC)*, 2021, pp. 685–690, doi: 10.1109/CDC45484.2021.9683691.
[144] M. W. Spong, "Partial feedback linearization of underactuated mechanical systems," in *Proc. IEEE/RSJ Int. Conf. Intell. Robots Syst. (IROS)*, 1994, vol. 1, pp. 314–321, doi: 10.1109/IROS.1994.407375.
[145] S. Li, A. Kruszewski, T.-M. Guerra, and A.-T. Nguyen, "Equivalent-input-disturbance-based dynamic tracking control for soft robots via reduced-order finite-element models," *IEEE/ASME Trans. Mechatron.*, vol. 27, no. 5, pp. 4078–4089, Oct. 2022, doi: 10.1109/TMECH.2022.3144353.
[146] G. Rizzello, D. Naso, B. Turchiano, and S. Seelecke, "Robust position control of dielectric elastomer actuators based on LMI optimization," *IEEE Trans. Control Syst. Technol.*, vol. 24, no. 6, pp. 1909–1921, Nov. 2016, doi: 10.1109/TCST.2016.2519839.
[147] G.-Y. Gu, J. Zhu, L.-M. Zhu, and X. Zhu, "A survey on dielectric elastomer actuators for soft robots," *Bioinspiration Biomimetics*, vol. 12, no. 1, Jan. 2017, Art. no. 011003, doi: 10.1088/1748-3190/12/1/011003.
[148] J. van der Weijde, H. Vallery, and R. Babuška, "Closed-loop control through self-sensing of a joule-heated twisted and coiled polymer muscle," *Soft Robot.*, vol. 6, no. 5, pp. 621–630, Oct. 2019, doi: 10.1089/soro.2018.0165.
[149] A. Pedram, H. N. Pishkenari, and M. Sitti, "Optimal controller design for 3D manipulation of buoyant magnetic microrobots via constrained linear quadratic regulation approach," *J. Micro-Bio Robot.*, vol. 15, no. 2, pp. 105–117, Dec. 2019, doi: 10.1007/s12213-019-00121-3.
[150] S. Jeon et al., "A magnetically controlled soft microrobot steering a guidewire in a three-dimensional phantom vascular network," *Soft Robot.*, vol. 6, no. 1, pp. 54–68, Feb. 2019, doi: 10.1089/soro.2018.0019.
[151] M. Azizkhani, I. S. Godage, and Y. Chen, "Dynamic control of soft robotic arm: A simulation study," *IEEE Robot. Autom. Lett.*, vol. 7, no. 2, pp. 3584–3591, Apr. 2022, doi: 10.1109/LRA.2022.3148437.
[152] B. Siciliano and W. J. Book, "A singular perturbation approach to control of lightweight flexible manipulators," *Int. J. Robot. Res.*, vol. 7, no. 4, pp. 79–90, Aug. 1988, doi: 10.1177/027836498800700404.
[153] M. Bridges, D. M. Dawson, and C. Abdallah, "Contril of rigid-link, flexible-joint robots: A survey of backstepping approaches," *J. Robot Syst.*, vol. 12, no. 3, pp. 199–216, Mar. 1995, doi: 10.1002/rob.4620120305.
[154] M. A. Khosravi and H. D. Taghirad, "Dynamic modeling and control of parallel robots with elastic cables: Singular perturbation approach," *IEEE Trans. Robot.*, vol. 30, no. 3, pp. 694–704, Jun. 2014, doi: 10.1109/TRO.2014.2298057.
[155] B. Taheri, D. Case, and E. Richer, "Force and stiffness backstepping-sliding mode controller for pneumatic cylinders," *IEEE/ASME Trans. Mechatronics*, vol. 19, no. 6, pp. 1799–1809, Dec. 2014, doi: 10.1109/TMECH.2013.2294970.
[156] S. B. F. Asl and S. S. Moosapour, "Adaptive backstepping fast terminal sliding mode controller design for ducted fan engine of thrust-vectored aircraft," *Aerosp. Sci. Technol.*, vol. 71, pp. 521–529, Dec. 2017, doi: 10.1016/j.ast.2017.10.001.
[157] P. Carbonell, Z. Jiang, and D. Repperger, "Nonlinear control of a pneumatic muscle actuator: Backstepping vs. sliding-mode," in *Proc. IEEE Int. Conf. Contr. Appl. (CCA) (Cat. No. 01CH37204)*, 2001, pp. 167–172, doi: 10.1109/CCA.2001.973858.
[158] T. Wang, Y. Zhang, Z. Chen, and S. Zhu, "Parameter identification and model-based nonlinear robust control of fluidic soft bending actuators," *IEEE/ASME Trans. Mechatronics*, vol. 24, no. 3, pp. 1346–1355, Jun. 2019, doi: 10.1109/TMECH.2019.2909099.
[159] E. Franco, T. Ayatullah, A. Sugiharto, A. Garriga-Casanovas, and V. Virdyawan, "Nonlinear energy-based control of soft continuum pneumatic manipulators," *Nonlinear Dyn.*, vol. 106, no. 1, pp. 229–253, Sep. 2021, doi: 10.1007/s11071-021-06817-1.
[160] M. Stölzle and C. D. Santina, "Piston-driven pneumatically-actuated soft robots: Modeling and backstepping control," *IEEE Contr. Syst. Lett.*, vol. 6, pp. 1837–1842, 2022, doi: 10.1109/LCSYS.2021.3134165.
[161] C. D. Santina, A. Bicchi, and D. Rus, "Dynamic control of soft robots with internal constraints in the presence of obstacles," in *Proc. IEEE/RSJ Int. Conf. Intell. Robots Syst. (IROS)*, 2019, pp. 6622–6629, doi: 10.1109/IROS40897.2019.8967668.
[162] C. M. Best, M. T. Gillespie, P. Hyatt, L. Rupert, V. Sherrod, and M. D. Killpack, "A new soft robot control method: Using model predictive control for a pneumatically actuated humanoid," *IEEE Robot. Autom. Mag.*, vol. 23, no. 3, pp. 75–84, Sep. 2016, doi: 10.1109/MRA.2016.2580591.
[163] P. Hyatt and M. D. Killpack, "Real-time nonlinear model predictive control of robots using a graphics processing unit," *IEEE Robot. Autom. Lett.*, vol. 5, no. 2, pp. 1468–1475, Apr. 2020, doi: 10.1109/LRA.2020.2965393.
[164] S. Tonkens, J. Lorenzetti, and M. Pavone, "Soft robot optimal control via reduced order finite element models," 2020, *arXiv:2011.02092*.
[165] Y. Bailly and Y. Amirat, "Modeling and control of a hybrid continuum active catheter for aortic aneurysm treatment," in *Proc. IEEE Int. Conf. Robot. Automat.*, 2005, pp. 924–929, doi: 10.1109/ROBOT.2005.1570235.
[166] D. B. Camarillo, C. R. Carlson, and J. K. Salisbury, "Configuration tracking for continuum manipulators with coupled tendon drive," *IEEE Trans. Robot.*, vol. 25, no. 4, pp. 798–808, Aug. 2009, doi: 10.1109/TRO.2009.2022426.
[167] T. Mahl, A. Hildebrandt, and O. Sawodny, "A variable curvature continuum kinematics for kinematic control of the bionic handling assistant," *IEEE Trans. Robot.*, vol. 30, no. 4, pp. 935–949, Aug. 2014, doi: 10.1109/TRO.2014.2314777.
[168] J. M. Bern, G. Kumagai, and S. Coros, "Fabrication, modeling, and control of plush robots," in *Proc. IEEE/RSJ Int. Conf. Intell. Robots Syst. (IROS)*, 2017, pp. 3739–3746, doi: 10.1109/IROS.2017.8206223.
[169] T. M. Bieze, F. Largilliere, A. Kruszewski, Z. Zhang, R. Merzouki, and C. Duriez, "Finite element method-based kinematics and closed-loop control of soft, continuum manipulators," *Soft Robot.*, vol. 5, no. 3, pp. 348–364, Jun. 2018, doi: 10.1089/soro.2017.0079.
[170] M. T. Chikhaoui, J. Granna, J. Starke, and J. Burgner-Kahrs, "Toward motion coordination control and design optimization for dual-arm concentric tube continuum robots," *IEEE Robot. Autom. Lett.*, vol. 3, no. 3, pp. 1793–1800, Jul. 2018, doi: 10.1109/LRA.2018.2800037.
[171] P. Chiacchio, S. Chiaverini, L. Sciavicco, and B. Siciliano, "Closed-loop inverse kinematics schemes for constrained redundant manipulators with task

space augmentation and task priority strategy," *Int. J. Robot. Res.*, vol. 10, no. 4, pp. 410–425, Aug. 1991, doi: 10.1177/027836499101000409.
[172] S. R. Buss, "Introduction to inverse kinematics with Jacobian transpose, pseudoinverse and damped least squares methods," *IEEE J. Robot. Autom.*, vol. 17, no. 1, p. 16, May 2004.
[173] S. Chiaverini, G. Oriolo, and A. A. Maciejewski, "Redundant robots," in *Springer Handbook of Robotics*, B. Siciliano and O. Khatib, Eds. Berlin, Germany: Springer-Verlag, 2016, pp. 221–242.
[174] B. Benhabib, A. A. Goldenberg, and R. G. Fenton, "A solution to the inverse kinematics of redundant manipulators," *J. Robot. Syst.*, vol. 2, no. 4, pp. 373–385, 1985, doi: 10.1002/rob.4620020404.
[175] P. Falco and C. Natale, "On the stability of closed-loop inverse kinematics algorithms for redundant robots," *IEEE Trans. Robot.*, vol. 27, no. 4, pp. 780–784, Aug. 2011, doi: 10.1109/TRO.2011.2135210.
[176] A. Kapadia and I. D. Walker, "Task-space control of extensible continuum manipulators," in *Proc. IEEE/RSJ Int. Conf. Intell. Robots Syst.*, 2011, pp. 1087–1092, doi: 10.1109/IROS.2011.6094873.
[177] J. Burgner-Kahrs, D. C. Rucker, and H. Choset, "Continuum robots for medical applications: A survey," *IEEE Trans. Robot.*, vol. 31, no. 6, pp. 1261–1280, Dec. 2015, doi: 10.1109/TRO.2015.2489500.
[178] T. da Veiga et al., "Challenges of continuum robots in clinical context: A review," *Prog. Biomed. Eng.*, vol. 2, no. 3, Jul. 2020, Art. no. 032003, doi: 10.1088/2516-1091/ab9f41.
[179] F. Campisano et al., "Closed-loop control of soft continuum manipulators under tip follower actuation," *Int. J. Robot. Res.*, vol. 40, nos. 6–7, pp. 923–938, Mar. 2021, doi: 10.1177/0278364921997167.
[180] D. C. Rucker et al., "Sliding mode control of steerable needles," *IEEE Trans. Robot.*, vol. 29, no. 5, pp. 1289–1299, Oct. 2013, doi: 10.1109/TRO.2013.2271098.
[181] A. A. Alqumsan, S. Khoo, and M. Norton, "Robust control of continuum robots using cosserat rod theory," *Mech. Mach. Theory*, vol. 131, pp. 48–61, Jan. 2019, doi: 10.1016/j.mechmachtheory.2018.09.011.
[182] F. Xu, H. Wang, W. Chen, and Y. Miao, "Visual servoing of a cable-driven soft robot manipulator with shape feature," *IEEE Robot. Autom. Lett.*, vol. 6, no. 3, pp. 4281–4288, Jul. 2021, doi: 10.1109/LRA.2021.3067285.
[183] Z. Zhang, T. M. Bieze, J. Dequidt, A. Kruszewski, and C. Duriez, "Visual servoing control of soft robots based on finite element model," in *Proc. IEEE/RSJ Int. Conf. Intell. Robots Syst. (IROS)*, 2017, pp. 2895–2901, doi: 10.1109/IROS.2017.8206121.
[184] J. Till, C. E. Bryson, S. Chung, A. Orekhov, and D. C. Rucker, "Efficient computation of multiple coupled cosserat rod models for real-time simulation and control of parallel continuum manipulators," in *Proc. IEEE Int. Conf. Robot. Automat. (ICRA)*, 2015, pp. 5067–5074, doi: 10.1109/ICRA.2015.7139904.
[185] O. Khatib, "A unified approach for motion and force control of robot manipulators: The operational space formulation," *IEEE J. Robot. Automat.*, vol. 3, no. 1, pp. 43–53, Feb. 1987, doi: 10.1109/JRA.1987.1087068.
[186] J. Nakanishi, R. Cory, M. Mistry, J. Peters, and S. Schaal, "Operational space control: A theoretical and empirical comparison," *Int. J. Robot. Res.*, vol. 27, no. 6, pp. 737–757, Jun. 2008, doi: 10.1177/0278364908091463.
[187] A. Dietrich and C. Ott, "Hierarchical impedance-based tracking control of kinematically redundant robots," *IEEE Trans. Robot.*, vol. 36, no. 1, pp. 204–221, Feb. 2020, doi: 10.1109/TRO.2019.2945876.
[188] I. S. Godage, D. T. Branson, E. Guglielmino, and D. G. Caldwell, "Path planning for multisection continuum arms," in *Proc. IEEE Int. Conf. Mechatronics Automat.*, 2012, pp. 1208–1213, doi: 10.1109/ICMA.2012.6283423.
[189] A. D. Marchese, R. K. Katzschmann, and D. Rus, "Whole arm planning for a soft and highly compliant 2D robotic manipulator," in *Proc. IEEE/RSJ Int. Conf. Intell. Robots Syst.*, 2014, pp. 554–560, doi: 10.1109/IROS.2014.6942614.
[190] J. Lai, B. Lu, Q. Zhao, and H. K. Chu, "Constrained motion planning of a cable-driven soft robot with compressible curvature modeling," *IEEE Robot. Autom. Lett.*, vol. 7, no. 2, pp. 4813–4820, Apr. 2022, doi: 10.1109/LRA.2022.3152318.
[191] A. Bicchi, "Intrinsic contact sensing for soft fingers," in *Proc. IEEE Int. Conf. Robot. Automat.*, 1990, pp. 968–973, doi: 10.1109/ROBOT.1990.126117.
[192] J. K. Salisbury, "Active stiffness control of a manipulator in cartesian coordinates," in *Proc. 19th IEEE Conf. Decis. Contr. Including Symp. Adaptive Process.*, 1980, pp. 95–100, doi: 10.1109/CDC.1980.272026.
[193] S.-F. Chen and I. Kao, "Conservative congruence transformation for joint and cartesian stiffness matrices of robotic hands and fingers," *Int. J. Robot. Res.*, vol. 19, no. 9, pp. 835–847, Sep. 2000, doi: 10.1177/02783640022067201.
[194] K. Suzumori, S. Iikura, and H. Tanaka, "Applying a flexible microactuator to robotic mechanisms," *IEEE Control Syst. Mag.*, vol. 12, no. 1, pp. 21–27, Feb. 1992, doi: 10.1109/37.120448.
[195] M. T. Gillespie, C. M. Best, and M. D. Killpack, "Simultaneous position and stiffness control for an inflatable soft robot," in *Proc. IEEE Int. Conf. Robot. Automat. (ICRA)*, 2016, pp. 1095–1101, doi: 10.1109/ICRA.2016.7487240.
[196] S. M. Mustaza, C. M. Saaj, F. J. Comin, W. A. Albukhanajer, D. Mahdi, and C. Lekakou, "Stiffness control for soft surgical manipulators," *Int. J. Humanoid Robot.*, vol. 15, no. 5, 2018, Art. no. 1850021, doi: 10.1142/S0219843618500214.
[197] G. Rizzello, P. Serafino, D. Naso, and S. Seelecke, "Towards sensorless soft robotics: Self-sensing stiffness control of dielectric elastomer actuators," *IEEE Trans. Robot.*, vol. 36, no. 1, pp. 174–188, Feb. 2020, doi: 10.1109/TRO.2019.2944592.
[198] A. Albu-Schaffer, M. Fischer, G. Schreiber, F. Schoeppe, and G. Hirzinger, "Soft robotics: What cartesian stiffness can obtain with passively compliant, uncoupled joints?" in *Proc. IEEE/RSJ Int. Conf. Intell. Robots Syst. (IROS) (IEEE Cat. No. 04CH37566)*, 2004, vol. 4, pp. 3295–3301.
[199] A. Ajoudani, N. G. Tsagarakis, J. Lee, M. Gabiccini, and A. Bicchi, "Natural redundancy resolution in dual-arm manipulation using configuration dependent stiffness (CDS) control," in *Proc. IEEE Int. Conf. Robot. Automat. (ICRA)*, 2014, pp. 1480–1486, doi: 10.1109/ICRA.2014.6907047.
[200] J. M. Bern and D. Rus, "Soft IK with stiffness control," in *Proc. IEEE 4th Int. Conf. Soft Robot. (RoboSoft)*, 2021, pp. 465–471, doi: 10.1109/RoboSoft51838.2021.9479195.
[201] M. Mahvash and P. E. Dupont, "Stiffness control of surgical continuum manipulators," *IEEE Trans. Robot.*, vol. 27, no. 2, pp. 334–345, Apr. 2011, doi: 10.1109/TRO.2011.2105410.
[202] C. Ott, *Cartesian Impedance Control of Redundant and Flexible-Joint Robots*. Berlin, Germany: Springer-Verlag, 2008.
[203] A. Bajo and N. Simaan, "Hybrid motion/force control of multi-backbone continuum robots," *Int. J. Robot. Res.*, vol. 35, no. 4, pp. 422–434, 2016, doi: 10.1177/0278364915584806.
[204] R. Yasin and N. Simaan, "Joint-level force sensing for indirect hybrid force/position control of continuum robots with friction," *Int. J. Robot. Res.*, vol. 40, nos. 4–5, pp. 764–781, 2021, doi: 10.1177/0278364920979721.
[205] Z. Zhang, J. Dequidt, J. Back, H. Liu, and C. Duriez, "Motion control of cable-driven continuum catheter robot through contacts," *IEEE Robot. Autom. Lett.*, vol. 4, no. 2, pp. 1852–1859, Apr. 2019, doi: 10.1109/LRA.2019.2898047.
[206] E. Coevoet, A. Escande, and C. Duriez, "Soft robots locomotion and manipulation control using FEM simulation and quadratic programming," in *Proc. 2nd IEEE Int. Conf. Soft Robot. (RoboSoft)*, 2019, pp. 739–745, doi: 10.1109/ROBOSOFT.2019.8722815.
[207] W. J. Book, S. Le, and V. Sangveraphunsiri, "Bracing strategy for robot operation," in *Theory and Practice of Robots and Manipulators*, A. Morecki, G. Bianchi, and K. Kędzior, Eds. Boston, MA, USA: Springer, 1985, pp. 179–185.
[208] M. Selvaggio, L. Ramirez, N. Naclerio, B. Siciliano, and E. Hawkes, "An obstacle-interaction planning method for navigation of actuated vine robots," in *Proc. IEEE Int. Conf. Robot. Automat. (ICRA)*, 2020, pp. 3227–3233, doi: 10.1109/ICRA40945.2020.9196587.
[209] S. P. Nageshrao, G. A. Lopes, D. Jeltsema, and R. Babuška, "Port-hamiltonian systems in adaptive and learning control: A survey," *IEEE Trans. Autom. Control*, vol. 61, no. 5, pp. 1223–1238, May 2016, doi: 10.1109/TAC.2015.2458491.
[210] L. Buşoniu, T. de Bruin, D. Tolić, J. Kober, and I. Palunko, "Reinforcement learning for control: Performance, stability, and deep approximators," *Annu. Rev. Contr.*, vol. 46, pp. 8–28, 2018, doi: 10.1016/j.arcontrol.2018.09.005.
[211] C. De Persis and P. Tesi, "Formulas for data-driven control: Stabilization, optimality, and robustness," *IEEE Trans. Autom. Control*, vol. 65, no. 3, pp. 909–924, Mar. 2020, doi: 10.1109/TAC.2019.2959924.
[212] J. Berberich, J. Köhler, M. A. Muller, and F. Allgower, "Data-driven model predictive control with stability and robustness guarantees," *IEEE Trans. Autom. Control*, vol. 66, no. 4, pp. 1702–1717, Apr. 2021, doi: 10.1109/TAC.2020.3000182.
[213] M. Sznaier, "Control oriented learning in the era of big data," *IEEE Contr. Syst. Lett.*, vol. 5, no. 6, pp. 1855–1867, Dec. 2021, doi: 10.1109/LCSYS.2020.3045664.
[214] C. Laschi et al., "A survey on learning based control in soft robots (Provisional Title)," *IEEE Control Mag.*, to be published.
[215] K. J. Åström and B. Wittenmark, *Adaptive Control*. North Chelmsford, MA, USA: Courier Corporation, 2013.
[216] P. Tomei, "Adaptive PD controller for robot manipulators," *IEEE Trans. Robot. Autom. (1989–June 2004)*, vol. 7, no. 4, pp. 565–570, Aug. 1991, doi: 10.1109/70.86088.
[217] J.-J. E. Slotine and W. Li, "On the adaptive control of robot manipulators," *Int. J. Robot. Res.*, vol. 6, no. 3, pp. 49–59, Sep. 1987, doi: 10.1177/027836498700600303.
[218] H. Wang, B. Yang, Y. Liu, W. Chen, X. Liang, and R. Pfeifer, "Visual servoing of soft robot manipulator in constrained environments with an adaptive controller," *IEEE/ASME Trans. Mechatronics*, vol. 22, no. 1, pp. 41–50, Feb. 2017, doi: 10.1109/TMECH.2016.2613410.
[219] E. H. Skorina, M. Luo, W. Tao, F. Chen, J. Fu, and C. D. Onal, "Adapting to flexibility: Model reference adaptive control of soft bending actuators," *IEEE Robot. Autom. Lett.*, vol. 2, no. 2, pp. 964–970, Apr. 2017, doi: 10.1109/LRA.2017.2655572.

[220] Z. Q. Tang, H. L. Heung, K. Y. Tong, and Z. Li, "Model-based online learning and adaptive control for a 'Human-Wearable Soft Robot' integrated system," *Int. J. Robot. Res.*, vol. 40, no. 1, pp. 256–276, 2021, doi: 10.1177/02783649 19873379.
[221] D. Bruder, X. Fu, R. B. Gillespie, C. D. Remy, and R. Vasudevan, "Data-driven control of soft robots using koopman operator theory," *IEEE Trans. Robot.*, vol. 99, pp. 1–14, Dec. 2020, doi: 10.1109/TRO.2020.3038693.
[222] J. S. Terry, J. Whitaker, R. W. Beard, and M. D. Killpack, "Adaptive control of large-scale soft robot manipulators with unknown payloads," in *Proc. Dyn. Syst. Contr. Conf.*, American Society of Mechanical Engineers, 2019, vol. 59162, pp. V003T20A003.
[223] P. Hyatt, C. Johnson, and M. D. Killpack, "Model reference predictive adaptive control for large-scale soft robots," *Frontiers Robot. AI*, vol. 7, Oct. 2020, Art. no. 558027, doi: 10.3389/frobt.2020.558027.
[224] M. Trumić, C. Della Santina, K. Jovanović, and A. Fagiolini, "Adaptive control of soft robots based on an enhanced 3D augmented rigid robot matching," *IEEE Contr. Syst. Lett.*, vol. 5, no. 6, pp. 1934–1939, Dec. 2021, doi: 10.1109/LCSYS.2020.3047737.
[225] L. Weerakoon and N. Chopra, "Bilateral teleoperation of soft robots under piecewise constant curvature hypothesis: An experimental investigation," in *Proc. IEEE Amer. Contr. Conf. (ACC)*, 2020, pp. 2124–2129, doi: 10.23919/ACC45564.2020.9147323.
[226] G. Zheng, "Control of a silicone soft tripod robot via uncertainty compensation," *IEEE Robot. Autom. Lett.*, vol. 5, no. 2, pp. 2801–2807, Apr. 2020, doi: 10.1109/LRA.2020.2974714.
[227] E. Franco, A. G. Casanovas, J. Tang, F. Rodriguez y Baena, and A. Astolfi, "Position regulation in cartesian space of a class of inextensible soft continuum manipulators with pneumatic actuation," *Mechatronics*, vol. 76, Jun. 2021, Art. no. 102573, doi: 10.1016/j.mechatronics.2021.102573.
[228] G. Cao, Y. Liu, Y. Jiang, F. Zhang, G. Bian, and D. H. Owens, "Observer-based continuous adaptive sliding mode control for soft actuators," *Nonlinear Dyn.*, vol. 105, pp. 371–386, Jul. 2021, doi: 10.1007/s11071-021-06606-w.
[229] R. M. Sanner and J.-J. E. Slotine, "Gaussian networks for direct adaptive control," in *Proc. IEEE Amer. Contr. Conf.*, 1991, pp. 2153–2159.
[230] M. M. Polycarpou, "Stable adaptive neural control scheme for nonlinear systems," *IEEE Trans. Autom. Control*, vol. 41, no. 3, pp. 447–451, Mar. 1996, doi: 10.1109/9.486648.
[231] C. Yang, T. Teng, B. Xu, Z. Li, J. Na, and C.-Y. Su, "Global adaptive tracking control of robot manipulators using neural networks with finite-time learning convergence," *Int. J. Contr., Automat. Syst.*, vol. 15, no. 4, pp. 1916–1924, Aug. 2017, doi: 10.1007/s12555-016-0515-7.
[232] D. A. Bristow, M. Tharayil, and A. G. Alleyne, "A survey of iterative learning control," *IEEE Control Syst. Mag.*, vol. 26, no. 3, pp. 96–114, Jun. 2006, doi: 10.1109/MCS.2006.1636313.
[233] S. Seok, C. D. Onal, K.-J. Cho, R. J. Wood, D. Rus, and S. Kim, "Meshworm: A peristaltic soft robot with antagonistic nickel titanium coil actuators," *IEEE/ASME Trans. Mechatronics*, vol. 18, no. 5, pp. 1485–1497, Oct. 2013, doi: 10.1109/TMECH.2012.2204070.
[234] H. Chi, X. Li, W. Liang, J. Cao, and Q. Ren, "Iterative learning control for motion trajectory tracking of a circular soft crawling robot," *Frontiers Robot. AI*, vol. 6, Nov. 2019, Art. no. 113, doi: 10.3389/frobt.2019.00113.
[235] M. Hofer and R. D'Andrea, "Design, fabrication, modeling and control of a fabric-based spherical robotic arm," *Mechatronics*, vol. 68, Jun. 2020, Art. no. 102369, doi: 10.1016/j.mechatronics.2020.102369.
[236] J. Zughaibi, M. Hofer, and R. D. Andrea, "A fast and reliable pick-and-place application with a spherical soft robotic arm," 2020, *arXiv:2011.04624*.
[237] G. Cao, B. Chu, and Y. Liu, "Analytical modeling and control of soft fast pneumatic networks actuators," in *Proc. 46th Annu. Conf. IEEE Ind. Electron. Soc. (IECON)*, 2020, pp. 2760–2765, doi: 10.1109/IECON43393.2020.9254517.
[238] Z. Q. Tang, H. L. Heung, K. Y. Tong, and Z. Li, "A novel iterative learning model predictive control method for soft bending actuators," in *Proc. IEEE Int. Conf. Robot. Automat. (ICRA)*, 2019, pp. 4004–4010, doi: 10.1109/ICRA.2019.8793871.
[239] L. Cenceschi, F. Angelini, C. Della Santina, and A. Bicchi, "Pi σ-pi σ continuous iterative learning control for nonlinear systems with arbitrary relative degree," in *Proc. IEEE Eur. Contr. Conf. (ECC)*, 2021, p. 1042, doi: 10.23919/ECC54610.2021.9655196.
[240] J. Rieffel, D. Knox, S. Smith, and B. Trimmer, "Growing and evolving soft robots," *Artif. Life*, vol. 20, no. 1, pp. 143–162, Jan. 2014, doi: 10.1162/ARTL_a_00101.
[241] N. Cheney, J. Bongard, and H. Lipson, "Evolving soft robots in tight spaces," in *Proc. Annu. Conf. Genetic Evol. Comput.*, 2015, pp. 935–942, doi: 10.1145/2739480.2754662.
[242] J. Tobin, R. Fong, A. Ray, J. Schneider, W. Zaremba, and P. Abbeel, "Domain randomization for transferring deep neural networks from simulation to the real world," in *Proc. IEEE/RSJ Int. Conf. Intell. Robots Syst. (IROS)*, 2017, pp. 23–30, doi: 10.1109/IROS.2017.8202133.
[243] J. Rojas, E. Sifakis, and L. Kavan, "Differentiable implicit soft-body physics," 2021, *arXiv:2102.05791*.
[244] S. Satheeshbabu, N. K. Uppalapati, T. Fu, and G. Krishnan, "Continuous control of a soft continuum arm using deep reinforcement learning," in *Proc. 3rd IEEE Int. Conf. Soft Robot. (RoboSoft)*, 2020, pp. 497–503, doi: 10.1109/RoboSoft48309.2020.9116003.
[245] M. Bächer, E. Knoop, and C. Schumacher, "Design and control of soft robots using differentiable simulation," *Current Robot. Rep.*, vol. 2, no. 51, pp. 1–11, Jun. 2021, doi: 10.1007/s43154-021-00052-7.
[246] W. Samek, T. Wiegand, and K.-R. Müller, "Explainable artificial intelligence: Understanding, visualizing and interpreting deep learning models," 2017, *arXiv:1708.08296*.
[247] J. Sjöberg et al., "Nonlinear black-box modeling in system identification: A unified overview," *Automatica*, vol. 31, no. 12, pp. 1691–1724, Dec. 1995, doi: 10.1016/0005-1098(95)00120-8.
[248] J. Schoukens and L. Ljung, "Nonlinear system identification: A user-oriented road map," *IEEE Control Syst. Mag.*, vol. 39, no. 6, pp. 28–99, Dec. 2019, doi: 10.1109/MCS.2019.2938121.
[249] D. Nguyen-Tuong and J. Peters, "Model learning for robot control: A survey," *Cogn. Process.*, vol. 12, no. 4, pp. 319–340, Apr. 2011, doi: 10.1007/s10339-011-0404-1.
[250] C. C. Johnson, T. Quackenbush, T. Sorensen, D. Wingate, and M. D. Killpack, "Using first principles for deep learning and model-based control of soft robots," *Frontiers Robot. AI*, vol. 8, May 2021, Art. no. 654398, doi: 10.3389/frobt.2021.654398.
[251] A. Tariverdi et al., "A recurrent neural-network-based real-time dynamic model for soft continuum manipulators," *Frontiers Robot. AI*, vol. 8, Mar. 2021, Art. no. 631303, doi: 10.3389/frobt.2021.631303.
[252] B. Deutschmann, T. Liu, A. Dietrich, C. Ott, and D. Lee, "A method to identify the nonlinear stiffness characteristics of an elastic continuum mechanism," *IEEE Robot. Autom. Lett.*, vol. 3, no. 3, pp. 1450–1457, Jan. 2018, doi: 10.1109/LRA.2018.2800098.
[253] L. Wang and N. Simaan, "Geometric calibration of continuum robots: Joint space and equilibrium shape deviations," *IEEE Trans. Robot.*, vol. 35, no. 2, pp. 387–402, Apr. 2019, doi: 10.1109/TRO.2018.2881049.
[254] J. M. Bern, Y. Schnider, P. Banzet, N. Kumar, and S. Coros, "Soft robot control with a learned differentiable model," in *Proc. 3rd IEEE Int. Conf. Soft Robot. (RoboSoft)*, 2020, pp. 417–423, doi: 10.1109/RoboSoft48309.2020.9116011.
[255] R. Lagneau, A. Krupa, and M. Marchal, "Active deformation through visual servoing of soft objects," in *Proc. IEEE Int. Conf. Robot. Automat. (ICRA)*, 2020, pp. 8978–8984, doi: 10.1109/ICRA40945.2020.9197506.
[256] T. G. Thuruthel, E. Falotico, F. Renda, and C. Laschi, "Learning dynamic models for open loop predictive control of soft robotic manipulators," *Bioinspiration Biomimetics*, vol. 12, no. 6, Oct. 2017, Art. no. 066003, doi: 10.1088/1748-3190/aa839f.
[257] S. Satheeshbabu, N. K. Uppalapati, G. Chowdhary, and G. Krishnan, "Open loop position control of soft continuum arm using deep reinforcement learning," in *Proc. IEEE Int. Conf. Robot. Automat. (ICRA)*, 2019, pp. 5133–5139, doi: 10.1109/ICRA.2019.8793653.
[258] M. T. Gillespie, C. M. Best, E. C. Townsend, D. Wingate, and M. D. Killpack, "Learning nonlinear dynamic models of soft robots for model predictive control with neural networks," in *Proc. IEEE Int. Conf. Soft Robot. (RoboSoft)*, 2018, pp. 39–45, doi: 10.1109/ROBOSOFT.2018.8404894.
[259] D. Bruder, B. Gillespie, C. D. Remy, and R. Vasudevan, "Modeling and control of soft robots using the koopman operator and model predictive control," 2019, *arXiv:1902.02827*.
[260] E. Kamenar, N. Ćrnjarić-Žic, D. Haggerty, S. Zelenika, E. Hawkes, and I. Mezić, "Prediction of the behavior of a pneumatic soft robot based on koopman operator theory," in *Proc. 43rd IEEE Int. Conv. Inf., Commun. Electron. Technol. (MIPRO)*, pp. 1169–1173, doi: 10.23919/MIPRO48935.2020.9245155.
[261] M. L. Castaño, A. Hess, G. Mamakoukas, T. Gao, T. Murphey, and X. Tan, "Control-oriented modeling of soft robotic swimmer with koopman operators," in *Proc. IEEE/ASME Int. Conf. Adv. Intell. Mechatronics (AIM)*, 2020, pp. 1679–1685, doi: 10.1109/AIM43001.2020.9159033.
[262] D. A. Haggerty, M. J. Banks, P. C. Curtis, I. Mezić, and E. W. Hawkes, "Modeling, reduction, and control of a helically actuated inertial soft robotic arm via the koopman operator," 2020, *arXiv:2011.07939*.